THE GEOLOGICAL SOCIETY
OF AMERICA®

Proterozoic–Phanerozoic tectonic evolution of the Qilian Shan and Eastern Kunlun Range, northern Tibet

Chen Wu[1,†], Jie Li[2], Andrew V. Zuza[3], Peter J. Haproff[4], Xuanhua Chen[5], and Lin Ding[1]
[1]*State Key Laboratory of Tibetan Plateau Earth System and Resources Environment, Institute of Tibetan Plateau Research, Chinese Academy of Sciences, Beijing 100101, China*
[2]*School of Earth Sciences and Resources, China University of Geosciences (Beijing), Beijing 100083, China*
[3]*Nevada Bureau of Mines and Geology, University of Nevada, Reno, Nevada 89557, USA*
[4]*Department of Earth and Ocean Sciences, University of North Carolina, Wilmington, North Carolina 28403, USA*
[5]*Chinese Academy of Geological Sciences, Beijing 100037, China*

ABSTRACT

The Proterozoic–Phanerozoic tectonic evolution of the Qilian Shan, Qaidam Basin, and Eastern Kunlun Range was key to the construction of the Asian continent, and understanding the paleogeography of these regions is critical to reconstructing the ancient oceanic domains of central Asia. This issue is particularly important regarding the paleogeography of the North China-Tarim continent and South China craton, which have experienced significant late Neoproterozoic rifting and Phanerozoic deformation. In this study, we integrated new and existing geologic field observations and geochronology across northern Tibet to examine the tectonic evolution of the Qilian-Qaidam-Kunlun continent and its relationships with the North China-Tarim continent to the north and South China craton to the south. Our results show that subduction and subsequent collision between the Tarim-North China, Qilian-Qaidam-Kunlun, and South China continents occurred in the early Neoproterozoic. Late Neoproterozoic rifting opened the North Qilian, South Qilian, and Paleo-Kunlun oceans. Opening of the South Qilian and Paleo-Kunlun oceans followed the trace of an early Neoproterozoic suture. The opening of the Paleo-Kunlun Ocean (ca. 600 Ma) occurred later than the opening of the North and South Qilian oceans (ca. 740–730 Ma). Closure of the North Qilian and South Qilian oceans occurred in the Early Silurian (ca. 440 Ma), whereas the final consumption of the Paleo-Kunlun Ocean occurred in the Devonian (ca. 360 Ma). Northward subduction of the Neo-Kunlun oceanic lithosphere initiated at ca. 270 Ma, followed by slab rollback beginning at ca. 225 Ma evidenced in the South Qilian Shan and at ca. 194 Ma evidenced in the Eastern Kunlun Range. This tectonic evolution is supported by spatial trends in the timing of magmatism and paleo-crustal thickness across the Qilian-Qaidam-Kunlun continent. Lastly, we suggest that two Greater North China and South China continents, located along the southern margin of Laurasia, were separated in the early Neoproterozoic along the future Kunlun-Qinling-Dabie suture.

INTRODUCTION

The Kunlun-Qaidam-Qilian continent, located along the northeastern margin of the Tethyan orogenic system, is a key continental fragment that contributed to the tectonic development of Asia (e.g., Şengör, 1984; Jiang et al., 1992; Yin and Harrison, 2000; Wu et al., 2016a; Xiao et al., 2009; Song et al., 2013; Zuza et al., 2018). Despite the regional importance of the Kunlun-Qaidam-Qilian continent, its Proterozoic–Phanerozoic evolution has remained inadequately examined. A major unresolved issue is the paleogeographic relationship of the Kunlun-Qaidam-Qilian continent with the North China-Tarim cratons and the adjacent Songpan-Ganzi continent of the South China craton (Fig. 1) (e.g., Wu et al., 2016a). These continental fragments are presently separated by the Cenozoic Qilian Shan-Nan Shan thrust belt to the north and left-slip Kunlun fault to the south. Several active structures deform Archean–Proterozoic basement rocks and overprint rocks emplaced during Mesozoic extension and punctuated magmatism during the Neoproterozoic–early Mesozoic (e.g., Xiao et al., 2009; Song et al., 2013, 2019a; Zuza et al., 2016, 2018; Wu et al., 2016a, 2019a; Dong et al., 2018; Yu et al., 2021), which has provided a challenge in understanding the evolution of northern Tibet.

Several important first-order questions regarding the evolution of the Qilian orogen remain unanswered: (1) the relationships between North, Central, and South Qilian Shan basement rocks with those of the North China, Tarim, and South China cratons, respectively; (2) whether subduction of the Qilian Ocean faced to the north (Song et al., 2013), south (Yin et al., 2007; Zuza et al., 2018), or was bi-directional (Xiao et al., 2009; Li et al., 2021); (3) whether final closure of the Qilian Ocean occurred during the Devonian or Silurian; (4) the number and composition (i.e., oceanic versus continental) of magmatic arcs involved; and (5) whether the North and South Qilian sutures formed via distinct ocean closure events (Fig. 1). Similarly, the number and closure timing of sutures of the Eastern Kunlun orogen remain debated. One set of models involve the one-time closure of a single Kunlun Ocean in the Neoproterozoic (Şengör et al., 1988; Wu et al., 2016a, 2019a) or Devonian (Stampfli and Borel, 2002). Alternatively, Yin and Harrison (2000) proposed that a single Kunlun Ocean suture existed prior to the Ordovician and closed once in the Early Carboniferous and again in the latest Triassic. A third set of models involve the closure of two to three oceans along distinct sutures (Jiang et al., 1992; Yang et al., 1996; Meng et al., 2013a, 2015; Dong et al., 2018).

Here we present findings of the structural framework of the Qilian and Eastern Kunlun orogens located between the Kunlun-Qaidam-Qilian, Tarim-North China, and Songpan-Ganzi continents based on a compilation of new and existing field observations from geologic mapping, geo-/thermochronologic ages, and geochemical data. Our results allowed us to construct regional tectonostratigraphic sections, constrain the spatial and temporal extents of arc magmatism, and

Chen Wu https://orcid.org/0000-0003-0647-3530
†wuchen@itpcas.ac.cn.

GSA Bulletin; https://doi.org/10.1130/B36306.1; 14 figures; 1 table; 1 supplemental file.
Published online 24 December 2021

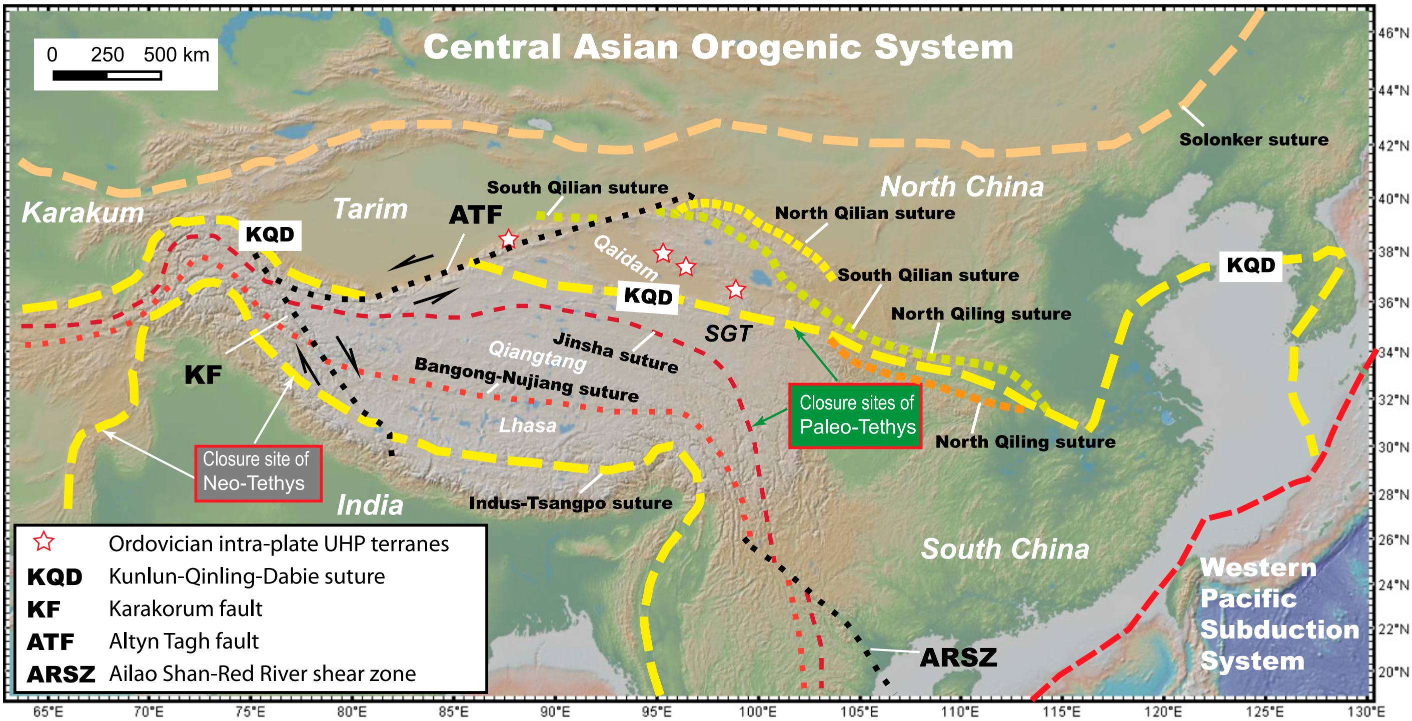

Figure 1. Simplified tectonic map across the Tibetan Plateau and central Asia, modified after Yin and Nie (1996) and Yin and Harrison (2000). UHP—ultrahigh pressure.

correlate basement rocks and assign possible provenance which provided new constraints on the Proterozoic–Phanerozoic tectonic evolution of the Qilian and Eastern Kunlun orogens and the formation of the Asian continent.

REGIONAL GEOLOGIC SETTING

The Qilian Shan is located along the northeastern margin of the Tibetan Plateau, separating the Hexi Corridor to the north from the Qaidam Basin to the south. The Qilian Shan is truncated to the northwest by the sinistral strike-slip Altyn Tagh fault and links to the east with the Qinling orogen (e.g., Yin and Harrison, 2000; Zuza et al., 2016) (Fig. 1). The early Paleozoic Qilian orogen exposed in the Qilian Shan contains ophiolitic mélange complexes of the North and South Qilian suture zones (Figs. 1 and 2) that formed during the collision of the Kunlun-Qaidam continent with the southern margin of the combined Tarim-North China cratons (e.g., Xiao et al., 2009; Song et al., 2013; Wu et al., 2017; Zuza et al., 2018; Fu et al., 2020; Li et al., 2021; Fu et al., 2019, 2021). In general, the Qilian orogen contains three tectonic units separated by the North and South Qilian sutures: (1) the North Qilian Shan consisting of Neoproterozoic passive-continent margin strata and post-collisional intrusions, (2) the Central Qilian Shan consisting of Precambrian basement intruded by 1.1–0.9 Ga plutons, and (3) the South Qilian Shan consisting of the early Paleozoic Qilian arc sequence emplaced atop Precambrian amphibolite-grade continental basement (e.g., Yin and Harrison, 2000; Pan et al., 2004; Wu et al., 2016a; Zuza et al., 2018) (Fig. 2). The southern margin of the North China craton and Kunlun-Qaidam continent may contain correlative Paleoproterozoic (ca. 2.3–1.8 Ga) basement rocks and overlying Mesoproterozoic cover sequences (e.g., Chen et al., 2013f; Yu et al., 2017b, 2019; Wu et al., 2017, 2021). The tectonostratigraphic evolution of the Qilian orogen is described by Zuza et al. (2018) and Wu et al. (2017). Key geologic relationships and geochronologic ages of the North, Central, and South Qilian Shan are summarized in a simplified tectonostratigraphic column (Fig. 3) and regional-scale geologic map (Fig. 4).

The Eastern Kunlun Range is located between the Qaidam Basin of the Kunlun-Qaidam continent to the north and the active left-slip Kunlun fault to the south, the latter of which follows the Triassic Neo-Kunlun suture (e.g., Jiang et al., 1992; Yang et al., 1996; Wu et al., 2016a, 2019a; Dong et al., 2018) (Fig. 4). The Eastern Kunlun orogen exposed in the range formed via three major deformation events in the Neoproterozoic, early Paleozoic, and late Paleozoic–early Mesozoic associated with collision of the Proto-, Paleo-, and Neo-Kunlun arcs, respectively (Wu et al., 2016a, 2019a) (Fig. 4). The late Paleozoic–early Mesozoic closure of the Neo-Kunlun ocean occurred as the Qaidam-Kunlun continent collided with the Songpan-Ganzi continent along the western margin of the South China craton (Wu et al., 2016a, 2019a). The Eastern Kunlun orogen primarily contains three tectonic units that consist from north to south of: (1) Paleoproterozoic basement rocks and Phanerozoic cover sequences along the southern margin of the Kunlun-Qaidam continent; (2) a central zone of volcanic and plutonic rocks associated with the Kunlun arc(s), and intermittently exposed ultramafic-mafic rocks and ophiolitic fragments that occur within Precambrian–early Paleozoic metamorphic complexes; and (3) the Triassic Neo-Kunlun suture that separates the Kunlun arc(s) to the north and South China craton basement rocks overlain by Triassic submarine-fan turbidite deposits of the Songpan-Ganzi flysch complex to the south (e.g., Yin and Harrison, 2000; Jiang et al., 1992; Yang et al., 1996; Ding et al., 2013; Wu et al., 2016a). Detailed descriptions of the Eastern Kunlun tectonostratigraphy are presented in Wu et al. (2016a, 2019a).

The northwest-striking, early Paleozoic intra-arc North Qaidam ultrahigh pressure (UHP) metamorphic belt is located along the northeastern margin of the Qaidam Basin and is truncated by the left-slip Altyn Tagh fault to

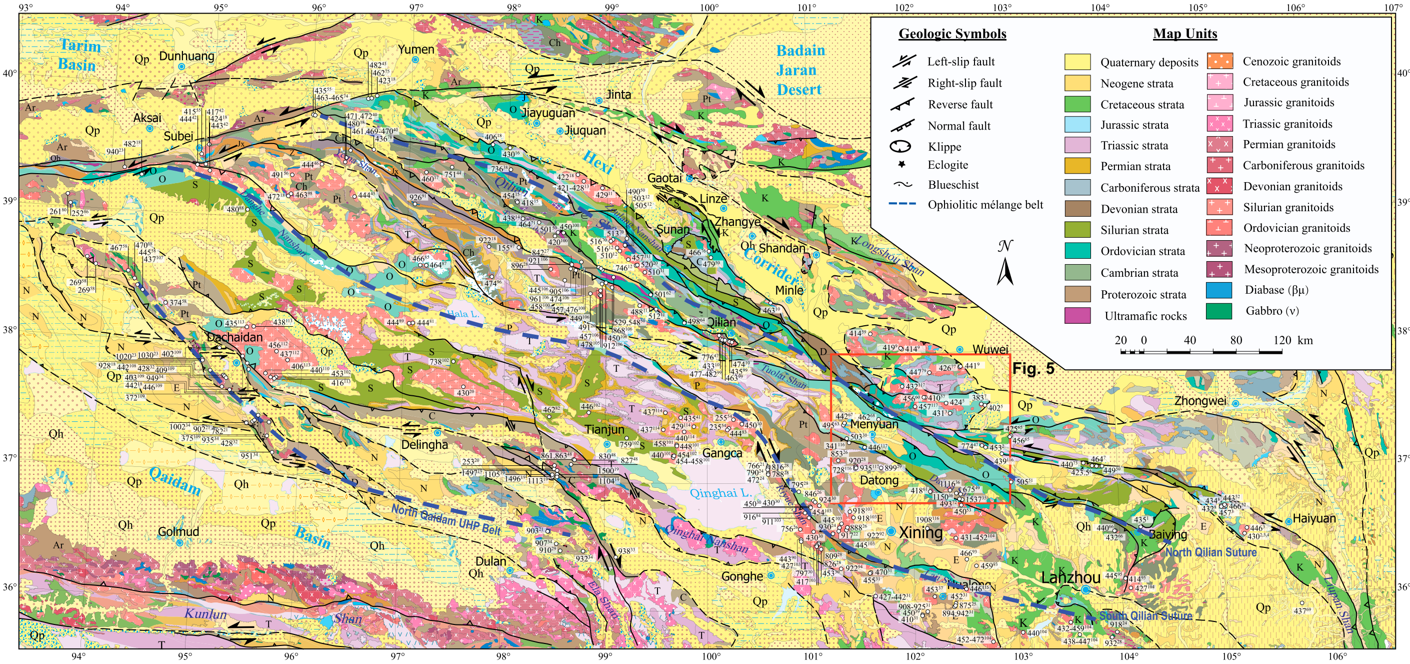

Figure 2. Geologic map of the Qilian Shan of northern Tibet showing regional geochronologic results of magmatic events. The map is compiled from Pan et al. (2004), Wang et al. (2013b), and this study. Data are compiled from: 1—H. Yang et al. (2020); 2—C.Y. Tseng et al. (2009); 3—S.Y. Yu et al. (2015); 4—S. Chen et al. (2016c); 5—Z.L. Xiong et al. (2012); 6—Q. Qian et al. (1998); 7—C.L. Wu et al. (2004b); 8—S. Chen et al. (2015a); 9—L.Q. Zhang et al. (2017b); 10—C.L. Wu et al. (2011a); 11—C.L. Wu et al. (2010); 12—Y.X. Chen et al. (2014); 13—H. Huang et al. (2017a); 14—Y.X. Chen et al. (2012c); 15—X.M. Zhao et al. (2014); 16—Y.S. Li et al. (2019); 17—J.W. Mao et al. (2000); 18—G.E. Gehrels et al. (2003b); 19—C.Y. Wang et al. (2021); 20—B. Li et al. (2021); 21—Y.B. Peng et al. (2019); 22—J.J. Guo et al. (2000); 23—Y.S. Wan et al. (2001, 2003); 24—K.A. Tung et al. (2007); 25—W.C. Xu et al. (2007); 26—Y. Yong et al. (2008); 27—N. Xue et al. (2009); 28—K.A. Tung et al. (2013); 29—S.Y. Yu et al. (2013a); 30—H. Huang et al. (2015); 31—Z. Yan et al. (2015); 32—J.X. Zhang et al. (2008b); 33—Y.L. Xu et al. (2011); 34—S.G. Song et al. (2012); 35—J.D. Liu et al. (2015); 36—J.S. Dong et al. (2015); 37—Z.P. Guo et al. (2015a); 38—M. Li et al. (2015c); 39—Z.W. Zhang et al. (2015b); 40—R.N. Hou et al. (2015); 41—J.P. Shi et al. (2015); 42—Z.W. Luo et al. (2015); 43—Z.B. Song et al. (2004); 44—J.P. Su et al. (2004a); 45—J.P. Su et al. (2004b); 46—J.P. Su et al. (2004c); 47—C.Y. Tseng et al. (2006); 48—J.J. Ma et al. (2018); 49—T.Z. Song et al. (2016, C.X. Tian et al. (2018); 50—S.G. Song et al. (2013); 51—H.P. Qin et al. (2014a); 52—H.P. Qin et al. (2014b); 53—M. Liu et al. (2014); 54—Q.F. Xie et al. (2014); 55—J.F. Li et al. (2010); 56—Z.B. Huang et al. (2014b); 57—Z.B. Huang et al. (2018); 58—C.L. Wu et al. (2009a); 59—Z.B. Huang et al. (2010); 60—Ding and Huang, 2019); 61—G.L. Wang et al. (2018a); 62—J. Wang et al. (2018b); 63—Y.B. Peng et al. (2017b); 64—B. Li et al. (2017); 65—X.M. Zhao et al. (2018); 66—G.B. Zhao et al. (2013); 67—Q. Liu et al. (2019); 68—Z.P. Guo et al. (2015a); 69—W.Z. Wu et al. (2019c); 70—L.T. Zhang et al. (2018a); 71—Y.X. Liu et al. (2018b); 72—B.S. Liu et al. (2016); 73—H.R. Zhang et al. (2019); 74—N. Wang et al. (2017a); 75—X.X. Fan et al. (2020); 76—T. Bu et al. (2019); 77—M.Q. Liu (2013); 78—Q.H. Wang et al. (2017b); 79—Y.J. Chen et al. (2019); 80—Z.L. Jia et al. (2017); 81—X.Y. Zhang et al. (2018d); 82—H. Liao et al. (2014b); 83—J.P. Shi et al. (2017); 84—X.L. Zhu et al. (2019); 85—W.F. Li et al. (2020); 86—W.L. Hu et al. (2016); 87—X.L. Yu et al. (2018a); 88—B. Ji et al. (2019); 89—X.L. Yu et al. (2018b); 90—Z.W. Zhang et al. (2012b); 91—G. Tao et al. (2017); 92—L. Gao et al. (2017); 93—J.S. Cao et al. (2019); 94—D.Y. Lv et al. (2021); 95—J.L. Chen et al. (2008a); 96—Y. Zheng et al. (2017); 97—J.M. Zhang et al. (2018b); 98—R.R. Qi (2012); 99—Q.L. Chen (2009); 100—L.L. Zhang (2014); 101—P.Y. Chang (2017); 102—Y. Qin (2018); 103—X.T. Liu (2019); 104—H. Yang (2016); 105—Y.L. An (2015); 106—A.V. Zuza et al. (2018); 107—X.H. Zhu et al. (2013); 108—B. Zhou et al. (2014); 109—C.L. Wu et al. (2007); 110—X.X. Lu et al. (2007); 111—X. Zhang et al. (2015a); 112—X.H. Zhu et al. (2016); 113—X.Y. He et al. (2020); 114—G.D. Zhang et al. (2016a); 115—J.W. Cui et al. (2016); 116—C. Wu et al. (2021); 117—this study.

the northwest (e.g., Yin et al., 2007; Yu et al., 2021; Song et al., 2013, 2019b) (Figs. 1 and 2). This UHP metamorphic belt includes the tightly folded eclogite blocks and ophiolitic rocks that experienced regional epidote-amphibolite facies metamorphism (Menold et al., 2009). The present-day exposure of the belt is strongly controlled by north-dipping Cenozoic thrust faults (e.g., Sobel and Arnaud, 1999, Yin et al., 2007) (Fig. 2) and thus is not interpreted to represent an in situ early Paleozoic suture. In the Qilian Shan, two or even three subparallel ophiolitic mélange belts have been identified (e.g., Song et al., 2013, 2019a; Fu et al., 2020) (Figs. 2 and 3). These ophiolitic mélange belts consist, from north to south, of: (1) the ca. 517–487 Ma forearc and ca. 490–445 Ma backarc North Qilian ophiolitic mélange belts; (2) the ca. 550–495 Ma Central Qilian ophiolitic mélange belt (?); and (3) the ca. 525–500 Ma South Qilian ophiolitic mélange belt. Similarly, three subparallel ophiolitic mélange belts have been identified in the Eastern Kunlun Range (Fig. 4) including: (1) the ca. 486–423 Ma(?) North Kunlun ophiolitic mélange zone; (2) the ca. 555–243 Ma(?) Central Kunlun ophiolitic mélange zone; and (3) the ca. 535–260 Ma(?) South Kunlun ophiolitic mélange zone (e.g., Yang et al., 1996; Meng et al., 2015; Dong et al., 2018; Yu et al., 2017a). Ophiolitic mélange belts exposed in the Qilian Shan

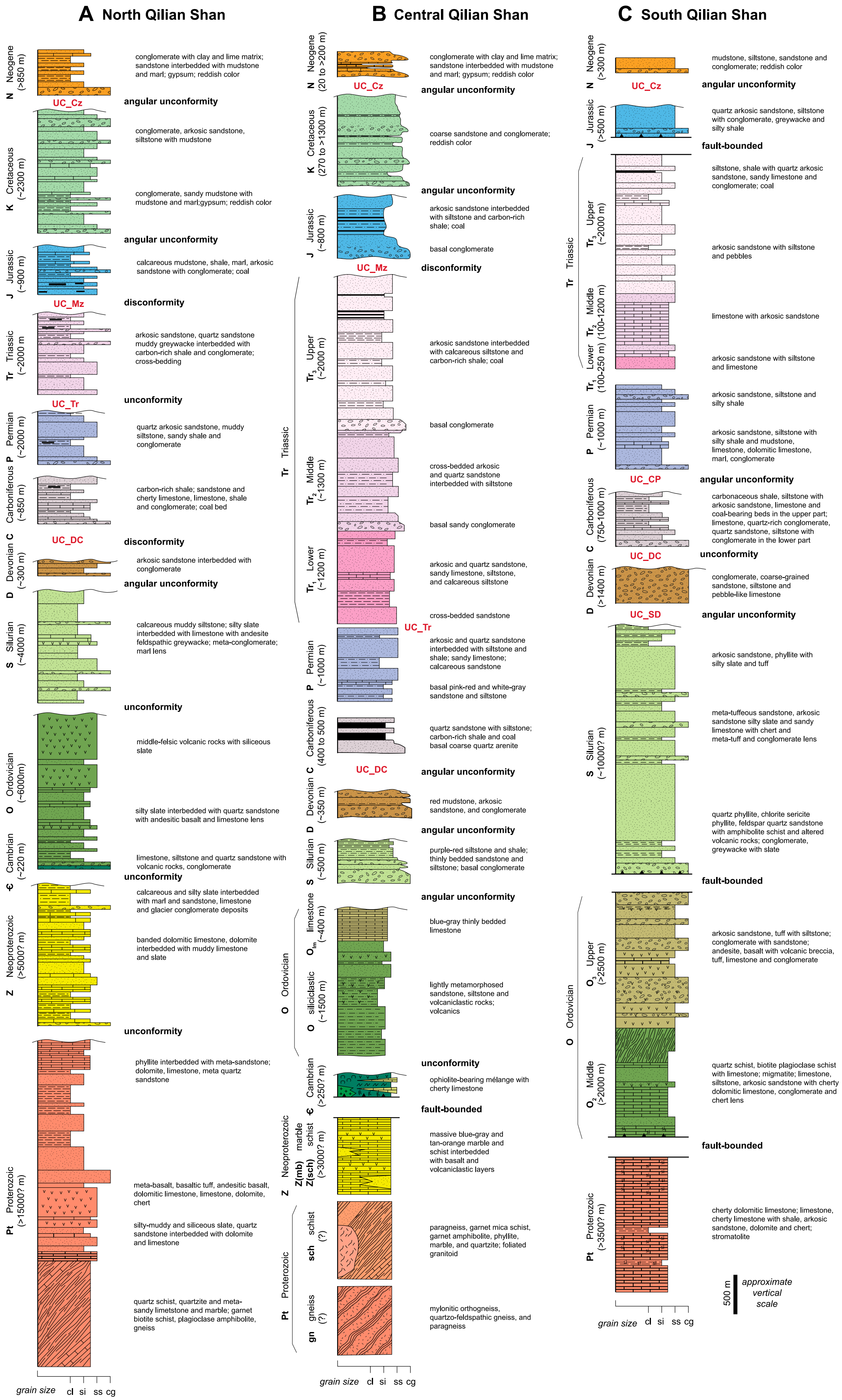

Figure 3. Lithostratigraphy of the North Qilian Shan, Central Qilian Shan, and South Qilian Shan of northern Tibet. Ages are compiled from Qinghai Bureau of Geology and Mineral Resources (1997), Pan et al. (2004), Wang et al. (2013c), and this study. cl—clay; si—silt; ss—sand; cg—conglomerate.

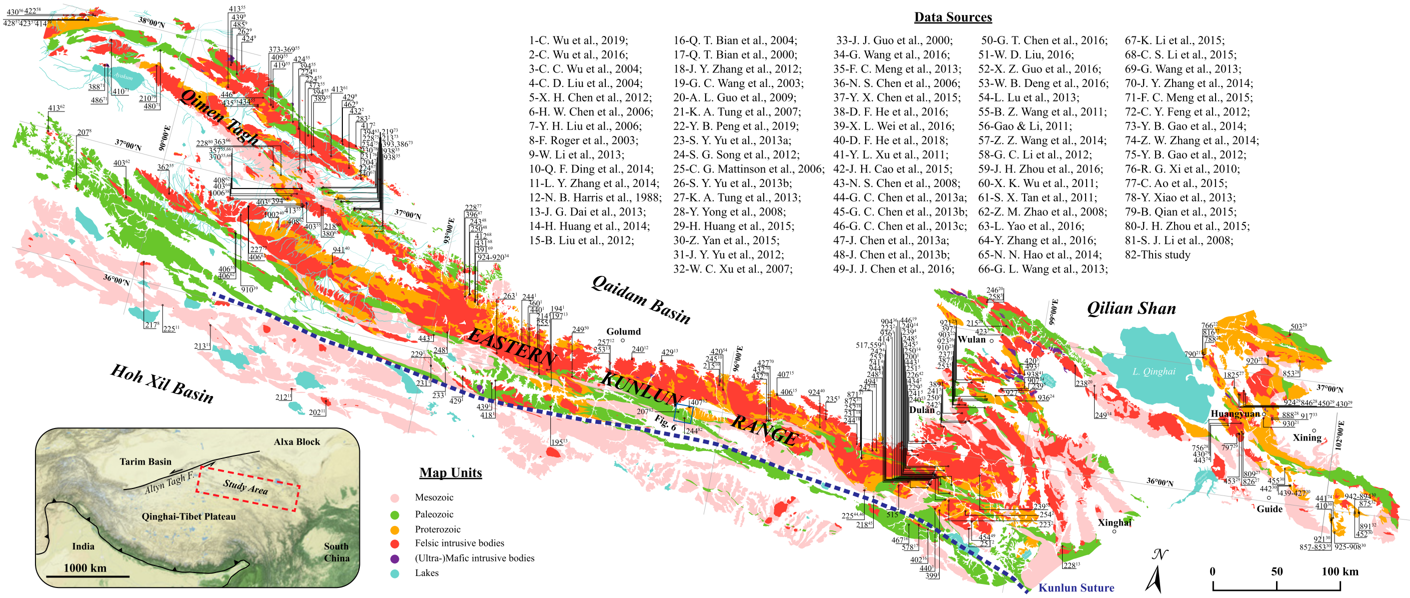

Figure 4. Simplified geologic map of the Eastern Kunlun Range of northern Tibet showing regional geochronologic results of magmatic events. The map is compiled from Pan et al. (2004), Wang et al. (2013c), and this study. Data are compiled from: 1—C. Wu et al. (2019a); 2—C. Wu et al. (2016a); 3—C.C. Wu et al. (2004a); 4—C.D. Liu et al. (2004); 5—X.H. Chen et al. (2012b); 6—H.W. Chen et al. (2006a); 7—Y.H. Liu et al. (2006a); 8—F. Roger et al. (2003); 9—W. Li et al. (2013); 10—Q.F. Ding et al. (2014); 11—L.Y. Zhang et al. (2014b); 12—N.B. Harris et al. (1988); 13—J.G. Dai et al. (2013); 14—H. Huang et al. (2014a); 15—B. Liu et al. (2012a); 16—Q.T. Bian et al. (2004); 17—Q.T. Bian et al. (2000); 18—J.Y. Zhang et al. (2012a); 19—G.C. Wang et al. (2003); 20—A.L. Guo et al. (2009); 21—K.A. Tung et al. (2007); 22—Y.B. Peng et al. (2019); 23—S.Y. Yu et al. (2013a); 24—S.G. Song et al. (2012); 25—C.G. Mattinson et al. (2006); 26—S.Y. Yu et al. (2013b); 27—K.A. Tung et al. (2013); 28—Y. Yong et al. (2008); 29—H. Huang et al. (2015); 30—Z. Yan et al. (2015); 31—J.Y. Yu et al. (2012); 32—W.C. Xu et al. (2007); 33—J.J. Guo et al. (2000); 34—G. Wang et al. (2016); 35—F.C. Meng et al. (2013b); 36—N.S. Chen et al. (2006b); 37—Y.X. Chen et al. (2015b); 38—D.F. He et al. (2016); 39—X.L. Wei et al. (2016); 40—D.F. He et al. (2018); 41—Y.L. Xu et al. (2011); 42—J.H. Cao et al. (2015); 43—N.S. Chen et al. (2008b); 44—G.C. Chen et al. (2013a); 45—G.C. Chen et al. (2013b); 46—G.C. Chen et al. (2013c); 47—J. Chen et al. (2013d); 48—J. Chen et al. (2013e); 49—J.J. Chen et al. (2016b); 50—G.T. Chen et al. (2016a); 51—W.D. Liu (2016); 52—X.Z. Guo et al. (2016); 53—W.B. Deng et al. (2016); 54—L. Lu et al. (2013); 55—B.Z. Wang et al. (2011); 56—Gao and Li (2011); 57—Z.Z. Wang et al. (2014); 58—G.C. Li et al. (2012); 59—J.H. Zhou et al. (2016); 60—X.K. Wu et al. (2011b); 61—S.X. Tan et al. (2011); 62—Z.M. Zhao et al. (2008); 63—L. Yao et al. (2016); 64—Y. Zhang et al. (2016b); 65—N.N. Hao et al. (2014); 66—G.L. Wang et al. (2013b); 67—K. Li et al. (2015b); 68—C.S. Li et al. (2015a); 69—G. Wang et al. (2013a); 70—J.Y. Zhang et al. (2014a); 71—F.C. Meng et al. (2015); 72—C.Y Feng (2012); 73—Y.B. Gao et al. (2014); 74—Z.W. Zhang et al. (2014c); 75—Y.B. Gao et al. (2012); 76—R.G. Xi et al. (2010); 77—C. Ao et al. (2015); 78—Y. Xiao et al. (2013); 79—B. Qian et al. (2015); 80—J.H. Zhou et al. (2015); 81—S.J. Li et al. (2008); 82—this study. F.—Fault.

and Eastern Kunlun Range are truncated to the northwest by the left-slip Altyn Tagh fault and occur in the hanging walls of Cenozoic thrusts (e.g., Yin et al., 2007) (Figs. 2 and 4). The trace of the South Qilian suture appears to link to the southeast with the North Qinling Erlangping suture (Yin and Nie, 1996; Tseng et al., 2009), whereas the Neo-Kunlun suture correlates with the Shangdan suture exposed in the central Qinling region to the east (Ratschbacher et al., 2003; Dong and Santosh, 2016). Whether the ophiolitic mélange belts exposed in the Qilian Shan and Eastern Kunlun Range represent individual in situ sutures formed via distinct ocean closure events or intracontinental and/or backarc processes remains debated.

Numerous Neoproterozoic and early Paleozoic granitoid plutons are exposed throughout the Qilian Shan (Fig. 2; Table S1[1]). These plutons have ages ranging between 1030 and 728 Ma and 520–340 Ma (Table S1), and have been mostly attributed to subduction-related arc magmatism and/or syn- to post-orogenic magmatism (e.g., Gehrels et al., 2003b; Wu et al., 2017; Zuza et al., 2018; Huang et al., 2015; Fu et al., 2018). In addition, ca. 235–269 Ma granitoids are distributed throughout the southern Qilian Shan along the northern margin of the Kunlun-Qaidam continent (Xie et al., 2014; Hu et al., 2016; Li et al., 2021; Jia et al., 2017; Wu et al., 2009a, 2009b). Three distinct generations of Neoproterozoic–Mesozoic granitoid plutons are exposed along the southern margin of the Kunlun-Qaidam terrane, two of which are widely exposed in the Eastern Kunlun Range (ca. 500–360 Ma and ca. 263–194 Ma) (Cowgill et al., 2003; Wu et al., 2016a, 2019a) (Fig. 4; Table S2; see footnote 1).

As part of this study, we performed local- and regional-scale geologic mapping of major tectonic units exposed in the eastern portion of the Qilian Shan (Fig. 5) and Wenquan area of the

[1]Supplemental Material. Table S1: Summary of Geochronology Results of Intrusive rocks in the Qilian Shan; Table S2: Summary of Geochronology Results of Intrusive rocks in the East Kunlun Range; Table S3: LA-ICP-MS results for zircons U-Pb ages of igneous, sandstone, and metamorphic sedimentary samples in this study; Table S4: Geochemistry Data for Plots of age against crustal thickness of the Qilian Shan; Table S5: Geochemistry Data for Plots of age against crustal thickness of the Eastern Kunlun Range. Please visit https://doi.org/10.1130/GSAB.S.17138867 to access the supplemental material, and contact editing@geosociety.org with any questions.

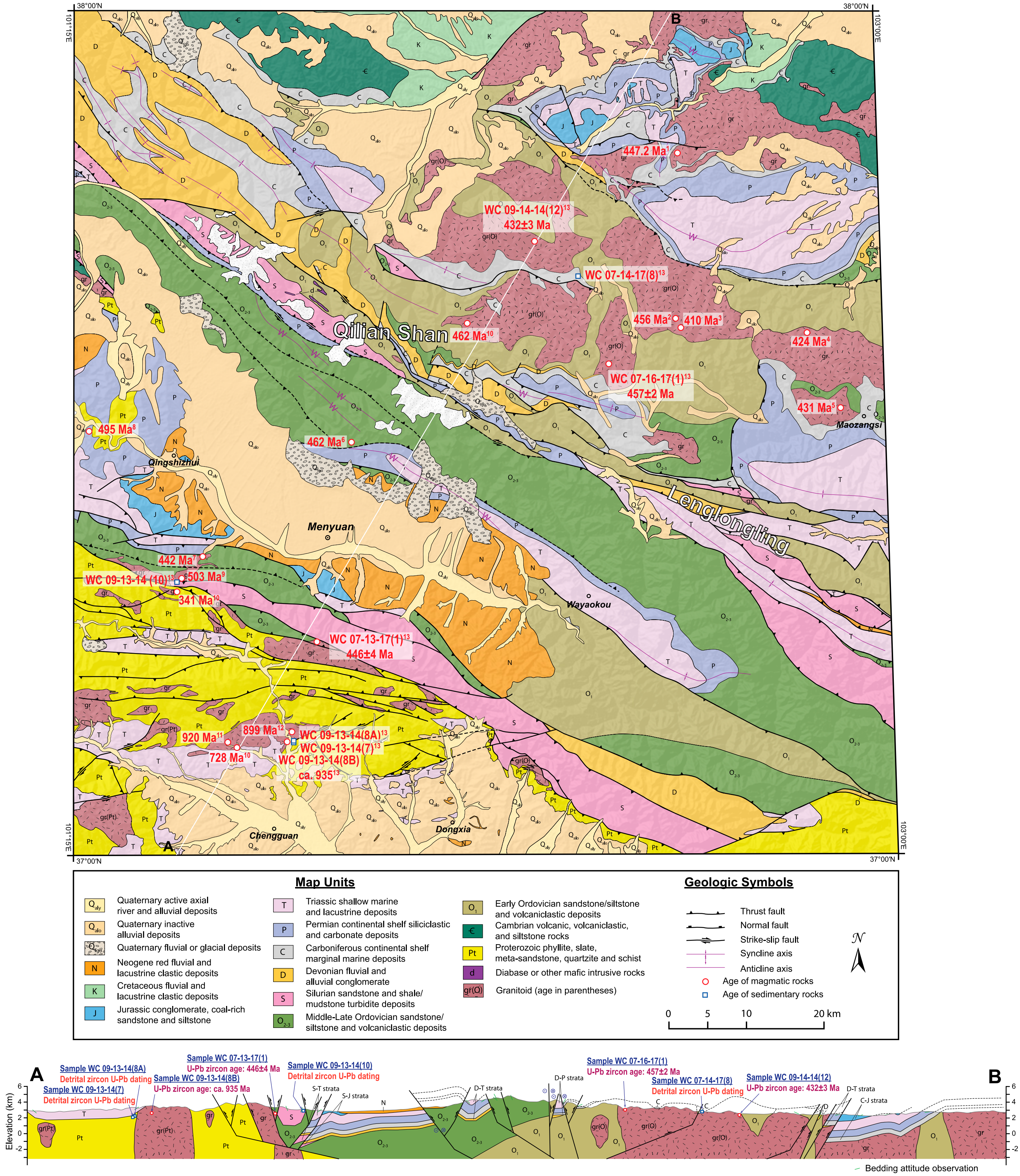

Figure 5. Geologic map of the eastern Qilian Shan of northern Tibet based on the results of this study, Pan et al. (2004), and Wu et al. (2021). The locations of the samples of this study are shown.

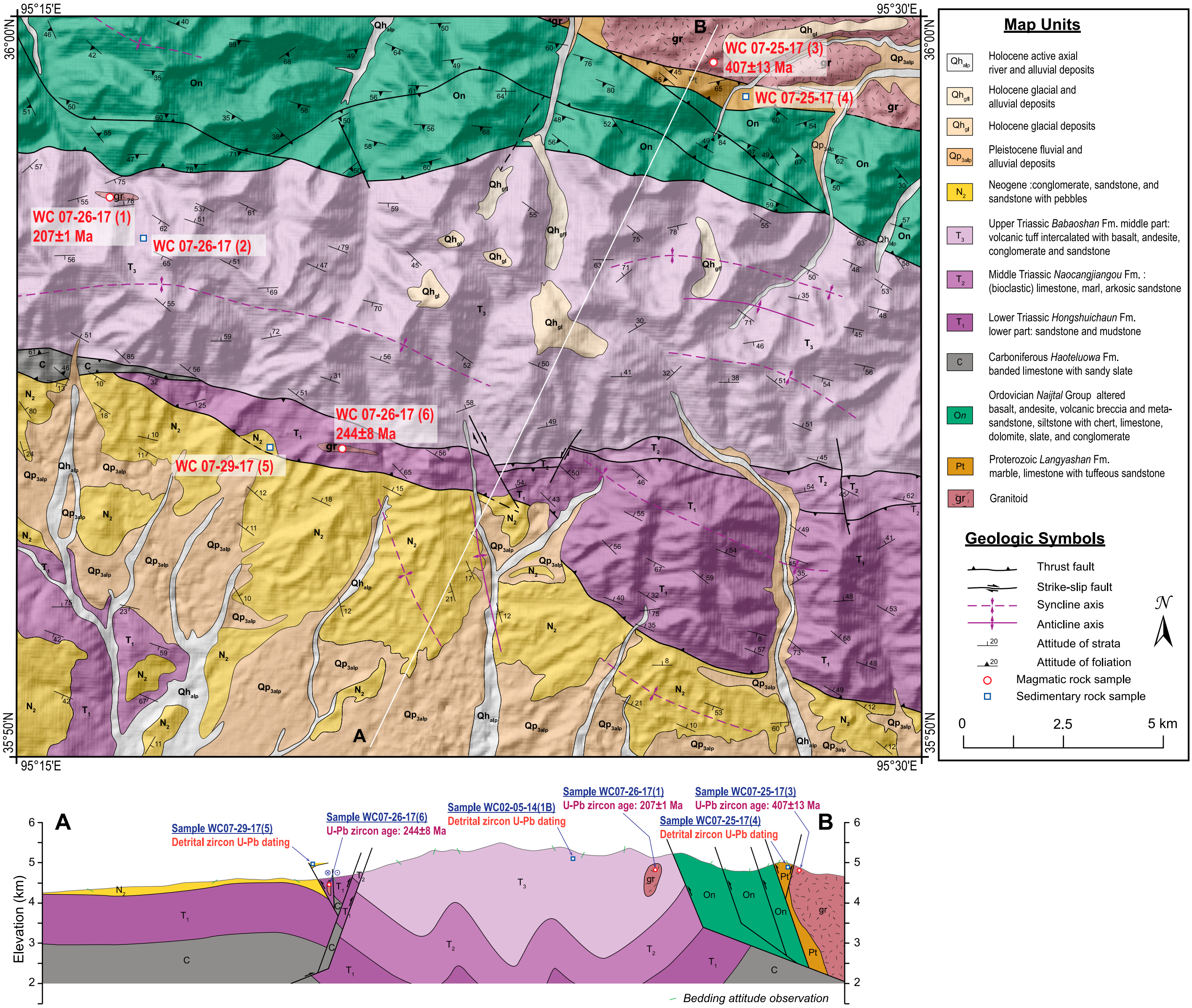

Figure 6. Geologic map of the Reshui region in the Eastern Kunlun Range of northern Tibet based on the results of this study and Pan et al. (2004). The locations of the samples of this study are shown. Fm.—Formation.

Eastern Kunlun Range (Fig. 6). In the following sections, we present the results of our mapping combined with constraints from existing geologic maps in the regions (e.g., Pan et al., 2004; Wu et al., 2021).

GEOLOGY OF THE EASTERN QILIAN SHAN

The eastern Qilian Shan region, including North and Central Qilian, exposes rocks varying in age from Neoproterozoic to Quaternary (Fig. 5). Precambrian metamorphic basement rocks are mainly exposed in the southern part of the mapping area and consist of porphyritic gneiss (Fig. 7A), phyllite, slate, meta-sandstone (Fig. 7B), quartzite (Fig. 7C), and schist. Cambrian volcanic, volcaniclastic, and siltstone rocks are exposed in the northern margin of the study area (Fig. 5). Ordovician rocks are widespread throughout the study area and consist of sandstone, siltstone, and volcaniclastic deposits. Ordovician rocks may represent a sequence of forearc, accretionary wedge, and foreland-basin strata (e.g., Xiao et al., 2009). Silurian rocks unconformably overlie Ordovician strata and often feature isoclinal folds and transposed bedding (Fig. 5). The Ordovician strata consist of minor conglomerate layers interbedded with siltstone, shale, and sandstone (Fig. 7D), which are considered to represent a flysch basin that transitions to a molasse sequence (e.g., Du et al., 2003; Yang et al., 2009; Yan et al., 2010).

Devonian strata do not exceed 350 m in thickness (Fig. 5) and consist of terrestrial conglomerate, sandstone, and minor volcanic rocks. These strata are interpreted to represent molasse that was deposited in intermontane and/or foreland basins during the Qilian orogeny (e.g., Xia et al., 2003; Yan et al., 2007). Devonian strata unconformably overlie deformed Proterozoic–early Paleozoic rocks. A disconformity forms the upper contact of the Devonian strata with Carboniferous strata (Zuza et al., 2018; Li et al., 2021). Throughout most of the eastern Qilian Shan,

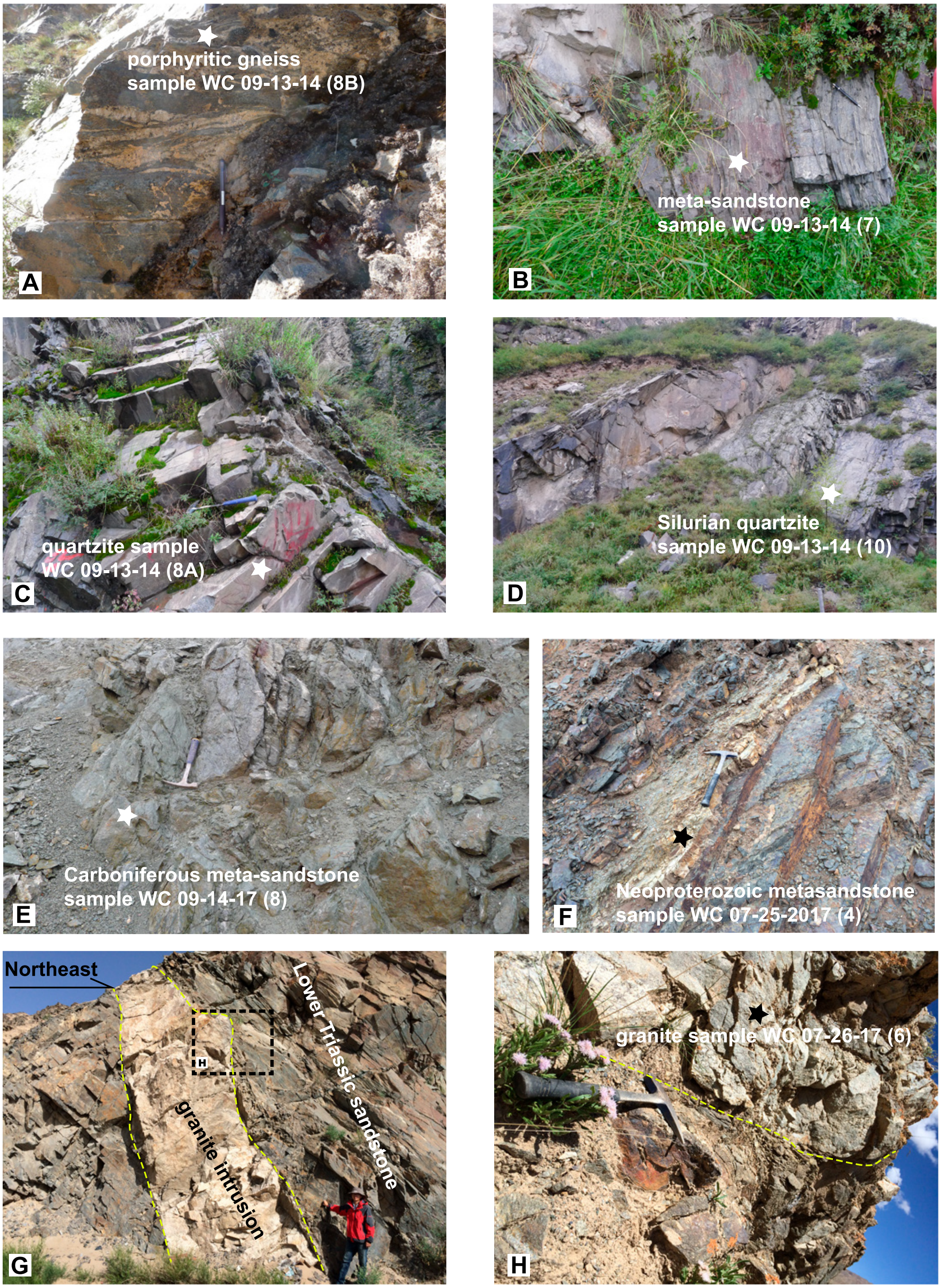

Figure 7. Field photographs of the Neoproterozoic Qilian Shan of northern Tibet metamorphic rocks including (A) porphyritic gneiss, (B) meta-sandstone, and (C) quartzite. Also shown are (D) Silurian quartzite, (E) Carboniferous slightly metamorphic sandstone, (F) Neoproterozoic metasandstone of the Langyashan Formation in the Eastern Kunlun Range, (G–H) a Triassic granite dike intruding Lower Triassic sandstone, (I) a Late Triassic granite dike intruding Upper Triassic sandstone, (J) weakly metamorphosed Lower Triassic sedimentary rocks thrust atop Cenozoic red deposits, and (K–M) granitoid samples collected as part of this study.

Carboniferous strata overlie Ordovician–Devonian rocks along an angular unconformity, and often feature isoclinal folds and transposed bedding (Zuza et al., 2018; Wu et al., 2021) (Fig. 5). Carboniferous strata consist of quartz sandstone (Fig. 7E) interbedded with siltstone and minor carbon-rich shale and coal. Permian strata consist of the coarse sandstone interbedded with siltstone and shale.

Triassic shallow marine and lacustrine strata conformably overlie Permian strata and consist of a basal conglomerate and overlying arkosic sandstone interbedded with calcareous siltstone (Fig. 5). Jurassic strata overlie Triassic strata along a regional disconformity and consist of a basal conglomerate and overlying arkosic sandstone interbedded with siltstone, shale, and numerous coal beds (Fig. 5). Overlying the Jurassic strata are Cretaceous and Cenozoic red-colored strata consisting of polymictic conglomerate and coarse sandstone. Gypsum layers are prevalent within the Cenozoic fluvial and lacustrine sediments (Fig. 5). The youngest strata are Quaternary alluvial and fluvial deposits (Fig. 5).

Four distinct Phanerozoic unconformities are recognized in the eastern Qilian Shan: (1) an oldest and most widespread unconformity between

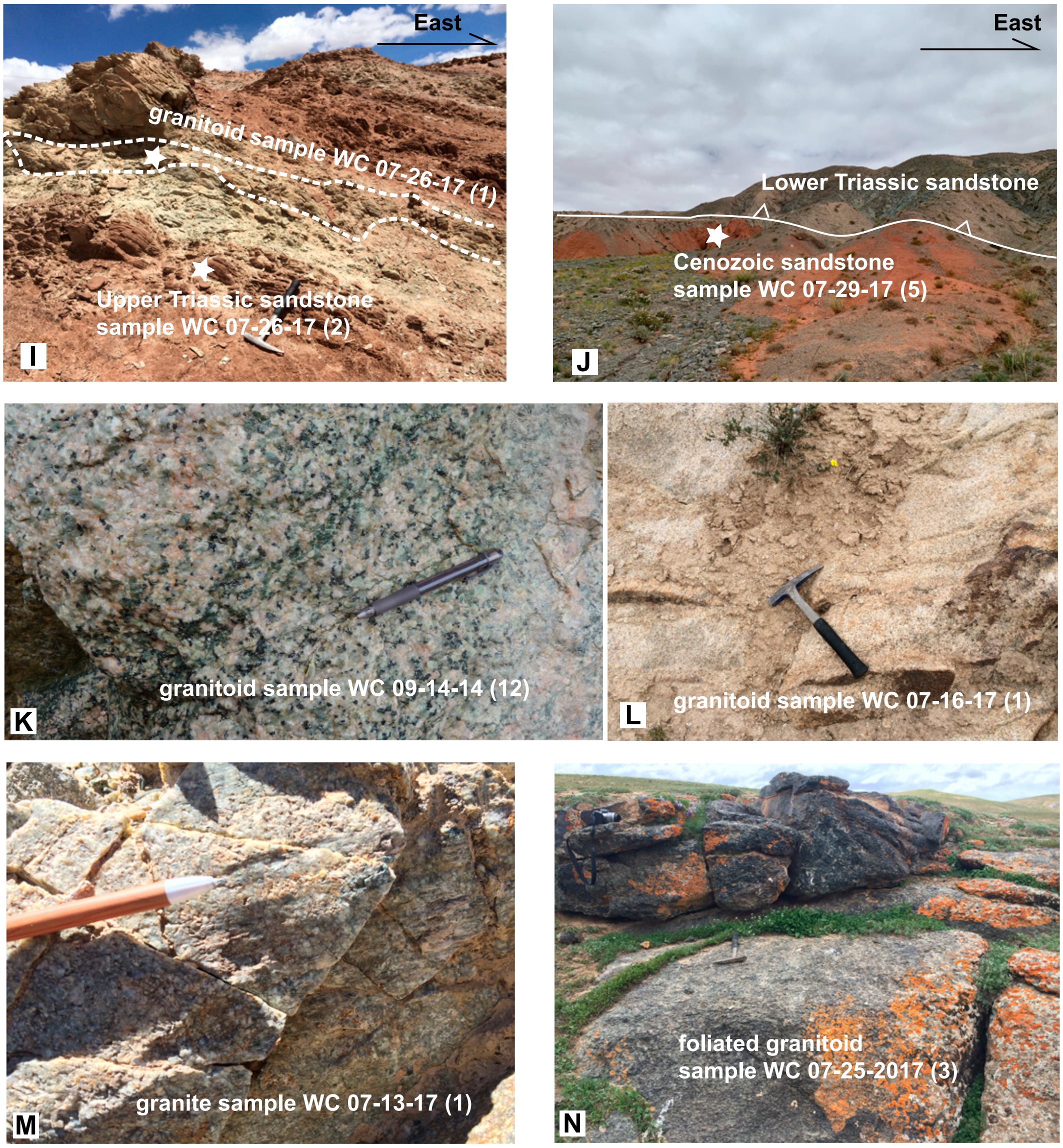

Figure 7. (***Continued***)

overlying Carboniferous strata (locally Devonian and/or Permian strata) and Proterozoic metamorphic basement and Ordovician–Silurian strata; (2) an unconformity between overlying Triassic strata and Carboniferous strata in the North Qilian; and (3) two youngest unconformities along the basal contacts of Cretaceous and Cenozoic strata. These youngest strata are interpreted to reflect regionally extensive tectonic events.

Numerous early Paleozoic granitoid plutons with ca. 503–424 Ma crystallization ages are exposed throughout the eastern Qilian Shan region (e.g., Chen et al., 2019; Ding and Huang, 2019; Huang et al., 2018; Xiong et al., 2012; Yu et al., 2013a, 2015; H. Huang et al., 2015; Guo et al., 2015a, 2015b; Liu et al., 2019; Peng et al., 2017a, 2017b; Tung et al., 2013; Wu et al., 2021; this study) (Fig. 5). In addition, Paleoproterozoic leucogranites (ca. 1.91 Ga), Neoproterozoic granitic intrusions (ca. 920–935 Ma), and late Paleozoic leucogranites (ca. 345 Ma) and alkaline rocks (ca. 410 Ma) are reported in the study area (e.g., Wu et al., 2021; Huang et al., 2018).

GEOLOGY OF THE EASTERN EASTERN KUNLUN RANGE

The oldest rocks exposed in the eastern Eastern Kunlun Range are Meso- to Neoproterozoic, low-grade metamorphic and unmetamorphosed strata of the Langyashan Formation (Fig. 6). These rocks are exposed in the northern corner of the mapping area and consist of marble and interbedded limestone and tuffeous sandstone (Zhang et al., 2018c) (Fig. 7F). The Langyashan Formation is thrust atop the Ordovician Naijtal Group which consists of weakly metamorphosed, shallow- and deep-marine clastic, carbonate, and volcaniclastic strata and volcanic rocks. Wu et al. (2019a) suggest that the Naijtal Group was deposited between ca. 447 and 440 Ma based on the detrital zircon U-Pb ages and the presence of Late Ordovician–Early Silurian granitoid intrusions. It remains unclear whether Paleozoic granitoids in the study area are thrust atop or intrude Proterozoic metamorphic rocks. The Carboniferous Haoteluowa Formation is thrust atop Triassic strata and volcanic rocks and consists of limestone interbedded with sandy slate (Fig. 6). Triassic rocks are divided into Lower, Middle, and Upper Triassic units, which are all intruded by granitic dikes (Figs. 7G–7I). The Lower Triassic Hongshuichuan Formation consists of a basal unit of massive cross-bedded gray sandstone overlain by siltstone and sandy slate (Figs. 7G and 7H). Middle Triassic strata are dominated by basal limestone

TABLE 1. SUMMARY OF SAMPLE LOCATIONS IN THE QILIAN SHAN AND EASTERN KUNLUN RANGE, NORTHERN TIBET

Sample number	Description	Latitude (°N)	Longitude (°E)	Elevation (m)	Crystallization age	MSWD	n
WC 07-26-17 (6)	granitoid	35°55′11.60″	95°20′03.39″	5312	244 ± 8 Ma	3.8	4 out of 18
WC 07-26-17 (1)	granitoid	35°57′30.93″	95°16′25.01″	4929	207 ± 1 Ma	0.79	17 out of 19
WC 07-25-17 (3)	granitoid	35°58′34.12″	95°26′03.87″	4765	407 ± 13 Ma	2.1	6 out of 7
WC 07-13-17 (1)	granitoid	37°15′22.54″	101°36′32.85″	3943	446 ± 4 Ma	0.63	3 out of 19
WC 07-16-17 (1)	granitoid	37°34′42.88″	102°02′18.27″	4406	457 ± 2 Ma	0.48	27 out of 27
WC 09-14-14 (12)	granitoid	37°43′12.14″	101°55′48.00″	2620	432 ± 3 Ma	0.31	12 out of 17
WC 07-29-17 (5)	sandstone	35°55′05.33″	95°18′46.06″	4655			100
WC 07-26-17 (2)	sandstone	35°57′05.83″	95°17′02.81″	5001			100
WC 07-25-17 (4)	meta-sandstone	35°57′52.55″	95°26′47.54″	4764			49
WC 09-13-14 (7)	meta-sandstone	37°07′59.77″	101°34′12.75″	2677			98
WC 09-13-14 (8A)	quartzite	37°08′09.23″	101°34′13.66″	2715			99
WC 09-13-14 (8B)	porphyritic gneiss	37°08′09.23″	101°34′13.66″	2715			99
WC 09-13-14 (10)	quartzite	37°19′29.46″	101°24′03.73″	3597			100
WC 09-14-17 (8)	quartz sandstone	37°41′19.50″	101°57′53.15″	3101			100

Note: MSWD—mean square weighted deviation.

overlain by cross-bedded arkosic sandstone with minor marble. Upper Triassic rocks consist of basal volcanics overlain by conglomerate and arkosic sandstone (Fig. 7I). The Triassic rocks are thrust over Cenozoic strata (Fig. 7J), which are predominantly Neogene and consist of red-colored fluvial conglomerate and sandstone and lacustrine mudstone with a clay, marble, or limestone matrix (Fig. 7J). The youngest rocks exposed in the study area are Quaternary alluvial, fluvial, and glaciofluvial strata.

Structures in the mapping area generally strike northwest, which parallels the strikes of sedimentary strata and metamorphic foliation and the trend of the range (Fig. 6). Cenozoic folds and faults are widespread in the mapping area (Fig. 6). Most faults cut Cenozoic and Quaternary strata with the exception of the thrust which places Paleozoic granitoids atop Proterozoic metamorphic rocks (Fig. 6).

RESULTS OF U-PB ZIRCON GEOCHRONOLOGY

Results of U-Pb zircon geochronology are presented in Table S3 (see footnote 1). Sample locations are shown in Table 1. The fractionation correction and U-Pb results were calculated using the program GLITTER 4.0. Common Pb was corrected following the method described by Andersen (2002). Age calculations and concordia plots were made using Isoplot (Ludwig, 2003). Most analyses are concordant or nearly concordant and cluster as single age populations. We report $^{206}Pb/^{238}U$ ages for grains younger than 1000 Ma and $^{207}Pb/^{206}Pb$ ages for grains older than 1000 Ma (Ludwig, 2003).

Seventeen zircon grains from granite sample WC 09-14-14 (12) (Fig. 7K) yield U-Pb ages ranging from 427 to 464 Ma. The weighted mean U-Pb age of 12 concordant zircon grains is 432 ± 3 Ma (mean square weighed deviation [MSWD] = 0.31) (Fig. 8A), which we interpret as the crystallization age of the granitoid sample.

Twenty-seven zircon grains from granitoid sample WC 07-16-17 (1) (Fig. 7L) yield concordant ages ranging from 452 to 466 Ma. The weighted mean U-Pb age of 27 concordant zircon grains is 457 ± 2 Ma (MSWD = 0.48) (Fig. 8B), which we interpret as the crystallization age.

Nineteen zircon grains from sample WC 07-13-17 (1) (Fig. 7M) yield ages ranging from 249 Ma ($^{206}Pb/^{238}U$) to 1924 Ma ($^{207}Pb/^{206}Pb$). The largest population of concordant analyses cluster at ca. 450 Ma and have a weighted mean age of 446 ± 4 Ma (MSWD = 0.63; n = 6) (Fig. 8C), which we interpret as the crystallization age.

Eighteen zircon grains from sample WC 07-26-17 (6) (Fig. 7H) yield ages ranging from 237 Ma ($^{206}Pb/^{238}U$) to 1434 Ma ($^{207}Pb/^{206}Pb$). The largest population of concordant analyses cluster at ca. 480 Ma and have a weighted mean age of 477 ± 7 Ma (MSWD = 2.1; n = 7). The youngest population of concordant zircon grains (n = 4) yields a weighted mean age of 244 ± 8 Ma (MSWD = 3.8) (Fig. 8D). We interpret that the oldest grains are inherited, and the youngest population represents the crystallization age of the granitoid sample.

Nineteen zircon grains from granitoid sample WC 07-26-17 (1) (Fig. 7I) yield concordant ages ranging from 204 to 233 Ma. The weighted mean U-Pb age of 17 concordant zircon grains is 207 ± 1 Ma (MSWD = 0.79) (Fig. 8E), which we interpret as the crystallization age.

Seven zircon grains from foliated granitoid sample WC 07-25-17 (3) (Fig. 7K) yield concordant ages ranging from 374 to 420 Ma. The weighted mean U-Pb age of 6 concordant zircon grains is 407 ± 13 Ma (MSWD = 2.1) (Fig. 8F), which we interpret as the crystallization age.

Ninety-nine spots from our porphyritic gneiss sample WC 09-13-14 (8B) (Fig. 7A) yield concordant ages ranging from ca. 732 Ma ($^{206}Pb/^{238}U$) to ca. 1091 Ma ($^{207}Pb/^{206}Pb$) (Fig. 8G). One dominant age population with a peak at ca. 935 Ma accounts for ~90% of the analyzed grains (Fig. 8G).

Ninety-eight detrital zircon grains were analyzed from meta-sandstone sample WC 09-13-14 (7) (Fig. 7B), of which 5 grains yield discordant ages. Ninety-three concordant ages range from ca. 734 Ma ($^{206}Pb/^{238}U$) to ca. 1039 Ma ($^{207}Pb/^{206}Pb$). This sample has a dominant zircon population between 824 and 1039 Ma (~95%) with a peak at ca. 920 Ma (Fig. 8H).

Ninety-nine detrital zircon grains were analyzed from quartzite sample WC 09-13-14 (8A) (Fig. 7C), of which 3 grains yield discordant ages. Ninety-six concordant ages range from ca. 839 Ma ($^{206}Pb/^{238}U$) to ca. 1181 Ma ($^{207}Pb/^{206}Pb$). The weighted mean of the three youngest concordant zircon grains is 846 ± 12 Ma (MSWD = 0.98) (Fig. 8I). We interpret this weighted mean age to represent the maximum depositional age of the quartzite sample. The sample has a major zircon population between 839 and 1016 Ma (~97%) with a peak at ca. 960 Ma (Fig. 8I).

One hundred detrital zircon grains were analyzed from quartzite sample WC 09-13-14 (10) (Fig. 7D), of which 5 grain yield discordant ages. Concordant ages range from ca. 445 Ma ($^{206}Pb/^{238}U$) to ca. 2939 Ma ($^{207}Pb/^{206}Pb$). The weighted mean of the three youngest concordant zircon grains is 460 ± 26 Ma (MSWD = 2.5) (Fig. 8J). We interpret this weighted mean age to represent the maximum depositional age of the quartzite sample. The sample has a major zircon population between 799 and 1845 Ma (~86%) with three peaks at ca. 900 Ma, ca. 1500 Ma, and ca. 1715 Ma (Fig. 8J). We note one minor age population at ca. 476 Ma. The oldest two zircon grains have $^{207}Pb/^{206}Pb$ ages of 2859 ± 18 and 2939 ± 9 Ma (Fig. 8J).

One hundred detrital zircon grains were analyzed from weakly metamorphosed quartz sandstone sample WC 09-14-17 (8) (Fig. 7E), of which 7 grains yield discordant ages.

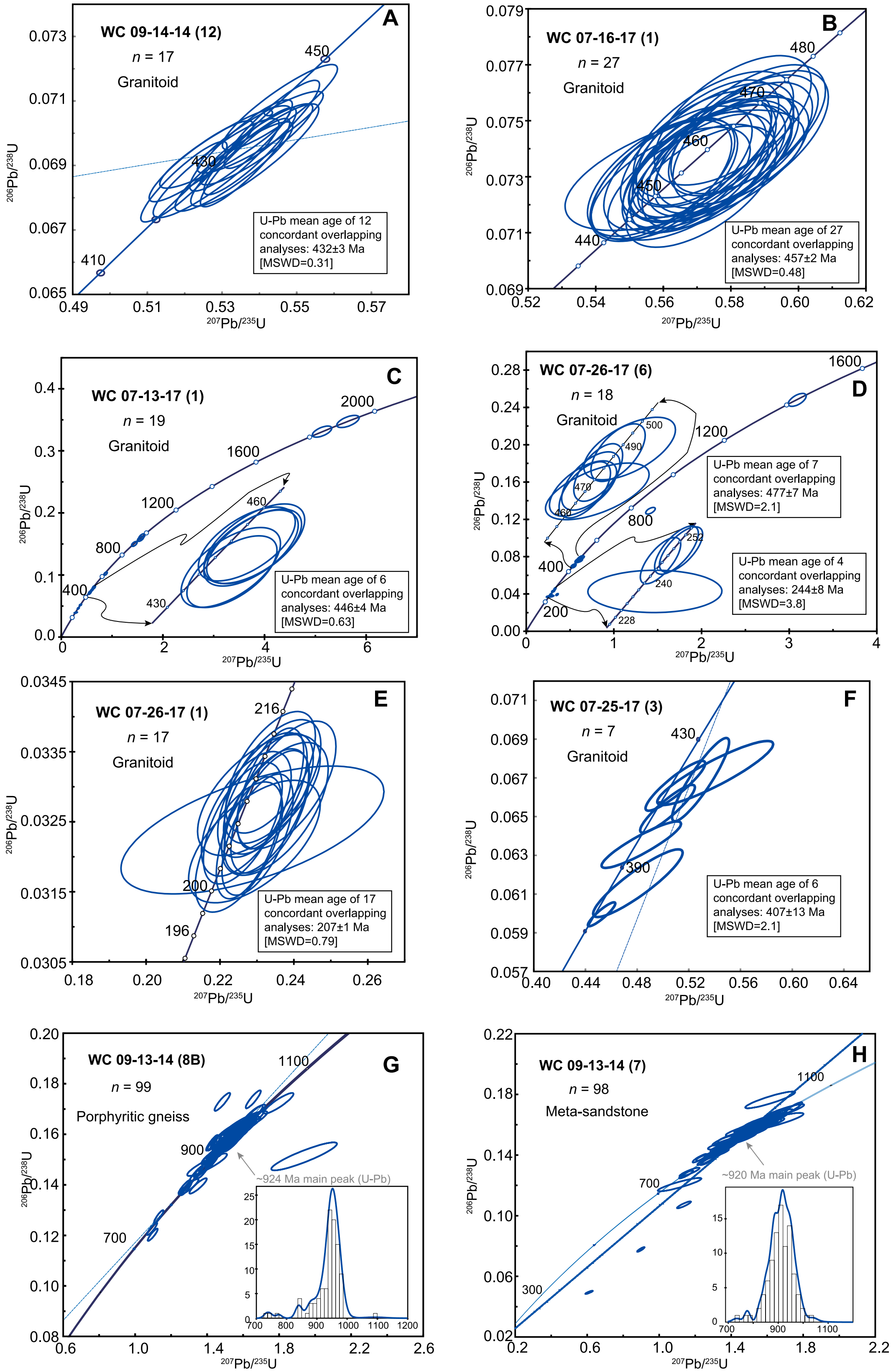

Figure 8. U-Pb concordia diagrams showing results of single-shot zircon analyses for each sample. (A) granitoid sample WC 09-14-14 (12); (B) granitoid sample WC 07-16-17 (1); (C) granitoid sample WC 07-13-17 (1); (D) granitoid sample WC 07-26-17 (6); (E) granitoid sample WC 07-26-17 (1); (F) granitoid sample WC 07-25-17 (3); (G) porphyritic gneiss sample WC 09-13-14 (8B); (H) meta-sandstone sample WC 09-13-14 (7); (I) quartzite sample WC 09-13-14 (8A); (J) sandstone sample WC 09-13-14 (10); (K) meta-sandstone sample WC 07-14-17 (8); (L) meta-sandstone sample WC 07-25-17 (4); (M) sandstone sample WC 07-26-17 (2); (N) sandstone sample WC 07-29-17 (5). Error ellipses are 2σ. MSWD—mean square weighed deviation.

Concordant ages range from 313 to 457 Ma. The weighted mean of the three youngest concordant zircon grains is 316 ± 8 Ma (MSWD = 2.9) (Fig. 8K). We interpret the weighted mean age to represent the maximum depositional age of the metasandstone sample. The sample has a major zircon population of 313–457 Ma (~100%) with two peaks at ca. 329 Ma and ca. 438 Ma (Fig. 8K).

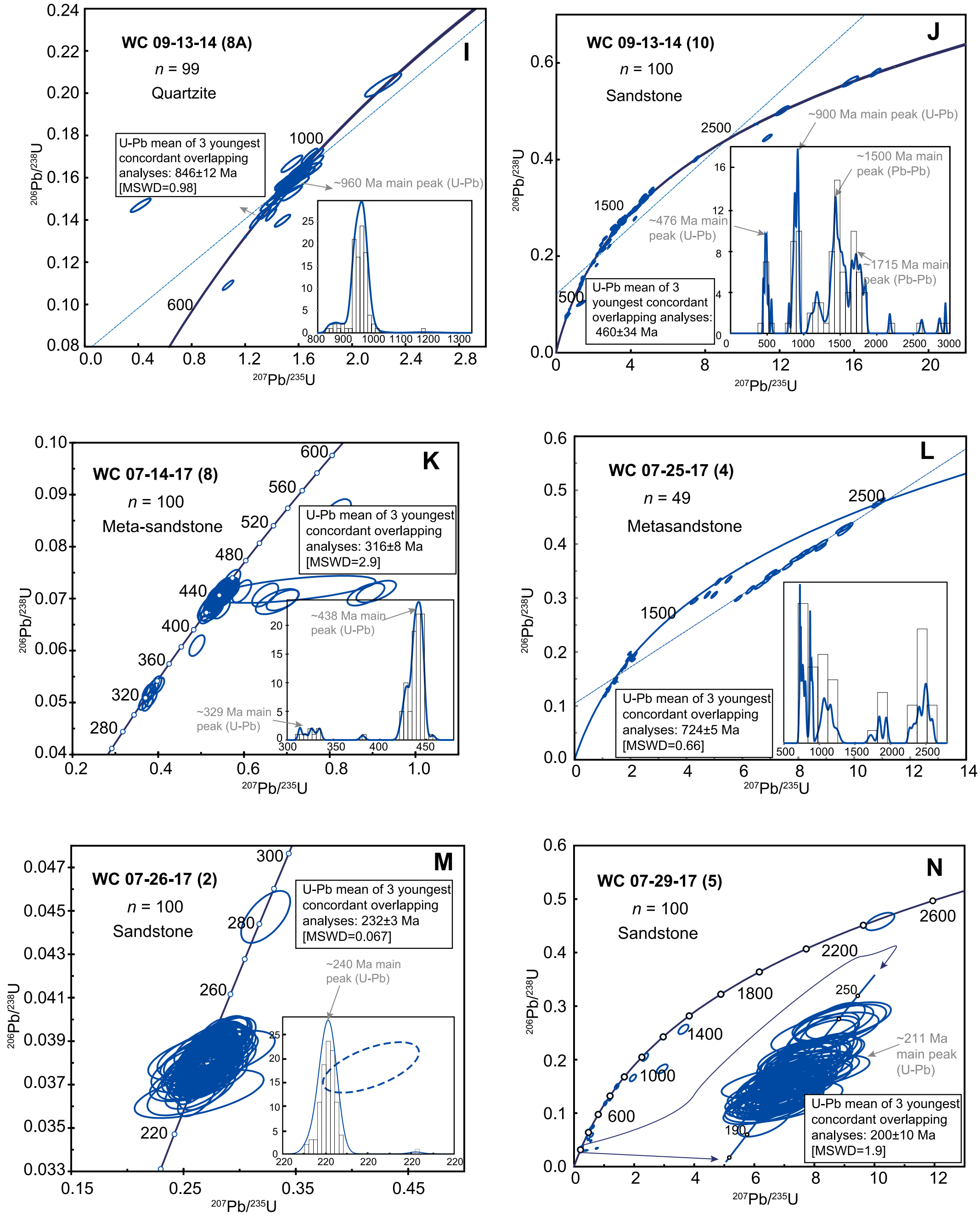

Figure 8. (*Continued*)

Forty-nine detrital zircon grains were analyzed from metasandstone sample WC 07-25-17 (4) (Fig. 7F), of which 26 grains yield discordant ages. Concordant ages range from ca. 717 Ma ($^{206}Pb/^{238}U$) to ca. 2595 Ma ($^{207}Pb/^{206}Pb$). The weighted mean of the three youngest concordant zircon grains is 724 ± 5 Ma (MSWD = 0.66) (Fig. 8L). We interpret the weighted mean age to represent the maximum depositional age of the metasandstone sample. The sample has two major zircon populations at 720–1100 Ma (~50%) and 2320–2595 Ma with two peaks at ca. 870 Ma and ca. 2500 Ma, respectively. We note one minor age population at ca. 1840 Ma (Fig. 8L).

One hundred detrital zircon grains were analyzed from sandstone sample WC 07-26-17 (2) (Fig. 7I), of which 1 grain yields a discordant age. Concordant ages range from 231 to 282 Ma. The weighted mean of the three youngest concordant zircon grains is 232 ± 3 Ma (MSWD = 0.067) (Fig. 8M). We interpret the weighted mean age to represent the maximum depositional age of the sandstone sample. The sample has a major zircon population at 231–247 Ma (~100%) with one peak at ca. 240 Ma (Fig. 8M).

One hundred detrital zircon grains were analyzed from sandstone sample WC 07-29-17 (5) (Fig. 7J), of which 7 grains yield discordant ages. Concordant ages range from ca. 196 Ma ($^{206}Pb/^{238}U$) to ca. 2469 Ma ($^{207}Pb/^{206}Pb$). The weighted mean of the three youngest concordant zircon grains is 200 ± 10 Ma (MSWD = 1.9) (Fig. 8N). We interpret the weighted mean age to represent the maximum depositional age of the sandstone sample. The sample has a major zircon population at 201–239 Ma (~90%) with one peak at ca. 211 Ma (Fig. 8N).

DISCUSSION

Our U-Pb geochronology results of six granitoid samples combined with existing ages in

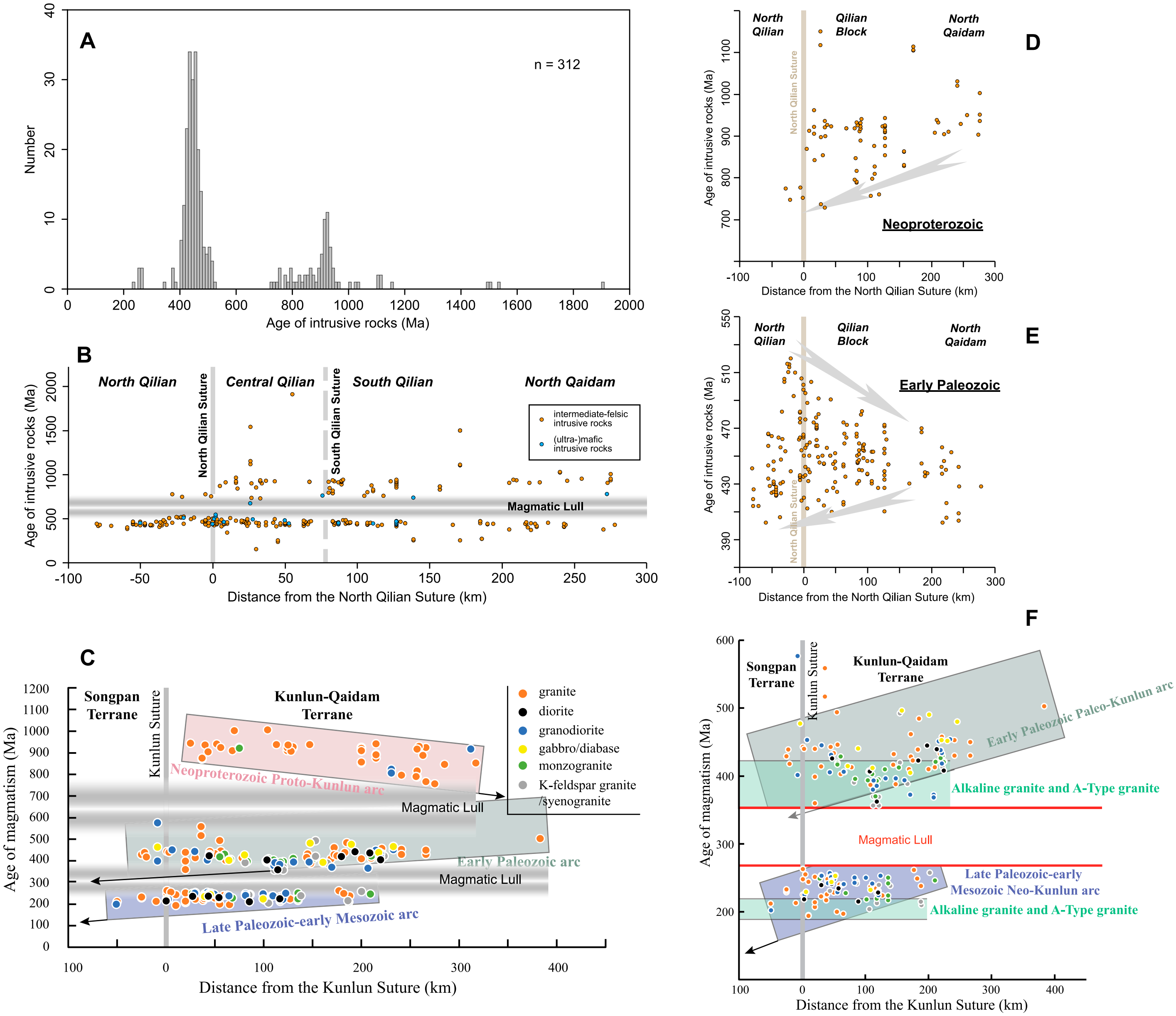

Figure 9. Crystallization ages and age versus distance plots of Neoproterozoic, Paleozoic, and Mesozoic plutons exposed in the Qilian Shan and Eastern Kunlun Range of northern Tibet.

northern Tibet show that Silurian–Late Ordovician granite bodies (432–457 Ma) intrude Lower Paleozoic strata in the eastern Qilian Shan and early Mesozoic (247–207 Ma) granites intrude Triassic sandstones and Neoproterozoic metamorphic rocks in the Eastern Kunlun Range. Combining these findings with new and existing detailed field observations allowed us to better understand the magmatic history of northern Tibet. In addition, detrital zircon U-Pb ages of Neoproterozoic metamorphic rocks and Phanerozoic sandstones provide key provenance information and age populations that can be compared between the Qilian Shan and Eastern Kunlun Range. Based on these findings, we better constrained the Proterozoic–Phanerozoic tectonic evolution of the Qilian Shan and Eastern Kunlun Range in northern Tibet.

Magmatic Records Across Northern Tibet

U-Pb zircon ages of intrusive rocks from the Qilian Shan mostly define with two age groups of 520–402 Ma and 961–728 Ma with peaks at ca. 445 Ma and ca. 920 Ma, respectively (Fig. 9A). Geochronologic results of granitoid samples from the Qilian Shan support the interpretation of a prominent magmatic lull in the region at 728–520 Ma (Fig. 9B). Permian-Triassic arc granitoids (235–269 Ma) and Late Devonian post-orogenic granitoids (392–372 Ma) occur in the South Qilian Shan and North Qaidam, respectively (e.g., Xie et al., 2014; Hu et al., 2016; Li et al., 2021; Jia et al., 2017; Wu et al., 2004b, 2007, 2009a; Zhou et al., 2021) (Fig. 9B). Mesoproterozoic granitic gneiss (ca. 1002–1537 Ma) occurs in the North Qaidam (Wang et al., 2021), whereas ca. 1116–1150 Ma granitic gneiss occurs in the North Qilian Shan (Dong et al., 2015) (Figs. 1 and 9B; Table S1). In addition, the youngest and oldest leucogranites in the region (ca. 341 Ma and ca. 1908 Ma, respectively) occur in the Central Qilian Shan (Wu et al., 2021). Gabbro with 550–529 Ma ages interpreted to represent fossil Qilian oceanic crust and/or supra-subduction ophiolite occurs in the North Qilian Shan (Shi et al., 2004; Song et al., 2013) (Fig. 9B). In contrast to the magmatic record of the Qilian Shan, zircon ages of granitoid samples in the Eastern Kunlun Range fall within three age groups at 944–904 Ma, 503–357 Ma, and 263–194 Ma (Wu et al., 2019a) (Figs. 4 and 9C).

The ca. 1.9 Ga and ca. 1.88 Ga leucogranites in the Qilian Shan and Longshou Shan to the north, respectively, are interpreted to correlate with the Paleoproterozoic northern North China orogen (Wu et al., 2018, 2021). The Qilian Shan, Qaidam, and Eastern Kunlun regions were intruded by 960–900 Ma arc plutons (i.e., the Proto-Kunlun arc in the Eastern Kunlun Range and the Proto-Qilian arc in the Qilian Shan), which suggests that the regions formed a contiguous continent by the start of the early Neoproterozoic. Early Neoproterozoic plutons have also been documented in the Altyn Tagh Range and Tarim to the west, and the Qinling to the southeast, suggesting the existence of a south-dipping Proterozoic subduction zone that roughly stretched from Tarim to Qinling (Guo et al., 2005; Wu et al., 2016a, 2021; Zuza et al., 2018) (Fig. 9D). The Proto-Kunlun arc is interpreted be associated with southward subduction of Proto-Kunlun oceanic lithosphere beneath the Qilian-Qaidam-Kunlun continent (Wu et al., 2016a, 2019a). Granitoids with 900–728 Ma ages along the northern margin of the Qilian-Kunlun-Qaidam continent have a northward younging trend, which is interpreted to reflect northward steepening of subducting Proto-Kunlun oceanic lithosphere (Fig. 9C).

The geochemical composition of ca. 820 Ma granitoids in the Qilian Shan suggest generation during continental breakup, which indicates that the rifting and ocean basin formation may have occurred earlier than this time (Wu et al., 2017). The occurrence of 797–728 Ma granitic intrusions in the Qilian Shan has been attributed to the rifting of the Qilian-Qaidam-Kunlun continent from the North China-Tarim craton and subsequent opening of the Qilian Ocean (Tseng et al., 2006; Song et al., 2013; Wu et al., 2016a, 2017, 2021; Zuza et al., 2018). Alternatively, ca. 675 Ma gabbro and ca. 600 Ma basalt interbedded with thick marble sequences may suggest that rifting from Tarim-North China and opening of the Qilian ocean(s) occurred later (Xu et al., 2015; Song et al., 2016; Tian et al., 2018). At least one ocean existed in the Qilian Shan between 550 and 449 Ma, as evidenced by widespread exposures of ophiolite fragments (e.g., Shi et al., 2004; Xia et al., 2003, 2016; Song et al., 2013; Tseng et al., 2007; Zhang et al., 2007; Xiao et al., 2009; Zuza et al., 2018; Fu et al., 2020, 2021). Widespread arc plutons in the Qilian Shan (i.e., Qilian arc) indicate that a major subduction system initiated by ca. 520 Ma and continued throughout the Ordovician, and younger accretion-related magmatism persisted until ca. 341 Ma. A major pulse of magmatism in the Qilian Shan at ca. 445 Ma and coeval metamorphism based on monazite ages are reported by Zuza et al. (2018). In addition, 454–442 Ma $^{39}Ar/^{40}Ar$ cooling ages (Liu et al., 2006b) and a ca. 442 Ma syncollisional granite in North Qaidam are documented by Zhang et al. (2017b), suggesting that collision between Kunlun-Qaidam and North China likely occurred at 445–440 Ma. A ca. 439 Ma leucogranite also contains Silurian–Devonian ages, which are consistent with intracontinental deformation during collision (Wu et al., 2021). Numerous syn-collisional 430–410 Ma magmatic intrusions occur throughout the Qilian Shan. We interpret that the southward younging trend of magmatic ages reflects southward subduction of Qilian oceanic lithosphere, whereas the northward younging trend of magmatic termination ages reflect northward steepening of subducting Qilian oceanic lithosphere (Fig. 9E).

The Cambrian–Devonian arc magmatic event observed in the Eastern Kunlun Range (i.e., Paleo-Kunlun arc) is interpreted to be related to subduction of Paleo-Kunlun oceanic lithosphere (Wu et al., 2016a, 2019a). Late Cambrian (ca. 494 Ma) granite with high Sr and Y contents reflects deep subduction of Paleo-Kunlun oceanic lithosphere, and arc-related plutons in the Eastern Kunlun Range indicate that subduction initiated by ca. 500 Ma and continued throughout the Early Devonian (ca. 399 Ma) (Wu et al., 2019a). Late Devonian (ca. 360 Ma) metaluminous granite provides an upper age bound on final consumption of Paleo-Kunlun oceanic lithosphere and subsequent continental collision of the Kunlun-Qaidam continent and Songpan-Ganzi continent of South China (Wu et al., 2019a). We interpret the southward younging trend of magmatic termination ages to reflect southward steepening of subducting Paleo-Kunlun oceanic lithosphere (Fig. 9F). Permo-Triassic granitoids (270–194 Ma, i.e., the Neo-Kunlun arc) are widespread in the Kunlun-Qaidam continent across the South Qilian Shan in the north and the Eastern Kunlun Range in the south, and are interpreted to be associated with subduction of Neo-Kunlun oceanic lithosphere. The geochemical composition of 263–229 Ma granites suggests that they are associated with subduction-related arc magmatism (e.g., Li et al., 2015d; Wu et al., 2016a, 2019a; Chen et al., 2017; this study), whereas ca. 209 Ma rhyolites (Shao et al., 2021) and 214–200 Ma A-type granitoids suggest generation in an extension setting during that time (Wu et al., 2019a). We interpret the southward younging trend of magmatic termination ages to reflect southward steepening of subducting Neo-Kunlun oceanic lithosphere (Fig. 9F).

Tectonic Evolution of Northern Tibet

Basement rocks of the Qilian-Qaidam-Kunlun continent consist of Mesoproterozoic passive margin strata in the west and Archean–Proterozoic metamorphic rocks in the east. The Archean–Paleoproterozoic Quanji Massif in the Qilian-Qaidam-Kunlun continent is composed of basement rocks (e.g., Lu, 2002; Wan et al., 2006; Wang et al., 2008; Gong et al., 2012; Yu et al., 2017b) that experienced amphibolite facies metamorphism at 1.95–1.93 Ga (Hao et al., 2004; Wang et al., 2008) and were subsequently intruded by ca. 1.83 Ga mafic dikes and ca. 1.8 Ga Rapakivi granite (Lu et al., 2006; Chen et al., 2012a; Liao et al., 2014a). The Archean–Paleoproterozoic Quanji Massif is unconformably overlain by the Neoproterozoic Quanji Group in North Qaidam. Detrital zircon ages of Mesoproterozoic metasedimentary rocks in northern Tibet contain a youngest zircon population of 1.15–1.25 Ga in addition to 1.4–1.5 Ga ages and Paleoproterozoic–Archean zircons that are remarkably similar to those of the Tarim-North China craton (e.g., Gehrels et al., 2003a; Wu et al., 2017, 2021; Liu et al., 2018a; Tung et al., 2007; Yu et al., 2017b; Zuza et al., 2018) (Fig. 10). Based on similar lithologies and ages of Paleo- and Mesoproterozoic basement rocks located north and south of the Paleo-Qilian suture, we interpret that opening of the Paleo-Qilian Ocean between the North China-Tarim craton and Qilian-Qaidam-Kunlun continent likely occurred within a Greater North China craton (Fig. 11) (e.g., Zuza and Yin, 2013; i.e., part of the larger Balkatach continent of Zuza and Yin, 2017).

Paleo- and Mesoproterozoic structures are overlain by a series of Neoproterozoic rift and passive margin sequences. The Neoproterozoic tectonic events in northern Tibet are debated, however, 1.0–0.8 Ga plutons and detrital zircon ages of Neoproterozoic strata of the Qilian-Qaidam-Kunlun continent may correlate with those of Tarim-North China (Gehrels et al., 2003a, 2011; Chen et al., 2006a, 2006b; Peng, 2010; Wang et al., 2012; Liu et al., 2012b; Dan et al., 2014; Yu et al., 2017b) or the South China craton (e.g., Tung et al., 2013). Neoproterozoic passive margin strata of the central Qilian Shan have a detrital zircon U-Pb age population at 732–1000 Ma with a prominent peak at ca. 950 Ma and youngest weighted mean age of 738 ± 12 Ma (MSWD = 0.64, n = 3),

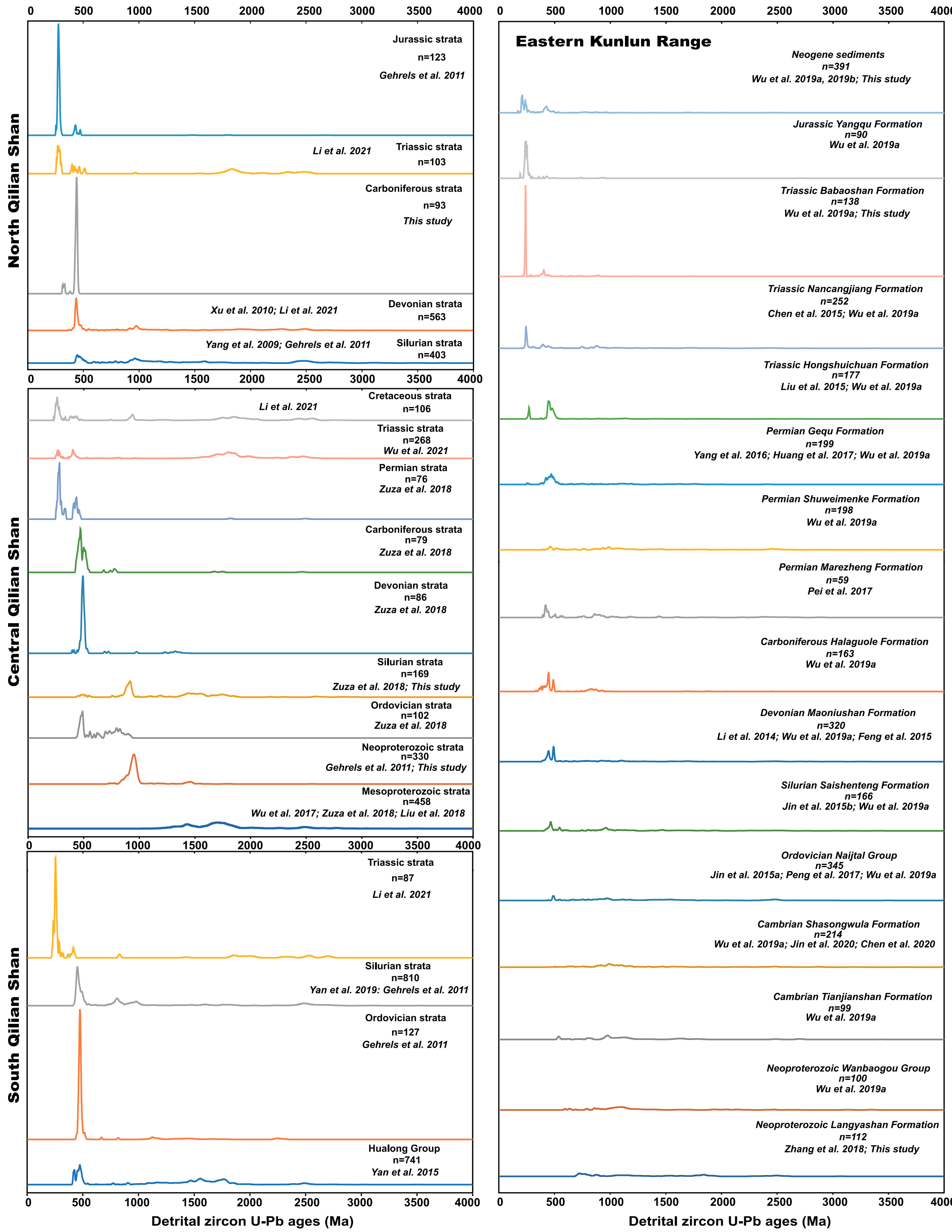

Figure 10. Mesoproterozoic–Cenozoic relative probability plots of detrital zircon ages of samples from the Qilian Shan and Eastern Kunlun Range of northern Tibet. Data are from Gehrels et al. (2011); Li et al. (2021); Xu et al. (2010); Yang et al. (2009); Zuza et al. (2018); Wu et al. (2021); Wu et al. (2017, 2019a, 2019b, 2021); Liu et al. (2018a); Yan et al. (2015, 2019); Zhang et al. (2018c); Li et al. (2014); Jin et al. (2015a, 2015b, 2020); Peng et al. (2017); Pei et al. (2017); Huang et al. (2017b); Yang et al. (2016); Liu et al. (2015); Chen (2015).

in addition to ages of 1.4–1.5 Ga, ca. 1.8 Ga, and 2.5 Ga (Gehrels et al., 2011; this study) (Fig. 10). The Neoproterozoic Langyashan Formation in the Eastern Kunlun Range has detrital zircon U-Pb age populations of 700–940 Ma with a youngest weighted mean age of 705 ± 10 Ma (MSWD = 0.66, n = 3), in addition to ages of ca. 1.05–1.25 Ga, 1.72–1.95 Ga with a peak of 1.84 Ga, and 2.35–2.60 Ga with a peak of 2.5 Ga (Zhang et al., 2018c; this study) (Fig. 10). The Neoproterozoic Hualong Group/Complex in the South Qilian Shan contains an age population at 940–780 Ma with a peak at ca. 906 Ma and youngest weighted mean age of 721 ± 3 Ma, in addition to ages of 1.47–1.78 Ga and 2.35–2.60 Ga with a peak at ca. 2.5 Ga (Yan et al., 2015). The Neoproterozoic Hualong Group/Complex also contains two early Paleozoic metamorphic ages of ca. 425 Ma and ca. 475 Ma (Yan et al., 2015) (Fig. 10). The lithologies and ages of Neoproterozoic metamorphic rocks located between the South Qilian Shan and Eastern Kunlun Range along the margins of the Kunlun-Qaidam continent are comparable, but distinct from those of the central Qilian Shan and late Neoproterozoic metamorphic rocks located along the southwestern margin of the North China craton. The common older ca. 2.5 Ga age peak represents typical North China basement (i.e., Wu et al., 2021). We suggest that two embayed seas existed within the North China craton, central Qilian Shan, and Kunlun-Qaidam continent, which are referred to as the North Qilian and South Qilian oceans, respectively (Fig. 11). Opening of the North and South Qilian oceans may have commenced by 740–730 Ma

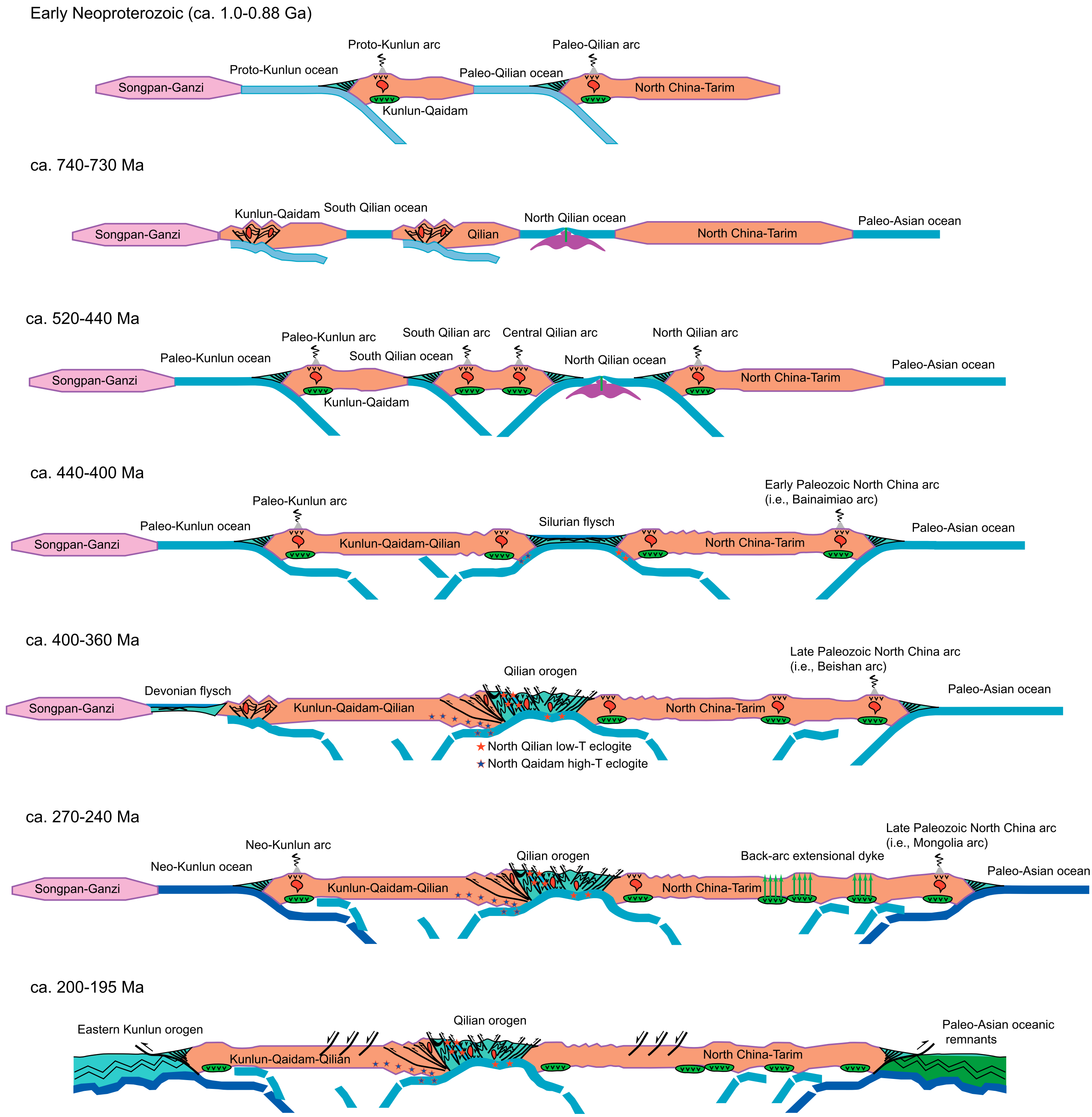

Figure 11. Neoproterozoic–Early Jurassic tectonic evolution of the Qilian-Qaidam-Kunlun continent of northern Tibet. T—temperature.

based on the exposure of ca. 738 Ma basalt and ca. 728 Ma arc granitoids (Wu et al., 2016a, 2021) (Fig. 11). Wu et al. (2016a) suggest that the trace of the South Qilian Ocean traces the tectonic contact between the North China craton and the Paleo-Qilian arc (Fig. 11). Magmatism across the Qilian Shan and southern margin of the North China craton, in addition to evidence from a magnetotelluric sounding profile across the northern Tibetan Plateau, support a model of bidirectional subduction of North Qilian oceanic lithosphere (e.g., Li et al., 2021) (Fig. 11).

Opening of the Paleo-Kunlun Ocean between the Kunlun-Qaidam continent and South China craton along the trace of the Proto-Kunlun arc is inferred to have initiated after ca. 608 Ma based on the youngest maximum deposition age of the Wanbaogou Group passive margin strata located along the southern margin of the Eastern Kunlun Range (Wu et al., 2019a). Thus, opening of the Paleo-Kunlun Ocean occurred later than the

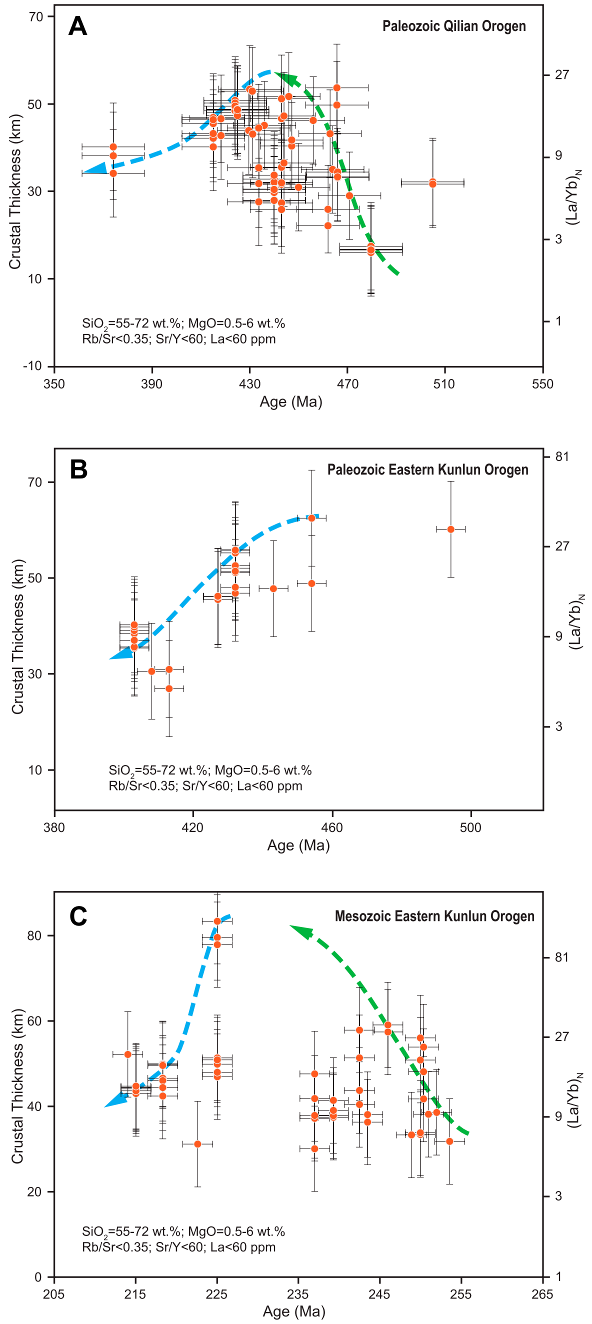

Figure 12. Plots of age versus crustal thickness of the Qilian Shan and Eastern Kunlun Range of northern Tibet using the La/Yb(n) calibration of Sundell et al. (2021). Geochemical data are listed in Tables S4 and S5 (see footnote 1).

openings of the North and South Qilian oceans. In addition, the onset of Paleo-Kunlun subduction along the southern margin of the Kunlun-Qaidam continent must have occurred prior to ca. 502 Ma (Fig. 11). The Cambrian–Ordovician arc sequence was deposited across the Qilian Shan and subsequently overlain by Silurian strata. A plot of paleo-crustal thickness versus crystallization age for the Qilian Shan granitoids shows a thickening trend from the Ordovician to Silurian (trace element calibration of Sundell et al., 2021) (Fig. 12A), which is supported by the presence of Phanerozoic unconformities. The North, Central, South Qilian Shan, and Eastern Kunlun Range share four major detrital zircon age populations at 448–550 Ma, 803–960 Ma, 1465–1750 Ma, and 2478–2590 Ma (Fig. 10). Given these similarities, we suggest that closure of the North Qilian and South Qilian oceans occurred during the Early Silurian (Fig. 11). In addition, paleo-crustal thickness constraints of the Qilian Shan shows an overall thinning trend from the Early Silurian to the Devonian–Early Carboniferous (trace element calibration of Sundell et al., 2021) (Fig. 12A). A-type Silurian granitoids emplaced during extension were coeval with Devonian intra-arc basin sedimentation in the Eastern Kunlun Range (Wu et al., 2016a). Exhumation of eclogite-bearing, high-grade metamorphic rocks and the emplacement of mafic and ultramafic bodies (Meng et al., 2013a and 2013b; Dong et al., 2018) in the Eastern Kunlun Range may have been associated with forearc thrusting (Wu et al., 2019a). This interpretation is supported by the overall thinning trend of the paleo-crustal thickness for the Ordovician to Early Devonian (trace element calibration of Sundell et al., 2021) (Fig. 12B). Devonian strata exposed across the Qilian-Qaidam-Kunlun continent were deposited in intermontane and/or foreland basins during the Qilian and Eastern Kunlun orogenies (Fig. 11). Devonian strata unconformably overlie deformed Proterozoic–early Paleozoic rocks and are disconformably overlain by younger strata. To the north, the early Paleozoic Bainaimiao arc were developed along the northern margin of the North China craton due to the southward subduction of the Paleo-Asian oceanic crust (Wu et al., 2016b) (Fig. 11).

Carboniferous strata in the North Qilian Shan have two major detrital zircon age peaks at ca. 329 Ma and ca. 438 Ma (Fig. 10). The ca. 329 Ma peak correlates with the crystallization ages of plutonic rocks in the North China craton to the north, whereas the ca. 438 Ma peak may reflect a source from the Qilian arc, Paleo-Kunlun arc, and North China craton. The magmatic lull across northern Tibet from 360 to 270 Ma was accompanied by passive continental margin sedimentation (i.e., Carboniferous Halaguole Formation and Lower Permian Marezheng Formation) in the Eastern Kunlun Range (Fig. 13) as the Songpan-Ganzi continent rifted away from the Qilian-Kunlun-Qaidam continent (Fig. 11). The Devonian Beishan arc and Permian Mongolia arc, placed at the southwestern and northern margin of the North China craton, respectively, are associated with the sustained subduction of the Paleo-Asian oceanic crust (Fig. 11). Early Permian mafic dike swarms are widespread between the southern portion of the Paleo-Asian tectonic domain and north of Qilian Shan (i.e., Zhang et al., 2017c).

Detrital zircon ages from Wu et al. (2019a) and the observation of ca. 244 Ma and ca. 207 Ma granitic dikes intruding Lower and Upper Triassic strata in the Eastern Kunlun Range (Figs. 7G–7I) place bounds on deposition of the Lower Triassic Hongshuichuan Formation and Upper Triassic Babaoshan Formation at 250–244 Ma and 220–207 Ma, respectively (Fig. 13). As discussed above, slab rollback probably occurred from ca. 225 Ma in the South Qilian Shan to ca. 194 Ma in the Eastern Kunlun Range (Fig. 11), as indicated by the Late Permian and Early Jurassic younging trend of

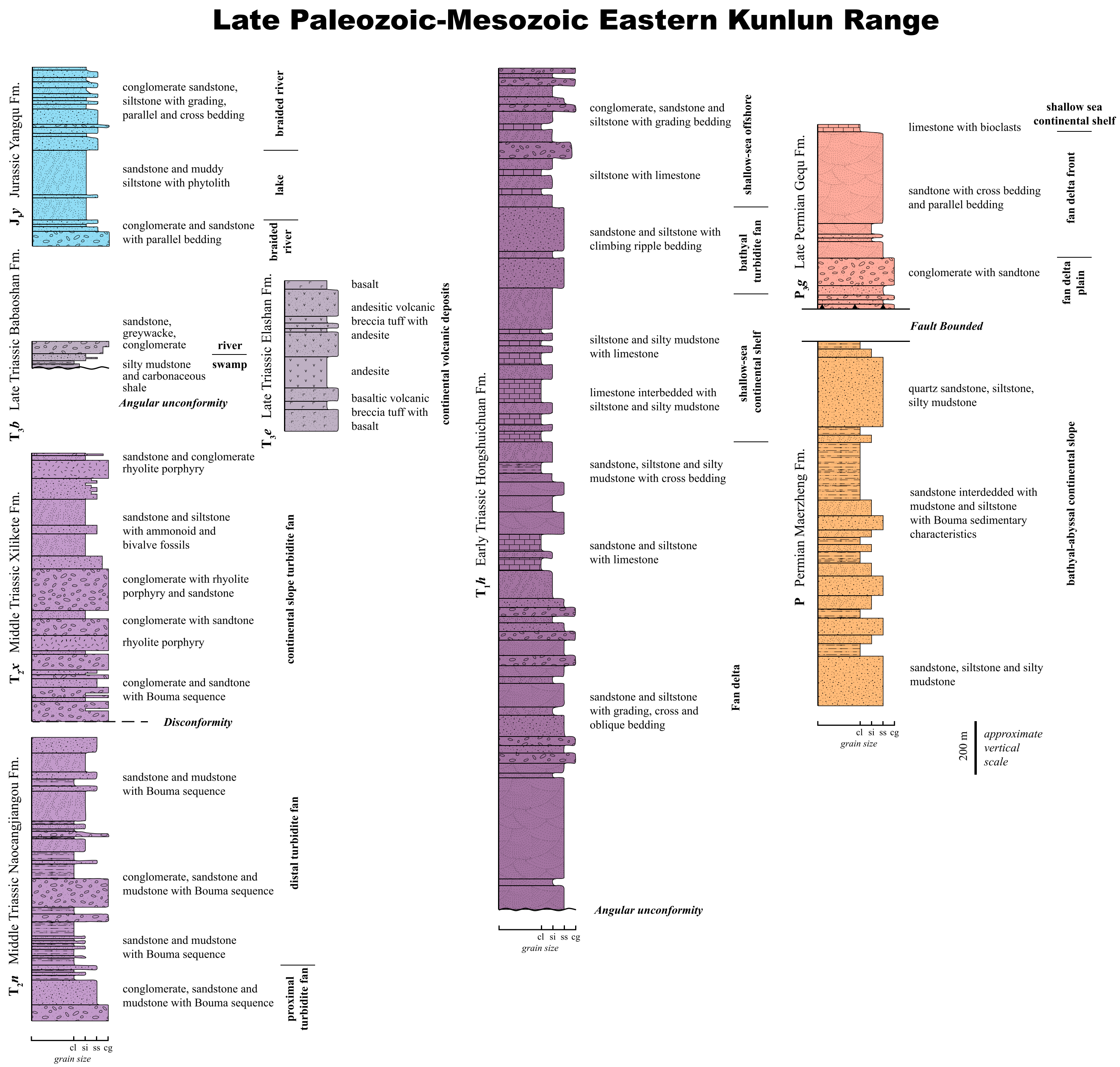

Figure 13. Permian–Jurassic lithostratigraphy of the Eastern Kunlun Range of northern Tibet. Fm.—Formation; cl—clay; si—silt; ss—sand; cg—conglomerate.

magmatism (Fig. 9F) and paleo-crustal thickness trends in the Eastern Kunlun Range (calibration of Sundell et al., 2021) (Fig. 12C). Jurassic extension resulted in exhumation of older strata, and the regional extension continued during the Cretaceous in northern Tibet (Fig. 13). Cenozoic strata show two major detrital zircon age peaks at ca. 212 Ma and ca. 427 Ma, and three minor age peaks at 820–960 Ma, ca. 1700 Ma, and ca. 2450 Ma (Fig. 10), reflecting provenance from the local Eastern Kunlun Range, although we acknowledge that recycling of older strata may have resulted in this age distribution (Wu et al., 2019a, 2019b).

This protracted Proterozoic–Paleozoic orogenic history established a framework of preexisting weak zones to be reactivated during the Cenozoic collision of India and Asia. (Yin et al., 2007; Zuza et al., 2019, 2020) (Fig. 11). The Qilian Shan is the northern limit of Cenozoic contractional deformation in the Himalayan-Tibetan orogen (Clark, 2012; Zuza et al., 2020), which deformed shortly after initial India-Asia collision (e.g., Yin et al., 2008a, 2008b; Li et al., 2020). We interpret that the spatial correlation between early strain and this complex pre-Cenozoic history of Paleozoic orogeny and suturing implies

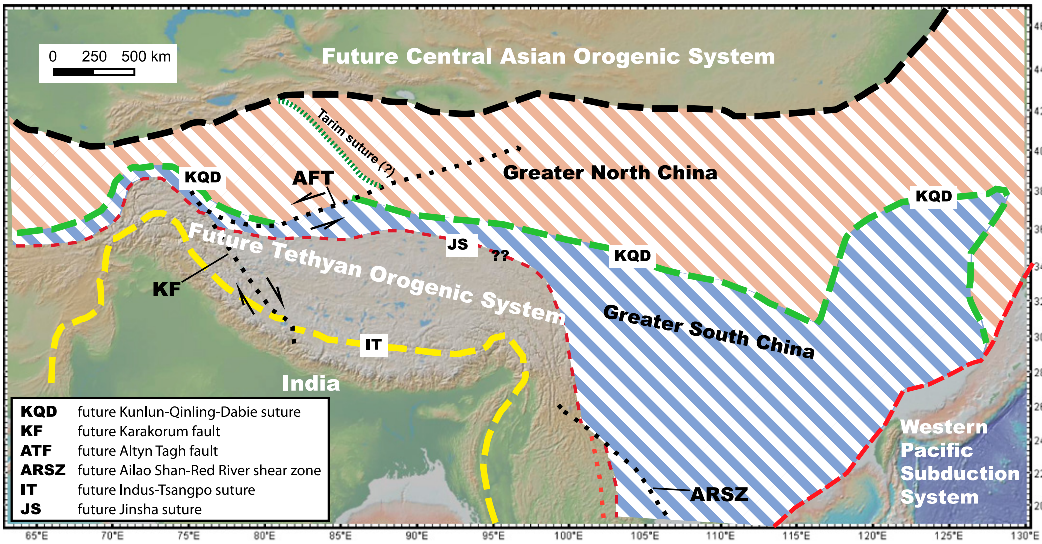

Figure 14. Simplified tectonic domain map showing the boundary between the Greater North China and South China continents of northern Tibet.

that the preexisting framework acted as significant lithospheric weakness (e.g., Heron et al., 2016). Although early Paleozoic Qilian ocean(s) subduction may have been bi-directional, significant collision-related continental subduction occurred to the south, as evidenced by the spatial location of UHP rocks exposed in the North Qaidam thrust belt (Yin et al., 2007; Zhang et al., 2008a, 2008b) (Fig. 11). Thus, the North China continent was underthrust south toward Moho depths, which may have established a south-dipping Moho-depth crustal ramp in the Paleozoic to be reactivated in the Cenozoic (e.g., Yin et al., 2007; Zuza et al., 2019; Chen et al., 2020b). It is likely that the Paleozoic–Mesozoic history of the Qilian Shan generated important crustal weaknesses in the northern Tibet crust and lithosphere that were exploited during Cenozoic crustal shortening, including multiple crustal subhorizontal detachments that may accommodate more shortening than observed at the Earth's surface. It remains unclear why the Paleo-Asian Ocean suture zones to the north (Fig. 1) were not so readily reactivated in the Cenozoic (Fig. 11). One hypothesis is that the volume of mafic island arcs and underplated mafic rocks (e.g., Windley et al., 2007) strengthened this crust (Liu and Furlong, 1994) to resist such strain. Alternatively, the Paleo-Asian oceanic domain was far enough from plate-boundary forces that stresses were not great enough to overcome the competition with gravitational potential energy, thus driving predominately strike-slip faulting (Cunningham et al., 1996; Webb and Johnson, 2006).

Neoproterozoic Paleogeography of Northern Tibet

Results of geologic mapping and geochronology indicate that Precambrian basement rocks of the Tarim Basin exposed in the Altyn Tagh Range are correlative with the North China basement rocks and Proterozoic cover sequences in the Qilian Shan and its foreland region (e.g., Gehrels et al., 2003a, 2003b; Cowgill et al., 2003; Guo et al., 2005; Wu et al., 2021). This correlation strengthens the interpretation that the Tarim and North China cratons were parts of a contiguous Precambrian craton (e.g., Heubeck, 2001; Kusky et al., 2007; Zuza and Yin, 2013, 2017). As discussed above, reconstruction of Cenozoic slip along the Altyn Tagh fault and removal of deformation related to early Paleozoic orogenic events in the Qilian Shan (e.g., Xiao et al., 2009; Song et al., 2012; Zuza et al., 2018; Wu et al., 2020) suggest that the combined Kunlun-Qaidam-Qilian continent was connected with the North China-Tarim craton in the Neoproterozoic. Full-scale plate reconstructions demonstrate that Tarim and North China have remained next to each other throughout the Phanerozoic (e.g., Domeier and Torsvik 2014). In addition, restoration of Cenozoic deformation in the westernmost Tian Shan (Avouac et al., 1993), Pamir (Burtman and Molnar, 1993), and western Kunlun Range (Cowgill et al., 2003) suggests that the Tarim craton extends farther westward to the Karakum block (e.g., Biske and Seltmann, 2010) (Fig. 14). A possible suture zone crossing the Tarim Basin separated North and South Tarim and joined in the Neoproterozoic (e.g., Guo et al., 2005; Zuza and Yin, 2017; Yang et al., 2018; Zhao et al., 2021) (Fig. 14), and therefore it is possible that Greater North China was fully assembled at this time. The shape of the northern margin of the North China-Tarim craton during the Neoproterozoic has been further modified by subsequent rifting during the Neoproterozoic–Cambrian. Neoproterozoic rift-related strata and bimodal volcanism are widespread in northern Tarim, North China, and the microcontinents of the Central Asian Orogenic System (e.g., Meert et al., 2011; Shu et al., 2011, Levashova et al., 2011).

The stratigraphy of the Songpan-Ganzi continent is well defined (Weislogel, 2008), however, its tectonic evolution is poorly understood (Burchfiel and Chen, 2012). Existing end-member models regarding the tectonic origin of the Songpan-Ganzi continent include: (1) an accretionary complex (Şengör et al., 1988); (2) remnant ocean basin (Yin and Nie, 1996); and (3) relic of backarc basin (Pullen et al., 2008). The Songpan-Ganzi continent is a narrow strip that extends from east to west through the Bayan Har, Hoh Xil, Tianshuihai, and Karakul-Mazar regions (Fig. 14). Geologic observations and geochronologic results suggest that the Songpan-Ganzi continent has been the western extension of the Yangtze craton of South China since the early Neoproterozoic and experienced extensional deformation in the Triassic (Wu et al., 2016a). Triassic flysch strata and underlying basement rocks are only exposed in its easternmost portion, whereas crystalline basement of the westernmost South China craton beneath a passive-margin sequence contains 825–750 Ma felsic arc rocks. Triassic granite of the eastern Songpan-Ganzi continent have a 0.9–1.1 Ga Nd model age, which is similar to those of the western South China craton (Roger et al., 2004) and the basement rocks of the South China craton that occur in Triassic gneiss domes of the eastern Songpan-Ganzi continent (Roger et al., 2010). Triassic granite in the central Songpan-Ganzi continent was sourced from 1.1 to 1.6 Ga basement based on the Nd model age, indicating correlation with the South China craton and Kunlun-Qaidam basement (Zhang et al., 2014b). High-grade gneiss with Triassic protolith ages occurs in the western Songpan-Ganzi continent (Robinson, 2015). A ca. 2.5 Ga meta-volcanic rock is reported in the basement (Ji et al., 2011), which is similar to the ca. 2.5 Ga Kangding orthogneiss in the western South China craton (Wang et al., 2013c) and correlatives to the North China craton. Due to a lack of studies on the basement of Qiangtang terrane, the southern extent of the Greater South China continent is not well constrained (Fig. 14).

In summary, we emphasize that plate reconstructions of central Asia should consider larger continents instead of smaller fragments. The relatively small continental fragments may be illusionary due to distributed deformation during collisions and subsequent reactivation by later phases of accretionary or collisional orogeny. Two Greater North China and South China continents, located along the southern margin of Laurasia, were separated in the early Neoproterozoic along the future Kunlun-Qinling-Dabie suture (i.e., Proto-Kunlun suture; Wu et al., 2019a) (Fig. 14). Subsequent Neoproterozoic rifting opened the Paleo-Asian and Tethyan oceans along the northern margins of Greater North China craton and Greater South China craton, respectively. Greater North China likely contributed the micro-continental fragments that were the eventual building blocks for the Paleozoic Central Asian Orogenic System, and this rifting also explains the heredity of some of the Central Asian microcontinents. Paleozoic–early Mesozoic arc-continent collisions across central Asia and later Cenozoic intra-continental deformation induced by the India-Asia collision significantly modified the original shape of the Greater North China and South China continents.

The existence of these *greater* continents is especially important for global plate reconstructions of Neoproterozoic Earth. For example, recent paleomagnetic data have individually placed Tarim and North China against western Laurentia (Wen et al., 2017, 2018; Ding et al., 2021). These distinct interpretations so far support the model of Zuza and Yin (2013, 2017) that the strip of Greater North China (Balkatach of Zuza and Yin, 2017) may have been affixed against western Laurentia in the Rodinian supercontinent. The rifting of Greater North China from Laurentia would have thus opened the twin Paleo-Pacific and Paleo-Asian oceans. Future geologic and paleomagnetic research should test this hypothesis while considering continuity between the Tarim and North China continents.

CONCLUSIONS

In this study, we present new constraints on the Proterozoic–Phanerozoic tectonic evolution of the Qilian Shan, Qaidam, and Eastern Kunlun Range of northern Tibet based on a synthesis of field observations and new U-Pb zircon geochronology. Our work shows that early Neoproterozoic subduction and subsequent collision occurred between the Tarim-North China, Qilian-Qaidam-Kunlun, and South China continents. Arc plutons generated along two subduction systems are exposed throughout the Qilian Shan and Eastern Kunlun Range. We suggest that Neoproterozoic rifting resulted in opening of the North Qilian, South Qilian, and Paleo-Kunlun marginal oceans, and separation of South Qilian and Paleo-Kunlun oceans occurred along the trace of an early Neoproterozoic suture zone. Opening of the Paleo-Kunlun Ocean at ca. 600 Ma occurred later compared to the openings of the North and South Qilian oceans at 740–730 Ma. The closure of the North Qilian and South Qilian oceans occurred during the Early Silurian (ca. 440 Ma), whereas final consumption of the Paleo-Kunlun Ocean may have lasted until the Devonian (ca. 360 Ma). The ca. 244 Ma granitic dike intruding the Lower Triassic Hongshuichuan Formation suggests that the unit was deposited between 250 and 244 Ma. Similarly, the ca. 207 Ma granitic dike intruding the Upper Triassic Babaoshan Formation suggests that the unit was deposited between 220 and 207 Ma. Northward subduction of Neo-Kunlun oceanic lithosphere initiated at ca. 270 Ma, followed by slab rollback at ca. 225 Ma recorded in the South Qilian Shan, and ca. 194 Ma recorded slab rollback in the Eastern Kunlun Range. Magmatic and paleo-crustal thickness histories across the Qilian-Qaidam-Kunlun continent supports the interpreted tectonic evolution of the region. In addition, after removing the effects of Phanerozoic deformation, we interpret that two Greater North China and South China continents, located south of Laurasia, were separated in the early Neoproterozoic along the future Kunlun-Qinling-Dabie suture.

ACKNOWLEDGMENTS

Discussions with supervisor Professor An Yin inspired and improved the ideas presented herein. This work would not be possible without his dedication, friendship, and guidance. We appreciate Editor Brad Singer, Associate Editor Tim Kusky, and two reviewers for their critical, careful, and very constructive reviews that have helped improve the clarity and interpretations of the original draft. This research was supported by grants from the Basic Science Center for Tibetan Plateau Earth System (grant no. 41988101-01), the Second Tibetan Plateau Scientific Expedition and Research Program (grant no. 2019QZKK0708), and the National Science Foundation (Division of Earth Sciences grant no. 1914501). This work was also supported by the China University of Geosciences (Beijing) and a grant from the SINO-Probe Program administered by the Chinese Academy of Geological Sciences (SinoProbe-08-01).

REFERENCES CITED

An, Y.L., 2015, Geochemistry, geochronology of the Dandeer intrusive rocks in the middle section of the Central Qilian Mountain and their tectonic significance [M.A. thesis] [in Chinese with English abstract]: Beijing, China, China University of Geosciences, 57 p.

Andersen, T., 2002, Correction of common lead in U-Pb analyses that do not report ^{204}Pb: Chemical Geology, v. 192, p. 59–79, https://doi.org/10.1016/S0009-2541(02)00195-X.

Ao, C., Sun, F.Y., Li, B.L., Wang, G., Li, L., Li, S.J., and Zhao, J.W., 2015, U-Pb dating, geochemistry and tectonic implications of Xiaojianshan gabbro in Qimantage Mountain, Eastern Kunlun Orogenic Belt [in Chinese with English abstract]: Geotectonica et Metallogenia, v. 39, no. 6, p. 1176–1184.

Avouac, J.P., Tapponnier, P., Bai, M., You, H., and Wang, G., 1993, Active thrusting and folding along the northern Tien Shan and late Cenozoic rotation of the Tarim relative to Dzungaria and Kazakhstan: Journal of Geophysical Research. Solid Earth, v. 98, p. 6755–6804, https://doi.org/10.1029/92JB01963.

Bian, Q.T., Luo, X.Q., Li, D.H., Zhao, D.S., Chen, H.H., Xu, G.Z., Chang, C.F., and Gao, Y.L., 2000, Discovery of Caledonian island-arc granodiorite-tonalite in Buqingshan, Qinghai Province: Progress in Natural Science, v. 10, no. 1, p. 74–78.

Bian, Q.T., Li, D.H., Pospelov, I., Yin, L.M., Li, H.S., Zhao, D.S., Chang, C.F., Luo, X.Q., Gao, S.L., Astrakhantsev, O., and Chamov, N., 2004, Age, geochemistry and tectonic setting of Buqingshan ophiolites, North Qinghai-Tibet Plateau, China: Journal of Asian Earth Sciences, v. 23, no. 4, p. 577–596, https://doi.org/10.1016/j.jseaes.2003.09.003.

Biske, Y.S., and Seltmann, R., 2010, Paleozoic Tian-Shan as a transitional region between the Rheic and Urals-Turkestan oceans: Gondwana Research, v. 17, p. 602–613, https://doi.org/10.1016/j.gr.2009.11.014.

Bu, T., Wang, G.Q., Tang, Z., Luo, G.G., Zhu, T., Ji, B., and Guo, L., 2019, Petrogenesis of the Middle Ordovician granite in the Yaodonggou area of the North Qilian orogenic belt: Constraints from zircon U-Pb geochronology and geochemistry [in Chinese with English abstract]: Acta Petrologica et Mineralogica, v. 38, no. 2, p. 145–159.

Burchfiel, B.C., and Chen, Z.L., 2012, Tectonics of the Southeastern Tibetan Plateau and Its Adjacent Foreland: Geological Society of America Memoirs, v. 210, 164 p., https://doi.org/10.1130/MEM210.

Burtman, V.S., and Molnar, P.H., 1993, Geological and Geophysical Evidence for Deep Subduction of Continental Crust beneath the Pamir: Geological Society of America Special Paper, v. 281, 76 p., https://doi.org/10.1130/SPE281-p1.

Cao, J.H., Yuan, W.M., Hao, N.N., Feng, Y.L., Chen, X.N., Duan, H.W., and Cheng, X.Q., 2015, Geochronology, geochemistry and geodynamic implications of the Gouli area granites in East Kunlun Mountains [in Chinese with English abstract]: Geological Science and Technology Information, v. 34, no. 2, p. 42–51.

Cao, J.S., Li, W.F., Wang, G.L., and Zhang, X.Y., 2019, The acid-intermediate intrusive rocks in the east section of middle Qilian Orogenic belt: LA-ICP-MS zircon U-Pb age and tectonic implications [in Chinese with English abstract]: Geology and Resources, v. 28, no. 5, p. 423–433.

Chang, P.Y., 2017, Analysis of Jiermeng granite pluton zircon U-Pb age and tectonic environments, South Qilian [M.A. thesis] [in Chinese with English abstract]: Beijing, China, China University of Geosciences, 69 p.

Cunningham, W.D., Windley, B.F., Dorjnamjaa, D., Badamgarov, J., and Saandar, M., 1996, Late Cenozoic transpression in southwestern Mongolia and the Gobi Altai-Tien Shan connection: Earth and Planetary Science Letters, v. 140, no. 1–4, p. 67–81, https://doi.org/10.1016/0012-821X(96)00048-9.

Chen, G.C., Pei, X.Z., Li, R.B., Li, Z.C., Pei, L., Liu, Z.Q., Chen, Y.X., Liu, C.J., Gao, J.M., and Wei, F.H., 2013a, Geochronology and genesis of the Helegang Xilikete granitic plutons from the southern margin of the East Kunlun Orogenic Belt and their tectonic significance [in

Chinese with English abstract]: Acta Geologica Sinica, v. 87, no. 10, p. 1525–1541.

Chen, G.C., Pei, X.Z., Li, R.B., Li, Z.C., Pei, L., Liu, Z.Q., Chen, Y.X., Liu, C.J., Gao, J.M., and Wei, F.H., 2013b, Zircon U-Pb geochronology, geochemical characteristics and geological significance of Cocoe A'Long quartz diorites body from the Hongshuichuan area in East Kunlun [in Chinese with English abstract]: Acta Geologica Sinica, v. 87, no. 2, p. 178–196.

Chen, G.C., Pei, X.Z., Li, R.B., Li, Z.C., Pei, L., Liu, Z.Q., Chen, Y.X., and Liu, C.J., 2013c, Late Triassic magma mixing in the East Kunlun orogenic belt: A case study of Helegang Xilikete granodiorites [in Chinese with English abstract]: Geology in China, v. 40, no. 4, p. 178–196.

Chen, G.T., Cai, H.J., and Liang, K.X., 2016a, Discovery and geological significance of Early Triassic granites in the west of East Kunlun [in Chinese with English abstract]: Gansu Metallurgy, v. 38, no. 4, p. 48–54, https://doi.org/10.16042/j.cnki.cn62-1053/tf.2016.04.015.

Chen, H.W., Luo, Z.H., Mo, X.X., Zhang, X.T., Wang, J., and Wang, B.Z., 2006a, SHRIMP ages of Kayakedengtage complex in the East Kunlun Mountains and their geological implications [in Chinese with English abstract]: Acta Petrologica et Mineralogica, v. 25, no. 1, p. 25–32.

Chen, J., Xie, Z.Y., Li, B., Tan, S.X., Ren, H., Zhang, Q.M., and Li, Y., 2013d, Petrogenesis of Devonian intrusive rocks in Lalingzaohuo area, eastern Kunlun, and its geological significance [in Chinese with English abstract]: Journal of Mineralogical and Petrological Sciences, v. 33, no. 2, p. 26–34.

Chen, J., Xie, Z.Y., Li, B., Li, S.P., Tan, S.X., Ren, H., and Zhang, Q.M., 2013e, Geological and geochemical characteristics of the ore-bearing intrusions from the Lalingzaohuo Mo polymetallic deposit and its metallogenic significance [in Chinese with English abstract]: Geology and Exploration, v. 49, no. 5, p. 813–824.

Chen, J.J., Fu, L.B., Wei, J.H., Tian, N., Xiong, L., Zhao, Y.J., Zhang, Y.J., and Qi, Y.Q., 2016b, Geochemical characteristics of Late Ordovician granodiorite in Gouli area, Eastern Kunlun Orogenic Belt, Qinghai Province: Implications on the evolution of Proto-Tethys Ocean [in Chinese with English abstract]: Earth Science, v. 41, no. 11, p. 1863–1882.

Chen, J., Wei, J., Fu, L., Li, H., Zhou, H., Zhao, X., and Tan, J., 2017, Multiple sources of the Early Mesozoic Gouli batholith, Eastern Kunlun Orogenic Belt, northern Tibetan Plateau: Linking continental crustal growth with oceanic subduction: Lithos, v. 292, p. 161–178, https://doi.org/10.1016/j.lithos.2017.09.006.

Chen, J.L., Xu, X.Y., Zeng, Z.X., Xiao, L., Wang, H.L., Wang, Z.Q., and Xiao, S.W., 2008a, Geochemical characters and LA-ICPMS zircon U-Pb dating constraints on the petrogenesis and tectonic setting of the Shichuan intrusion, east segment of the Central Qilian, NW China [in Chinese with English abstract]: Yanshi Xuebao, v. 24, no. 4, p. 841–854.

Chen, J., Li, B., Yu, F.C., and Chang, T., 2020a, Discovery of 4.0 Ga detrital zircon from the Cambrian strata in the south slope of East Kunlun, Qinghai Province [in Chinese with English abstract]: Mineralogy and Petrology, v. 40, no. 3, p. 20–25.

Chen, L., Liu, L., Capitanio, F.A., Gerya, T.V., and Li, Y., 2020b, The role of pre-existing weak zones in the formation of the Himalaya and Tibetan plateau: 3-D thermomechanical modelling: Geophysical Journal International, v. 221, no. 3, p. 1971–1983, https://doi.org/10.1093/gji/ggaa125.

Chen, N.S., Li, X.Y., Wang, X.Y., Chen, Q., Wang, Q.Y., and Wan, Y.S., 2006b, Zircon SHRIMP U-Pb age of Neoproterozoic metagranite in the North Kunlun unit on the southern margin of the Qaidam block in China [in Chinese with English abstract]: Geological Bulletin of China, v. 25, no. 11, p. 1311–1314.

Chen, N.S., Sun, M., Wang, Q.Y., Zhang, K.X., Wan, Y.S., and Chen, H.H., 2008b, U-Pb dating of zircon from the Central Zone of the East Kunlun Orogen and its implications for tectonic evolution: Science in China. Series D, Earth Sciences, v. 51, no. 7, p. 929–938, https://doi.org/10.1007/s11430-008-0072-x.

Chen, N.S., Zhang, L., Sun, M., Wang, Q., and Kusky, T.M., 2012a, U-Pb and Hf isotopic compositions of detrital zircons from the paragneisses of the Quanji Massif, NW China: Implications for its early tectonic evolutionary history: Journal of Asian Earth Sciences, v. 54, p. 110–130, https://doi.org/10.1016/j.jseaes.2012.04.006.

Chen, N., Liao, F., Wang, L., Santosh, M., Sun, M., Wang, Q., and Mustafa, H.A., 2013f, Late Paleoproterozoic multiple metamorphic events in the Quanji Massif: Links with Tarim and North China Cratons and implications for assembly of the Columbia supercontinent: Precambrian Research, v. 228, p. 102–116, https://doi.org/10.1016/j.precamres.2013.01.013.

Chen, Q.L., 2009, The petrology of Niuxinshan granitoids in the North Qilian and their zircon SHRIMP dating [M.A. thesis] [in Chinese with English abstract]: Beijing, China, Capital Normal University, 64 p.

Chen, S., Niu, Y., Sun, W., Zhang, Y., Li, J., Guo, P., and Sun, P., 2015a, On the origin of mafic magmatic enclaves (MMEs) in syn-collisional granitoids: Evidence from the Baojishan pluton in the North Qilian Orogen, China: Mineralogy and Petrology, v. 109, no. 5, p. 577–596, https://doi.org/10.1007/s00710-015-0383-5.

Chen, S., Niu, Y.L., Li, J.Y., Sun, W.L., Zhang, Y., Hu, Y., and Shao, F.L., 2016c, Syn-collisional adakitic granodiorites formed by fractional crystallization: Insights from their enclosed mafic magmatic enclaves (MMEs) in the Qumushan pluton, North Qilian Orogen at the northern margin of the Tibetan Plateau: Lithos, v. 248–251, p. 455–468, https://doi.org/10.1016/j.lithos.2016.01.033.

Chen, W.N., 2015, Geologic features, provenance analysis and structural evolution of Naocangjiangou Formation at the southern slope of the East Kunlun (east part) [M.A. thesis] [in Chinese with English abstract]: Chang'an University, Xi'an, China.

Chen, X.H., Gehrels, G., Yin, A., Li, L., and Jiang, R.B., 2012b, Paleozoic and Mesozoic basement magmatisms of Eastern Qaidam Basin, Northern Qinghai-Tibet Plateau: LA-ICP-MS zircon U-Pb geochronology and its geological significance: Acta Geologica Sinica, v. 86, no. 2, p. 350–369, https://doi.org/10.1111/j.1755-6724.2012.00665.x.

Chen, Y.J., Yang, K., Wu, B., Zhao, R.Y., Wang, G., and Gou, X.M., 2019, Zircon U-Pb dating and its geological implications in Beidaban granite, Northern Qilian, Gansu Province [Natural Science]: Journal of East China University of Technology, v. 42, no. 2, p. 108–115.

Chen, Y.X., Pei, X.Z., Li, Z.C., Li, R.B., Liu, C.J., Chen, G.C., Pei, L., and Wei, B., 2015b, Geochronology, geochemical features and geological significance of the granitic gneiss in Balong area [in Chinese with English abstract]: East Section of East Kunlun: Acta Petrologica Sinica, v. 31, no. 8, p. 2230–2244.

Chen, Y.X., Song, S., Niu, Y., and Wei, C., 2014, Melting of continental crust during subduction initiation: A case study from the Chaidanuo peraluminous granite in the North Qilian suture zone: Geochimica et Cosmochimica Acta, v. 132, p. 311–336, https://doi.org/10.1016/j.gca.2014.02.011.

Chen, Y.X., Xia, X., and Song, S., 2012c, Petrogenesis of Aoyougou high-silica adakite in the North Qilian orogen, NW China: Evidence for decompression melting of oceanic slab: Chinese Science Bulletin, v. 57, no. 18, p. 2289–2301, https://doi.org/10.1007/s11434-012-5069-3.

Clark, M.K., 2012, Continental collision slowing due to viscous mantle lithosphere rather than topography: Nature, v. 483, p. 74–77, https://doi.org/10.1038/nature10848.

Cowgill, E., Yin, A., Harrison, T.M., and Wang, X.F., 2003, Reconstruction of the Altyn Tagh fault based on U-Pb geochronology: Role of back thrusts, mantle sutures, and heterogeneous crustal strength in forming the Tibetan Plateau: Journal of Geophysical Research. Solid Earth, v. 108, no. B7, https://doi.org/10.1029/2002JB002080.

Cui, J.W., Zheng, Y.Y., Sun, X., Wu, S., Gao, S.B., Tian, L.M., Sun, J.Y., and Yang, C., 2016, Origin of granodiorite and mafic microgranular enclave in Saizhisi, Qinghai Province: Zircon U-Pb geochronological, geochemical and Sr-Nd-Hf isotopic constraints [in Chinese with English abstract]: Earth Science, v. 41, no. 7, p. 1156–1170.

Dai, J.G., Wang, C.S., Hourigan, J., and Santosh, M., 2013, Multi-stage tectono-magmatic events of the Eastern Kunlun Range, northern Tibet: Insights from U-Pb geochronology and (U-Th)/He thermochronology: Tectonophysics, v. 599, p. 97–106, https://doi.org/10.1016/j.tecto.2013.04.005.

Dan, W., Li, X.H., Wang, Q., Wang, X.C., and Liu, Y., 2014, Neoproterozoic S-type granites in the Alxa Block, westernmost North China and tectonic implications: In situ zircon U-Pb-Hf-O isotopic and geochemical constraints: American Journal of Science, v. 314, p. 110–153, https://doi.org/10.2475/01.2014.04.

Deng, W.B., Pei, X.Z., Liu, C.J., Li, Z.C., Li, R.B., Chen, Y.X., Chen, G.C., Yang, S., Chen, G., Sang, J.Z., and Wang, X.B., 2016, LA-ICP-MS zircon U-Pb dating of the Chahantaolegai syenogranites in Xiangride area of East Kunlun and its geological significance [in Chinese with English abstract]: Geological Bulletin of China, v. 35, no. 5, p. 687–699.

Ding, J., Zhang, S., Evans, D.A., Yang, T., Li, H., Wu, H., and Chen, J., 2021, North China craton: The conjugate margin for northwestern Laurentia in Rodinia: Geology, v. 49, no. 7, p. 773–778, https://doi.org/10.1130/G48483.1.

Ding, L., Yang, D., Cai, F.L., Pullen, A., Kapp, P., Gehrels, G.E., Zhang, L.Y., Zhang, Q.H., Lai, Q.Z., Yue, Y.H., and Shi, R.D., 2013, Provenance analysis of the Mesozoic Hoh-Xil-Songpan-Ganzi turbidites in northern Tibet: Implications for the tectonic evolution of the eastern Paleo-Tethys Ocean: Tectonics, v. 32, p. 34–48, https://doi.org/10.1002/tect.20013.

Ding, Q.F., and Huang, Z.B., 2019, U-Pb ages and geochemistry of Maozangsi granodiorite in North Qilian Mountains, China [in Chinese with English abstract]: Northwest Geology, v. 52, no. 4, p. 53–62.

Ding, Q.F., Jiang, S.Y., and Sun, F.Y., 2014, Zircon U-Pb geochronology, geochemical and Sr-Nd-Hf isotopic compositions of the Triassic granite and diorite dikes from the Wulonggou mining area in the Eastern Kunlun Orogen, NW China: Petrogenesis and tectonic implications: Lithos, v. 205, p. 266–283, https://doi.org/10.1016/j.lithos.2014.07.015.

Domeier, M., and Torsvik, T.H., 2014, Plate tectonics in the late Paleozoic: Geoscience Frontiers, v. 5, no. 3, p. 303–350, https://doi.org/10.1016/j.gsf.2014.01.002.

Dong, J.S., Tan, X.Y., Liu, J.D., and Yin, Z.H., 2015, The geological significance and determination of age of the metamorphic intrusion of Paleoproterozoic Tuolai rock Group in the mid-eastern part of the North Qilian Mountains [Natural Science]: Journal of Qinghai University, v. 33, no. 3, p. 73–79.

Dong, Y., He, D., Sun, S., Liu, X., Zhou, X., Zhang, F., and Li, J., 2018, Subduction and accretionary tectonics of the East Kunlun orogen, western segment of the Central China orogenic system: Earth-Science Reviews, v. 186, p. 231–261, https://doi.org/10.1016/j.earscirev.2017.12.006.

Dong, Y.P., and Santosh, M., 2016, Tectonic architecture and multiple orogeny of the Qinling orogenic belt, Central China: Gondwana Research, v. 29, no. 1, p. 1–40, https://doi.org/10.1016/j.gr.2015.06.009.

Du, Y., Wang, J., Han, X., and Shi, G.R., 2003, From flysch to molasse-sedimentary and tectonic evolution of late Caledonian–early Hercynian foreland basin in North Qilian Mountains: Journal of China University of Geosciences, v. 14, no. 1, p. 1–7.

Fan, X.X., Kong, W.J., Yang, Z.X., Zhao, J.C., and Li, Y.X., 2020, U-Pb chronology, geochemical characteristics and petrogenesis of the Chelugou pluton in the western part of North Qilian orogenic belt [in Chinese with English abstract]: Geology in China, v. 47, no. 3, p. 755–766.

Feng, C.Y., Wang, S., Li, G.C., Ma, S.C., and Li, D.S., 2012, Middle to Late Triassic granitoids in the Qimantage area, Qinghai Province, China: Chronology, geochemistry and metallogenic significances [in Chinese with English abstract]: Yanshi Xuebao, v. 28, no. 2, p. 665–678.

Feng, Q., Qin, Y., Fu, S.T., Liu, Y.Q., Zhou, D.W., Ma, D.D., Wang, L.Q., Ren, J.H., and Wang, C.Y., 2015, U-Pb age of detrital zircons and its geological significance from Maoniushan Formation in the Wulan County, northern

margin of Qaidam Basin [in Chinese with English abstract]: Chenji Xuebao, v. 33, no. 3, p. 486–499.
Fu, C.L., Yan, Z., Wang, Z.Q., Buckman, S., Aitchison, J.C., Niu, M.L., Cao, B., Guo, X.Q., Li, X.C., Li, Y.S., and Li, J.L., 2018, Lajishankou Ophiolite Complex: Implications for Paleozoic multiple accretionary and collisional events in the South Qilian Belt: Tectonics, v. 37, no. 5, p. 1321–1346, https://doi.org/10.1029/2017TC004740.
Fu, D., Kusky, T., Wilde, S.A., Polat, A., Huang, B., and Zhou, Z., 2019, Early Paleozoic collision-related magmatism in the eastern North Qilian orogen, northern Tibet: A linkage between accretionary and collisional orogenesis: Geological Society of America Bulletin, v. 131, no. 5–6, p. 1031–1056, https://doi.org/10.1130/B35009.1.
Fu, D., Kusky, T.M., Wilde, S.A., Windley, B.F., Polat, A., Huang, B., and Zhou, Z., 2020, Structural anatomy of the early Paleozoic Laohushan ophiolite and subduction complex: Implications for accretionary tectonics of the Proto-Tethyan North Qilian orogenic belt, northeastern Tibet: Geological Society of America Bulletin, v. 132, p. 2175–2201, https://doi.org/10.1130/B35442.1.
Fu, D., Huang, B., Johnson, T.E., Wilde, S., Jourdan, F., Polat, A., Windley, B.F., Hu, Z.C., and Kusky, T., 2021, Boninitic blueschists record subduction initiation and subsequent accretion of an arc-forearc in the northeast Proto-Tethys Ocean: Geology, https://doi.org/10.1130/G49457.1.
Gao, L., Ren, E.F., Li, J., and Kang, W.H., 2017, The geochemical characteristics and chronological significance of Baihuagou pluton at the eastern section of central Qilian [in Chinese with English abstract]: Journal of Qinghai University, v. 35, no. 4, p. 1–7.
Gao, Y.B., and Li, W.Y., 2011, Petrogenesis of granites containing tungsten and tin ores in the Baiganhu deposit, Qimantage, NW China: Constraints from petrology, chronology and geochemistry [in Chinese with English abstract]: Geochimica, v. 40, no. 4, p. 324–336.
Gao, Y.B., Li, W.Y., Ma, X.G., Zhang, Z.W., and Tang, Q.Y., 2012, Genesis, geochronology and Hf isotopic compositions of the magmatic rocks in Galinge iron deposit, eastern Kunlun [Natural Sciences]: Journal of Lanzhou University, v. 48, no. 2, p. 36–47.
Gao, Y.B., Li, W.Y., Qian, B., Li, K., Li, D.S., He, S.Y., Zhang, Z.W., and Zhang, J.W., 2014, Geochronology, geochemistry and Hf isotope compositions of the granitic rocks related with iron mineralization in Yemaquan deposit, East Kunlun, NW China [in Chinese with English abstract]: Yanshi Xuebao, v. 30, no. 6, p. 1647–1665.
Gehrels, G., Kapp, P., DeCelles, P., Pullen, A., Blakey, R., Weislogel, A., Ding, L., Guynn, J., Martin, A., McQuarrie, N., and Yin, A., 2011, Detrital zircon geochronology of pre-Tertiary strata in the Tibetan-Himalayan orogen: Tectonics, v. 30, no. 5, https://doi.org/10.1029/2011TC002868.
Gehrels, G.E., Yin, A., and Wang, X.F., 2003a, Detrital-zircon geochronology of the northeastern Tibetan plateau: Geological Society of America Bulletin, v. 115, no. 7, p. 881–896, https://doi.org/10.1130/0016-7606(2003)115<0881:DGOTNT>2.0.CO;2.
Gehrels, G.E., Yin, A., and Wang, X.F., 2003b, Magmatic history of the northeastern Tibetan Plateau: Journal of Geophysical Research. Solid Earth, v. 108, no. B9, https://doi.org/10.1029/2002jb001876.
Gong, S., Chen, N., Wang, Q., Kusky, T.M., Wang, L., Zhang, L., Ba, J., and Liao, F., 2012, Early Paleoproterozoic magmatism in the Quanji Massif, northeastern margin of the Qinghai–Tibet Plateau and its tectonic significance: LA-ICPMS U-Pb zircon geochronology and geochemistry: Gondwana Research, v. 21, p. 152–166, https://doi.org/10.1016/j.gr.2011.07.011.
Guo, A.L., Zhang, G.W., Qiang, J., Sun, Y.G., Li, G., and Yao, A.P., 2009, Indosinian Zongwulong orogenic belt on the northeastern margin of the Qinghai-Tibet plateau [in Chinese with English abstract]: Yanshi Xuebao, v. 25, no. 1, p. 1–12.
Guo, J.J., Zhao, F.Q., Li, H.K., Li, H.M., and Zuo, Y.C., 2000, New chronological evidence of the age of Huangyuan Group in the eastern segment of Mid-Qilian massif and its geological significance [in Chinese with English abstract]: Regional Geology of China, v. 19, no. 1, p. 26–31.
Guo, X.Z., Jia, Q.Z., Kong, H.L., Jia, Y.Z., Li, J.C., Ma, Z.Y., and Wang, Y., 2016, Zircon U-Pb geochronology and geochemistry of Harizha quartz diorite in the eastern section from East Kunlun [in Chinese with English abstract]: Geological Science and Technology Information, v. 35, no. 5, p. 18–26.
Guo, Z.J., Yin, A., Robinson, A., and Jia, C.Z., 2005, Geochronology and geochemistry of deepdrill-core samples from the basement of the central Tarim Basin: Journal of Asian Earth Sciences, v. 25, p. 45–56, https://doi.org/10.1016/j.jseaes.2004.01.016.
Guo, Z.P., Li, W.Y., Zhang, Z.W., Gao, Y.B., Zhang, J.W., Li, K., Kong, H.L., and Qian, B., 2015a, Petrogenesis of Lumanshan granites in Hualong area of southern Qilian Mountain: Constraints from geochemistry, zircon U-Pb geochronology and Hf isotope [in Chinese with English abstract]: Geology in China, v. 42, no. 4, p. 864–880.
Guo, Z.P., Zhao, X.M., Bai, Y., Zhang, J.W., and Kong, H.L., 2015b, Zircon U-Pb and molybdenite Re-Os dating of the Langlike copper deposit in North Qilian Mountain and its geological implications [in Chinese with English abstract]: Geology in China, v. 42, no. 3, p. 691–670.
Hao, G.J., Lu, S.N., Xin, H.T., Wang, H.C., and Yuan, G.B., 2004, The constitution and importance geological events of Pre-Devonian in the Dulan: Qinghai [in Chinese with English abstract]: Journal of Jilin University, v. 34, p. 495–501.
Hao, N.N., Yuan, W.M., Cao, J.H., Feng, Y.L., Cheng, X.Q., and Zhang, A.K., 2014, The recognition of Late Devonian granodiorite and its geological implications in Kayakedengtage, East Kunlun Mountain, Qinghai-Tibet Plateau [in Chinese with English abstract]: Northwest Geology, v. 47, no. 1, p. 107–115.
Harris, N.B.W., Xu, R.H., Lewis, C.L., Hawkesworth, C.J., and Zhang, Y.Q., 1988, Isotope geochemistry of the 1985 Tibet Geotraverse, Lhasa to Golmud: Philosophical Transactions of the Royal Society of London, v. 327, p. 263–285, https://doi.org/10.1098/rsta.1988.0129.
He, D.F., Dong, Y.P., Zhang, F.F., Yang, Z., Sun, S.S., Cheng, B., Zhou, B., and Liu, X.M., 2016, The 1.0 Ga S-type granite in the East Kunlun Orogen, Northern Tibetan Plateau: Implications for the Meso- to Neoproterozoic tectonic evolution: Journal of Asian Earth Sciences, v. 130, p. 46–59, https://doi.org/10.1016/j.jseaes.2016.07.019.
He, D.F., Dong, Y.P., Liu, X.M., Zhou, X.H., Zhang, F.F., and Sun, S.S., 2018, Zircon U-Pb geochronology and Hf isotope of granitoids in East Kunlun: Implications for the Neoproterozoic magmatism of Qaidam Block, Northern Tibetan Plateau: Precambrian Research, v. 314, p. 377–393, https://doi.org/10.1016/j.precamres.2018.06.017.
He, X.Y., Yang, X.K., Wang, Y., Guo, R.H., Liao, Y.Y., and Fan, Y.H., 2020, Petrology, geochemistry and zircon U-Pb geochronology of the Chaidamushan granite from the southern margin of Qilianshan [in Chinese with English abstract]: Acta Geologica Sinica, v. 94, no. 4, p. 1248–1263.
Heron, P.J., Pysklywec, R.N., and Stephenson, R., 2016, Identifying mantle lithosphere inheritance in controlling intraplate orogenesis: Journal of Geophysical Research. Solid Earth, v. 121, no. 9, p. 6966–6987, https://doi.org/10.1002/2016JB013460.
Heubeck, C., 2001, Assembly of central Asia during the middle and late Paleozoic, *in* Hendrix, M.S., and Davis, G.A., eds., Paleozoic and Mesozoic Tectonic Evolution of Central Asia: From Continental Assembly to Intracontinental Deformation: Geological Society of America Memoirs, v. 194, 22 p.
Hou, R.N., Wang, S.H., Zhang, X., Hou, K.X., Zhang, C., and Wang, J.R., 2015, Geochemical characteristics and tectonic significance of the granitoids in the western section of the Mid-Qilian [in Chinese with English abstract]: Diqiu Kexue Jinzhan, v. 30, no. 9, p. 1034–1049.
Hu, W.L., Jia, Z.L., Wang, J.R., Hou, K.X., and Wang, S.H., 2016, Geochronology and geochemistry characteristics of the granites from the Huashigou area, south Qilian and their tectonic significance [in Chinese with English abstract]: Gaoxiao Dizhi Xuebao, v. 22, no. 2, p. 242–253.
Huang, H., Niu, Y., Nowell, G., Zhao, Z., Yu, X., Zhu, D.-C., Mo, X.X., and Ding, S., 2014a, Geochemical constraints on the petrogenesis of granitoids in the East Kunlun Orogenic belt, northern Tibetan Plateau: Implications for continental crust growth through syn-collisional felsic magmatism: Chemical Geology, v. 370, p. 1–18, https://doi.org/10.1016/j.chemgeo.2014.01.010.
Huang, H., Niu, Y., Nowell, G., Zhao, Z., Yu, X., and Mo, X., 2015, The nature and history of the Qilian Block in the context of the development of the Greater Tibetan Plateau: Gondwana Research, v. 28, no. 1, p. 209–224, https://doi.org/10.1016/j.gr.2014.02.010.
Huang, H., Niu, Y., and Mo, X., 2017a, Garnet effect on Nd-Hf isotope decoupling: Evidence from the Jinfosi batholith, Northern Tibetan Plateau: Lithos, v. 274–275, p. 31–38, https://doi.org/10.1016/j.lithos.2016.12.025.
Huang, X.H., Zhang, H.J., Wang, X.L., Wang, X., Wang, Z.Y., and Qi, Y.J., 2017b, LA-ICP-MS U-Pb dating of detrital zircons from the Upper Permian Gequ Formation on the southern margin of the East Kunlun Mountains and its tectonics implications [in Chinese with English abstract]: Geological Bulletin of China, v. 36, no. 2/3, p. 258–269.
Huang, Z.B., Li, B.H., Jin, X., and Liu, M.Q., 2010, Discussion on the petrogenesis and tectonic setting of Beidaban granitic pluton in North Qilian Mountain [in Chinese with English abstract]: Journal of Mineral Petrology, v. 30, no. 4, p. 62–68.
Huang, Z.B., Zheng, J.P., Li, B.H., Wei, Z.J., Qi, W., and Xu, Y.L., 2014b, The discovery of Late Cambrian adakite in the western Central Qilian Mountain and its geological implications [in Chinese with English abstract]: Acta Petrologica et Mineralogica, v. 33, no. 6, p. 1008–1018.
Huang, Z.B., Zheng, J.P., Li, B.H., Dong, X.Y., Fu, T.Y., Xu, L., and Gao, K.L., 2018, U-Pb ages, Hf isotopic composition and geochemistry of alkaline complex from the Ganshaebo REE Deposit in North Qilian Mountains, China [in Chinese with English abstract]: Acta Geologica Sinica, v. 92, no. 12, p. 2420–2436.
Ji, B., Huang, B.T., Li, X.M., and Wang, L., 2019, Geochronology and geochemical characteristics of the Early Ordovician granite from Hongmiaogou area in northwest margin of South Qilian and its geological significance [in Chinese with English abstract]: Northwest Geology, v. 52, no. 4, p. 63–75.
Ji, W.H., Li, R.S., Chen, S.J., He, S.P., Zhao, Z.M., Bian, X.W., Zhu, H.P., Cui, J.G., and Ren, J.G., 2011, The discovery of Palaeoproterozoic volcanic rocks in the Bulunkuoler Group from the Tianshuihai Massif in Xinjiang of Northwest China and its geological significance: Science China. Earth Sciences, v. 54, p. 61–72, https://doi.org/10.1007/s11430-010-4043-7.
Jia, Z.L., Chen, W.F., Sha, X., and Wang, J.R., 2017, Discovery of Middle Permian adakitic rocks in south Qilian area, Gansu and implications for tectonics and Cu(Au) [in Chinese with English abstract]: Mineralization: Geotectonica et Metallogenia, v. 41, no. 1, p. 222–234.
Jiang, C.F., Yang, J.S., Feng, B.G., Zhu, Z.Z., Zhao, M., Chai, Y.C., Shi, X.D., Wang, H.D., and Ha, J.Q., 1992, Opening Closing Tectonics of Kunlun Mountains: Geological Memoirs [in Chinese with English abstract]: Beijing, China, Geological Publishing House, 224 p.
Jin, L.J., Zhou, H.W., Wang, J.L., Zhu, Y.H., and Lin, Q.X., 2015a, LA-ICP-MS U-Pb dating of the detrital zircons from clastic rocks of Naij Tal Group in East Kunlun and its geological implications [in Chinese with English abstract]: Geological Bulletin of China, v. 34, no. 10, p. 1848–1859.
Jin, L.J., Zhou, H.W., Zhu, Y.H., and Lin, Q.X., 2015b, U-Pb age of the detrital zircon from the Serteng Formation in East Kunlun: Constraints on its provenance and formation time [in Chinese with English abstract]: Geotectonica et Metallogenia, v. 39, no. 4, p. 691–703.
Jin, L.J., Wang, J.L., Zhao, T.Q., Zhou, H.W., Sun, T.H., Li, C.J., Han, Z.X., and Jia, W.W., 2020, The provenance of Salawula Formation in East Kunlun and the tectonic thermal events of provenance: The evidence from U-Pb chronology of detrital zircons [in Chinese with English abstract]: Geological Bulletin of China, v. 39, no. 7, p. 1025–1034.
Kusky, T.M., Li, J.H., and Santosh, M., 2007, The Paleoproterozoic North Hebei orogen: North China craton's

collisional suture with the Columbia supercontinent: Gondwana Research, v. 12, no. 1–2, p. 4–28, https://doi.org/10.1016/j.gr.2006.11.012.

Levashova, N.M., Meert, J.G., Gibsher, A.S., Grice, W.C., and Bazhenov, M.L., 2011, The origin of microcontinents in the Central Asian Orogenic Belt: Constraints from paleomagnetism and geochronology: Precambrian Research, v. 185, p. 37–54, https://doi.org/10.1016/j.precamres.2010.12.001.

Li, B., Hu, D.G., Chen, X.H., Zhang, Y.L., Wu, H.H., and Wang, C.Q., 2017, Zircon U-Pb age of granite porphyry within Youhulugou ophiolite in the suture zone of North Qilian Mountains and its geological implications [in Chinese with English abstract]: Geoscience, v. 31, no. 6, p. 1170–1176.

Li, B., Zuza, A.V., Chen, X., Wang, Z.Z., Shao, Z., Levy, D.A., Wu, C., Xu, S.L., and Sun, Y., 2021, Pre-cenozoic evolution of the northern Qilian Orogen from zircon geochronology: Framework for early growth of the northern Tibetan Plateau: Palaeogeography, Palaeoclimatology, Palaeoecology, v. 562, no. 110091, https://doi.org/10.1016/j.palaeo.2020.110091.

Li, C.S., Zhang, Z.W., Li, W.Y., Wang, Y.L., Sun, T., and Ripley, E.M., 2015a, Geochronology, petrology and Hf-S isotope geochemistry of the newly-discovered Xiarihamu magmatic Ni–Cu sulfide deposit in the Qinghai–Tibet plateau, western China: Lithos, v. 216–217, p. 224–240, https://doi.org/10.1016/j.lithos.2015.01.003.

Li, G.C., Feng, C.Y., Wang, R.J., Ma, S.C., Li, H.M., and Zhou, A.S., 2012, SIMS zircon U-Pb age, petrochemistry and tectonic implications of granitoids in Northeastern Baiganhue W-Sn Orefield, Xinjiang [in Chinese with English abstract]: Acta Geoscientica Sinica, v. 33, no. 2, p. 216–226.

Li, J.F., Zhang, Z.C., and Han, B.F., 2010, Geochronology and geochemistry of Early Paleozoic granitic plutons from Subei and Shibaocheng areas, the western segment of Central Qilian and their geological implications [in Chinese with English abstract]: Yanshi Xuebao, v. 26, no. 8, p. 2431–2444.

Li, K., Gao, Y.B., Qian, B., He, S.Y., Liu, Y.L., Zhang, Z.W., Zhang, J.W., and Wang, Y.L., 2015b, Geochronology, geochemical characteristics and Hf isotopic compositions of granite in the Hutouya deposit, Qimantag, East Kunlun [in Chinese with English abstract]: Geology in China, v. 42, no. 3, p. 630–645.

Li, M., Wang, C., Li, R.S., and Peng, Y., 2015c, Petrogenesis and LA-ICP-MS zircon U-Pb dating of late Neoproterozoic granitic gneisses in western Qilian Mountain [in Chinese with English abstract]: Geological Bulletin of China, v. 34, no. 8, p. 1438–1446.

Li, S.J., Sun, F.Y., Feng, C.Y., Liu, Z.H., Zhao, J.W., Li, Y.C., and Wang, S., 2008, Geochronological study on the Yazigou polymetallic deposit in Eastern Kunlun, Qinhai Province [in Chinese with English abstract]: Acta Geologica Sinica, v. 82, no. 7, p. 949–955.

Li, W., Neubauer, F., Liu, Y.J., Genser, J., Ren, S.M., Han, G.Q., and Liang, C.Y., 2013, Paleozoic evolution of the Qimantagh magmatic arcs, Eastern Kunlun Mountains: Constraints from zircon dating of granitoids and modern river sands: Journal of Asian Earth Sciences, v. 77, p. 183–202, https://doi.org/10.1016/j.jseaes.2013.08.030.

Li, W.F., Zhang, X.Y., Cao, J.S., Wang, G.L., Wang, C.T., Wang, W., Qiao, G.D., Liu, J.D., and Chen, L.J., 2020, Geochemical characteristics and chronological significance of Middle Ordovician granite in Halahu area of southern Qilian Mountain [in Chinese with English abstract]: Geological Bulletin of China, v. 39, no. 2–3, p. 215–223.

Li, X.B., Pei, X.Z., Chen, Y.X., Liu, C.J., Li, R.B., Li, Z.C., Chen, G.C., Xu, T., Yang, J., and Hu, N., 2014, Metamorphosed polymictic conglomerate layer zircon U-Pb age and its geological significance at Balong area in east part of Eastern Kunlun Mountains [in Chinese with English abstract]: Dizhi Lunping, v. 60, no. 6, p. 1212–1230.

Li, X., Huang, X., Luo, M., Dong, G., and Mo, X., 2015d, Petrogenesis and geodynamic implications of the Mid-Triassic lavas from East Kunlun, northern Tibetan Plateau: Journal of Asian Earth Sciences, v. 105, p. 32–47, https://doi.org/10.1016/j.jseaes.2015.03.009.

Li, Y.S., Xu, L.J., Yu, S.Y., Zhang, J.X., Guo, J., Peng, Y.B., and Zhou, G.S., 2019, Partial melting of thickened lower crust in post-collisional setting: Evidence from high silicon adakitic granites in the North Qilian orogen: Geological Journal, v. 55, no. 5, p. 3990–4007, https://doi.org/10.1002/gj.3645.

Liao, F.X., Zhang, L., Chen, N.S., Sun, M., Santosh, M., Wang, Q.Y., and Hassan, A.M., 2014a, Geochronology and geochemistry of meta-mafic dykes in the Quanji Massif, NW China: Paleoproterozoic evolution of the Tarim Craton and implications on the assembly of the Columbia supercontinent: Precambrian Research, v. 249, p. 33–56, https://doi.org/10.1016/j.precamres.2014.04.015.

Liao, H., Hu, D.G., Zhang, X.J., Yu, W.L., and Guo, T., 2014b, Zircon U-Pb age for granite of the Ordovician formation and its tectonic significance in the Southern Qilian [in Chinese with English abstract]: Journal of Geodynamics, v. 20, no. 3, p. 292–298.

Liu, B., Ma, C.Q., Zhang, J.Y., Xiong, F.H., Huang, J., and Jiang, H.A., 2012a, Petrogenesis of Early Devonian intrusive rocks in the east part of Eastern Kunlun Orogen and implication for early Palaeozoic orogenic processes [in Chinese with English abstract]: Yanshi Xuebao, v. 28, no. 6, p. 1785–1807.

Liu, B.S., Cai, J.F., Lei, X.Q., Wang, T.S., and Meng, H., 2016, Discovery and geological significance of Early Permian mafic dike intrusion into Tuolai Paleo-Proterozoic rock in Yulongtan region [in Chinese with English abstract]: Northwest Geology, v. 49, no. 4, p. 43–50.

Liu, C.D., Mo, X.X., Luo, Z.H., Yu, X.H., Chen, H.W., Li, S.W., and Zhao, X., 2004, Mixing events between the crust- and mantle-derived magmas in Eastern Kunlun: Evidence from zircon SHRIMP II chronology: Chinese Science Bulletin, v. 49, no. 8, p. 828–834, https://doi.org/10.1007/BF02889756.

Liu, C.F., Wu, C., Zhou, Z.G., Zhu, Y., Jiang, T., Song, Z.J., Liu, W., Yang, X., and Zhang, H., 2018a, U-Pb detrital zircon geochronology from the basement of the Central Qilian terrane: Implications for tectonic evolution of northeastern Tibetan Plateau: International Journal of Earth Sciences, v. 107, p. 673–686, https://doi.org/10.1007/s00531-017-1522-5.

Liu, J.D., Wang, C.T., Li, W.F., Zhang, X.Y., and Dong, J.S., 2015, Geological characteristics and formation of Proterozoic basement north Qilian Langshidang area [in Chinese with English abstract]: Gansu Metallurgy, v. 37, no. 4, p. 96–102.

Liu, M.Q., 2013, Single-grain zircon U-Pb ages and geological significance of the Lianhuashan granites from Wuwei (Gansu) in the Northern Qilian orogenic belt [Natural Sciences]: Journal of Lanzhou University, v. 49, no. 4, p. 448–452.

Liu, M., and Furlong, K.P., 1994, Intrusion and underplating of mafic magmas: Thermal-rheological effects and implications for Tertiary tectonomagmatism in the North American Cordillera: Tectonophysics, v. 237, no. 3–4, p. 175–187, https://doi.org/10.1016/0040-1951(94)90253-4.

Liu, M., Zhang, Z.H., Xiang, J.F., Cao, D.Z., and Yang, G.H., 2014, Zircon U-Pb isotopic dating and lithogeochemical features of the biotite monzonitic granite in Daheishan tungsten deposit, Qinghai Province, China [in Chinese with English abstract]: Yanshi Xuebao, v. 30, no. 1, p. 139–151.

Liu, Q., Wang, G., and Wang, D.K., 2019, Geochronology and its geological significance for granodiorite porphyry in the Songshunangou Au deposit [in Chinese with English abstract]: North Qilian Mountains: Acta Geologica Sichuan, v. 39, no. 1, p. 15–21.

Liu, S., Hu, R., Gao, S., Feng, C., Coulson, I.M., Feng, G., et al., 2012b, U-Pb zircon age, geochemical and Sr-Nd isotopic data as constraints on the petrogenesis and emplacement time of the Precambrian mafic dyke swarms in the North China Craton (NCC): Lithos, v. 140, p. 38–52, https://doi.org/10.1016/j.lithos.2012.01.002.

Liu, T.J., 2015, Geologic features, provenance nature and tectonic significance of Hongshuichuan formation located in the southern slope of the East Kunlun orogenic belt (eastern part) [M.A. thesis] [in Chinese with English abstract]: Chang'an University, Xi'an, China.

Liu, W.D., 2016, Study on rock age and formation mechanism of intrusive rocks in Early Triassic in Xiangride area in East Kunlun Orogenic [in Chinese with English abstract]: Shandong Land and Resources, v. 32, no. 12, p. 1–7.

Liu, X.T., 2019, Spatial-temporal distribution and tectonic implications of the granitoids from Qilian block [Ph.D. thesis] [in Chinese with English abstract]: Qinghai, China, Qinghai Institute of Salt Lakes, Chinese Academy of Sciences, 138 p.

Liu, Y.H., Mo, X.X., Yu, X.H., Zhang, X.T., and Xu, G.W., 2006a, Zircon SHRIMP U-Pb dating of the Jingren granite, Yemaquan region of the east Kunlun and its geological significance [in Chinese with English abstract]: Yanshi Xuebao, v. 22, no. 10, p. 2457–2463.

Liu, Y.J., Neubauer, F., Genser, J., Takasu, A., Ge, X.H., and Handler, R., 2006b, $^{40}Ar/^{39}Ar$ ages of blueschist facies politic schists from Qingshuigou in the Northern Qilian Mountains, western China: The Island Arc, v. 15, p. 187–198, https://doi.org/10.1111/j.1440-1738.2006.00508.x.

Liu, Y.X., Sha, X., Ma, Z., and Wang, J.R., 2018b, Geochemical characteristics and tectonic implication of the Shuanglong mafic-ultramafic rocks in western section of the North Qilian [in Chinese with English abstract]: Yanshi Xuebao, v. 34, no. 2, p. 383–397.

Lu, L., Zhang, Y.L., Wu, Z.H., and Hu, D.G., 2013, Zircon U-Pb dating of early Paleozoic granites from the East Kunlun Mountains and its geological significance [in Chinese with English abstract]: Acta Geoscientica Sinica, v. 34, no. 4, p. 447–454.

Lu, S.N., 2002, Preliminary Study of Precambrian Geology in the North Tibet-Qinghai Plateau [in Chinese]: Beijing, China, Geological Publishing House, 125 p.

Lu, S.N., Yu, H.F., and Li, H.K., 2006, Research on Precambrian Major Problems in China [in Chinese with English abstract]: Beijing, China, Geological Publishing Press, 206 p.

Lu, X.X., Sun, Y.G., Zhang, X.T., Xiao, Q.H., Wang, X.X., Wei, X.D., and Gu, D.M., 2007, The SHRIMP age of Tatalin Rapakivi granite at the north margin of Qaidam Basin [in Chinese with English abstract]: Acta Geologica Sinica, v. 81, no. 5, p. 626–634.

Ludwig, K.R., 2003, User's Manual for Isoplot 3.00: A Geochronological Toolkit for Microsoft Excel: Berkeley Geochronology Center Special Publication, v. 4, 70 p.

Luo, Z.W., Zhang, Z.C., Li, J.F., Feng, Z.S., and Tang, W.H., 2015, Geochronology of two kinds of Paleozoic granitic plutons from Sangewatang in Subei, the western margin of Central-south Qilian and their geological implications [in Chinese with English abstract]: Yanshi Xuebao, v. 31, no. 1, p. 176–188.

Lv, D.Y., Ren, E.F., Yang, Q.P., and Xiong, W.S., 2021, Geochemical characteristics and geochronological significance of the rock mass of Shangmoji in the eastern part of the middle Qilian mountains [in Chinese with English abstract]: Journal of Qinghai University, v. 39, no. 1, p. 101–108.

Ma, J.J., Wang, H., He, C., Wang, L., Wang, Q.Y., and Chen, N.S., 2018, Neoproterozoic post-collision magmatism in south Qilian orogen, China: Evidenced by geochronology and geochemistry [in Chinese with English abstract]: Diqiu Kexue Yu Huanjing Xuebao, v. 40, no. 2, p. 133–154.

Mao, J.W., Zhang, Z.H., Bernd, L., Zhang, Z.C., Yang, J.M., and Wang, Z.L., 2000, The Yeniutan granodiorite in Sunan County, Gansu Province, China: Petrological features, geological setting and relationship to tungsten mineralization: Episodes, v. 23, no. 3, p. 163–171, https://doi.org/10.18814/epiiugs/2000/v23i3/003.

Mattinson, C.G., Wooden, J.L., Liou, J.G., Bird, D.K., and Wu, C.L., 2006, Geochronology and tectonic significance of Middle Proterozoic granitic orthogneiss, North Qaidam HP/UHP terrane, Western China: Mineralogy and Petrology, v. 88, no. 1–2, p. 227–241, https://doi.org/10.1007/s00710-006-0149-1.

Meert, J.G., Gibsher, A.S., Levashova, N.M., Grice, W.C., Kamenov, G.D., and Ryabinin, A.B., 2011, Glaciation and ~770 Ma Ediacara (?) fossils from the Lesser Karatau microcontinent, Kazakhstan: Gondwana Research, v. 19, p. 867–880, https://doi.org/10.1016/j.gr.2010.11.008.

Meng, F.C., Zhang, J.X., and Cui, M.H., 2013a, Discovery of early Paleozoic eclogite from the East Kunlun, western

China, and its tectonic significance: Gondwana Research, v. 23, p. 825–836, https://doi.org/10.1016/j.gr.2012.06.007.

Meng, F.C., Cui, M.H., Wu, X.K., Wu, J.F., and Wang, J.H., 2013b, Magmatic and metamorphic events recorded in granitic gneisses from the Qimantag, East Kunlun Mountains, Northwest China [in Chinese with English abstract]: Yanshi Xuebao, v. 29, no. 6, p. 2107–2122.

Meng, F., Cui, M.H., Wu, X.K., and Ren, Y.F., 2015, Heishan mafic–ultramafic rocks in the Qimantag area of Eastern Kunlun, NW China: Remnants of an early Paleozoic incipient island arc: Gondwana Research, v. 27, p. 745–759, https://doi.org/10.1016/j.gr.2013.09.023.

Menold, C.A., Manning, C.E., Yin, A., Tropper, P., Chen, X.H., and Wang, X.F., 2009, Metamorphic evolution, mineral chemistry and thermobarometry of orthogneiss hosting ultrahigh-pressure eclogites in the North Qaidam metamorphic belt, western China: Journal of Asian Earth Sciences, v. 35, p. 273–284, https://doi.org/10.1016/j.jseaes.2008.12.008.

Pei, L., Li, R.B., Pei, X.Z., Liu, J.L., Li, Z.C., Liu, C.J., Chen, Y.X., Liu, Z.Q., Chen, G.C., Hu, N., and Gao, F., 2017, Sediment source analysis for the Maerzheng Formation sandstone in Gerizhuotuo area, southern margin of East Kunlun Region: Evidence for detrital zircon U-Pb geochronology [in Chinese with English abstract]: Acta Geologica Sinica, v. 91, no. 6, p. 1326–1344.

Pan, G.T., Ding, J., Yao, D., and Wang, L., 2004, Geological Map of Qinghai-Xiang (Tibet) Plateau and Adjacent Areas, Chengdu: Chengdu Institute of Geology and Mineral Resources, China Geological Survey, Chengdu Cartographic Publishing House, scale 1:1,500,000.

Peng, P., 2010, Reconstruction and interpretation of giant mafic dyke swarms: A case study of 1.78 Ga magmatism in the North China craton, *in* Kusky, T.M., Zhai, M.-G., and Xiao, W., eds., The Evolving Continents: Understanding Processes of Continental Growth: Geological Society of London Special Publication, v. 338, p. 163–178, https://doi.org/10.1144/SP338.8.

Peng, S.Z., Pei, X.Z., Li, R.B., Li, Z.C., Liu, C.J., Chen, Y.X., Yan, Q.Z., Wang, X., Zhang, Y., and Hu, C.G., 2017a, Detrital zircon U-Pb age and geological significance of the meta-sedimentary rocks from the Qingshuiquan area in the central tectonic mélange belt of East Kunlun [in Chinese with English abstract]: Northwest Geology, v. 50, no. 1, p. 212–226.

Peng, Y.B., Yu, S.Y., Zhang, J.X., Li, S.Z., Sun, D.Y., and Tong, L.X., 2017b, Early Paleozoic arc magmatism and metamorphism in the northern Qilian Block, western China: A case study of Menyuan-Kekeli [in Chinese with English abstract]: Yanshi Xuebao, v. 33, no. 12, p. 3925–3941.

Peng, Y.B., Yu, S., Li, S., Zhang, J., Liu, Y., Li, Y., and Santosh, M., 2019, Early Neoproterozoic magmatic imprints in the Altun-Qilian-Kunlun region of the Qinghai-Tibet Plateau: Response to the assembly and breakup of Rodinia supercontinent: Earth-Science Reviews, v. 199, p. 102954, https://doi.org/10.1016/j.earscirev.2019.102954.

Pullen, A., Kapp, P., Gehrels, G.E., Vervoort, J.D., and Ding, L., 2008, Triassic continental subduction in central Tibet and Mediterranean-style closure of the Paleo-Tethys Ocean: Geology, v. 36, p. 351–354, https://doi.org/10.1130/G24435A.1.

Qi, R.R., 2012, LA-ICP-MS zircon U-Pb ages and geological implications for the Bagadeerji granitic plutons in the central Qilian Mountains, Gansu [in Chinese with English abstract]: Chenji Yu Tetisi Dizhi, v. 32, no. 4, p. 86–93.

Qian, B., Gao, Y.B., Li, K., Zhang, Z.W., Zhou, A.S., and Wu, Y.S., 2015, Zircon U-Pb-Hf isotopes and whole rock geochemistry constraints on the petrogenesis of iron-rare metal mineralization related alkaline granitic intrusive rock in Yugouzi area, eastern Kunlun, Xinjiang [in Chinese with English abstract]: Yanshi Xuebao, v. 31, no. 9, p. 2508–2520.

Qian, Q., Wang, Y.M., Li, H.M., Jia, X.Q., Han, S., and Zhang, Q., 1998, Geochemical characteristics and genesis of diorites from Laohushan, Gansu Province [in Chinese with English abstract]: Yanshi Xuebao, v. 14, no. 4, p. 520–528.

Qin, H.P., Wu, C.L., Wang, C.S., Lei, M., Liu, C.H., and Li, M.Z., 2014a, LA-ICP-MS zircon U-Pb geochronology and geochemical characteristical of Xiagucheng granite in North Qilian [in Chinese with English abstract]: Acta Geologica Sinica, v. 88, no. 10, p. 1832–1842.

Qin, H.P., Wu, C.L., Wang, C.S., Li, X., Lei, M., Liu, C.H., and Li, M.Z., 2014b, LA-ICP-MS zircon U-Pb dating and geochemical characteristics of high Sr/Y-type granite from Xigela, eastern Qilian area [in Chinese with English abstract]: Yanshi Xuebao, v. 30, no. 12, p. 3759–3771.

Qin, Y., 2018, Neoproterozoic to early Paleozoic tectonic evolution in the South Qilian Orogen [Ph.D. thesis] [in Chinese with English abstract]: Xi'an, China, Northwest University, 153 p.

Qinghai Bureau of Geology and Mineral Resources, 1997, Regional Geology of Qinghai Province: Beijing, China, Geological Publishing House, 662 p.

Ratschbacher, L., Hacker, B.R., Calvert, A., Webb, L.E., Grimmer, J.C., McWilliams, M.O., Dong, S.W., and Hu, J., 2003, Tectonics of the Qinling (Central China): Tectonostratigraphy, geochronology, and deformation history: Tectonophysics, v. 366, p. 1–53, https://doi.org/10.1016/S0040-1951(03)00053-2.

Robinson, A.C., 2015, Mesozoic tectonics of the Gondwanan terranes of the Pamir plateau: Journal of Asian Earth Sciences, v. 102, p. 170–179, https://doi.org/10.1016/j.jseaes.2014.09.012.

Roger, F., Arnaud, N., Gilder, S., Tapponnier, P., Jolivet, M., Brunel, M., Malavieille, J., Xu, Z.Q., and Yang, J.S., 2003, Geochronological and geochemical constraints on Mesozoic suturing in east central Tibet: Tectonics, v. 22, no. 4, https://doi.org/10.1029/2002TC001466.

Roger, F., Malavieille, J., Leloup, P.H., Calassou, S., and Xu, Z., 2004, Timing of granite emplacement and cooling in the Songpan-Garzê fold belt (eastern Tibetan Plateau) with tectonic implications: Journal of Asian Earth Sciences, v. 22, p. 465–481, https://doi.org/10.1016/S1367-9120(03)00089-0.

Roger, F., Jolivet, M., and Malavieille, J., 2010, The tectonic evolution of the Songpan-Garzê (North Tibet) and adjacent areas from Proterozoic to present: A synthesis: Journal of Asian Earth Sciences, v. 39, no. 4, p. 254–269, https://doi.org/10.1016/j.jseaes.2010.03.008.

Şengör, A.M.C., 1984, The Cimmeride Orogenic System and the Tectonics of Eurasia: Geological Society of America Special Paper, v. 195, 74 p., https://doi.org/10.1130/SPE195-p1.

Şengör, A.M.C., Altıner, D., Cin, A., Ustaömer, T., and Hsü, K.J., 1988, Origin and assembly of the Tethyside orogenic collage at the expense of Gondwana Land, *in* Audley-Charles, M.G., and Hallam, A., eds., Gondwana and Tethys: Geological Society of London Special Publication, v. 37, p. 119–181, https://doi.org/10.1144/GSL.SP.1988.037.01.09.

Shao, F., Niu, Y., Kong, J., Liu, Y., Wang, G., and Zhang, Y., 2021, Petrogenesis and tectonic implications of the Triassic rhyolites in the East Kunlun Orogenic Belt, northern Tibetan Plateau: Geoscience Frontiers, v. 12, no. 6, no. 101243, https://doi.org/10.1016/j.gsf.2021.101243.

Shi, J.P., Huo, T.F., Lai, Q., Peng, X.H., Du, S.Y., and Yang, D.B., 2015, Petrogenesis of Early Silurian Gangchadasi granites in the eastern segment of the northern South Qilian Block: Constraints from LA-ICP-MS zircon U-Pb geochronology and geochemistry [in Chinese with English abstract]: Acta Geoscientica Sinica, v. 36, no. 6, p. 781–789.

Shi, J.P., Han, X.Z., Qiao, S.Y., Wang, Z.S., Huo, T.F., Yang, H.T., and Yang, D.B., 2017, The Late Ordovician tectonic evolution of the eastern section of the northern margin of the South Qilian Block: Evidences from geochronology, geochemistry and mineral chemistry of the Duozang hornblende gabbro [in Chinese with English abstract]: Earth Science Frontiers, v. 24, no. 6, p. 46–59.

Shi, R.D., Yang, J.S., and Wu, C.L., 2004, First SHRIMP dating for the formation of the late Sinian Yushigou ophiolite North Qilian Mountains [in Chinese with English abstract]: Acta Geologica Sinica, v. 78, p. 649–657.

Shu, L.S., Deng, X.L., Zhu, W.B., Ma, D.S., and Xiao, W.J., 2011, Precambrian tectonic evolution of the Tarim Block, NW China: New geochronological insights from the Quruqtagh domain: Journal of Asian Earth Sciences, v. 42, p. 774–790, https://doi.org/10.1016/j.jseaes.2010.08.018.

Sobel, E.R., and Arnaud, N., 1999, A possible middle Paleozoic suture in the Altyn Tagh, NW China: Tectonics, v. 18, p. 64–74, https://doi.org/10.1029/1998TC900023.

Song, S.G., Su, L., Li, X.H., Niu, Y.L., and Zhang, L.F., 2012, Grenville-age orogenesis in the Qaidam-Qilian block: The link between South China and Tarim: Precambrian Research, v. 220–221, p. 9–22, https://doi.org/10.1016/j.precamres.2012.07.007.

Song, S.G., Niu, Y.L., Su, L., and Xia, X., 2013, Tectonics of the North Qilian orogen, NW China: Gondwana Research, v. 23, no. 4, p. 1378–1401, https://doi.org/10.1016/j.gr.2012.02.004.

Song, S.G., Wu, Z.Z., Yang, L.M., Su, L., Xia, X.H., Wang, C., Dong, J.L., Zhou, C.A., and Bi, H.Z., 2019a, Ophiolite belts and evolution of the Proto-Tethys ocean in the Qilian Orogen: Yanshi Xuebao, v. 35, no. 10, p. 2948–2970, https://doi.org/10.18654/1000-0569/2019.10.2.

Song, S.G., Niu, Y.L., Zhang, G.B., and Zhang, L.F., 2019b, Two epochs of eclogite metamorphism link 'cold' oceanic subduction and 'hot' continental subduction, the North Qaidam UHP belt, NW China, ***in*** Zhang, L., Zhang, Z., Schertl, H.-P., and Wei, C., eds., HP–UHP Metamorphism and Tectonic Evolution of Orogenic Belts: Geological Society of London, Special Publications, v. 474, p. 275–289, https://doi.org/10.1144/SP474.2.

Song, T.Z., Liu, J.D., Li, J., Zhang, X.Y., Liang, K.X., and Zheng, Y., 2016, LA-ICP-MS zircon U-Pb age of gabbro and basalt in the Baimuxia area of North Qilian and its geological significance [in Chinese with English abstract]: Northwest Geology, v. 49, no. 4, p. 32–42.

Song, Z.B., Ren, Y.X., Li, Z.P., and Yang, J.G., 2004, A discussion on intrusion Epochs of granodiorites along the Bagexia-Heidaban zone in the western part of the North Qilian Mountains [in Chinese with English abstract]: Acta Geoscientica Sinica, v. 25, no. 2, p. 205–208.

Stampfli, G.M., and Borel, G.D., 2002, A plate tectonic model for the Paleozoic and Mesozoic constrained by dynamic plate boundaries and restored synthetic oceanic isochrones: Earth and Planetary Science Letters, v. 196, p. 17–33, https://doi.org/10.1016/S0012-821X(01)00588-X.

Su, J.P., Hu, N.G., Zhang, H.F., and Fu, G.M., 2004a, Single-zircon U-Pb dating and geological significance of the Diaodaban granitic gneiss in the western segment of North Qilian Mountains [in Chinese with English abstract]: Geological Science and Technology Information, v. 23, no. 3, p. 11–14.

Su, J.P., Hu, N.G., Zhang, H.F., and Feng, B.Z., 2004b, U-Pb zircon dating and genesis of the Heigouliangzi granitic intrusion in the western segment of the middle Qilian Mountains [in Chinese with English abstract]: Geoscience, v. 18, no. 1, p. 70–74.

Su, J.P., Zhang, X.H., Hu, N.G., Fu, G.M., and Zhang, H.F., 2004c, Geochemical characteristics and genesis of adakite-like granites at Yema Nanshan in the western segment of the central Qilian Mountains [in Chinese with English abstract]: Geology in China, v. 31, no. 4, p. 365–371.

Sundell, K.E., Laskowski, A.K., Kapp, P.A., Ducea, M.N., and Chapman, J.B., 2021, Jurassic to Neogene quantitative crustal thickness estimates in southern Tibet: GSA Today, v. 31, no. 6, https://doi.org/10.1130/GSATG461A.1.

Tan, S.X., Guo, T.Z., Dong, J.S., Chang, Y.Y., and Ma, W., 2011, Geological characteristics and significance of the peraluminous granite in Late Silurian epoch in Wulanwuzhuer region of Qinghai [Nature Science]: Journal of Qinghai University, v. 29, no. 1, p. 36–43.

Tao, G., Zhu, L.D., Li, Z.W., Ouyang, H.Z., Xie, L., Yang, W.G., and Yang, Z., 2017, Petrogenesis and geological significance of the North Liuhuangkuang granodiorite in the west segment of the Qilian Terrane: Evidences from geochronology, geochemistry, and Hf isotopes [in Chinese with English abstract]: Earth Science, v. 42, no. 12, p. 2258–2275.

Tian, C.X., Fu, Y.W., Zhang, J.M., and Zhang, Z.Q., 2018, Geochemical characteristics of Neoproterozoic gabbro from Cuolonggou area in North Qilian [in Chinese with English abstract]: Northwest Geology, v. 51, no. 1, p. 115–124.

Tseng, C.Y., Yang, H.Y., Wan, Y.S., Liu, D.Y.L., Wen, D.J., Lin, T.C., and Tung, K.A., 2006, Finding of

Neoproterozoic (~775 Ma) magmatism recorded in metamorphic complexes from the North Qilian orogen: Evidence from SHRIMP zircon U-Pb dating: Chinese Science Bulletin, v. 51, no. 8, p. 963–970, https://doi.org/10.1007/s11434-006-0963-1.

Tseng, C.Y., Yang, H.J., Yang, H.Y., Liu, D., Tsai, C.L., Wu, H., and Zuo, G., 2007, The Dongcaohe ophiolite from the North Qilian Mountains: A fossil oceanic crust of the Paleo-Qilian ocean: Chinese Science Bulletin, v. 52, p. 2390–2401, https://doi.org/10.1007/s11434-007-0300-3.

Tseng, C.Y., Yang, H.J., Yang, H.Y., Liu, D., Wu, C., Cheng, C.K., Chen, C.H., and Ker, C.M., 2009, Continuity of the North Qilian and North Qinling orogenic belts, Central Orogenic System of China: Evidence from newly discovered Paleozoic adakitic rocks: Gondwana Research, v. 16, no. 2, p. 285–293, https://doi.org/10.1016/j.gr.2009.04.003.

Tung, K.A., Yang, H.J., Yang, H.Y., Liu, D.Y., Zhang, J.X., Wan, Y.S., and Tseng, C.Y., 2007, SHRIMP U-Pb geochronology of the zircons from the Precambrian basement of the Qilian Block and its geological significances: Chinese Science Bulletin, v. 52, no. 19, p. 2687–2701, https://doi.org/10.1007/s11434-007-0356-0.

Tung, K.A., Yang, H.Y., Liu, D.Y., Zhang, J.X., Yang, H.J., Shau, Y.H., and Tseng, C.Y., 2013, The Neoproterozoic granitoids from the Qilian block, NW China: Evidence for a link between the Qilian and South China blocks: Precambrian Research, v. 235, p. 163–189, https://doi.org/10.1016/j.precamres.2013.06.016.

Wan, Y.S., Xu, Z.Q., Yang, J.S., and Zhang, J.X., 2001, Ages and compositions of the Precambrian high-grade basement of the Qilian Terrane and its adjacent areas: Acta Geologica Sinica, v. 75, no. 4, p. 375–384.

Wan, Y.S., Xu, Z.Q., Yang, J.S., and Zhang, J.X., 2003, The Precambrian high-grade basement of the Qilian terrane and neighboring areas: Its ages and compositions [in Chinese with English abstract]: Diqiu Xuebao, v. 24, no. 4, p. 319–324.

Wan, Y., Song, B., Liu, D., Wilde, S.A., Wu, J., Shi, Y., Yin, X., and Zhou, H., 2006, SHRIMP U-Pb zircon geochronology of Palaeoproterozoic metasedimentary rocks in the North China Craton: Evidence for a major late Palaeoproterozoic tectonothermal event: Precambrian Research, v. 149, p. 249–271, https://doi.org/10.1016/j.precamres.2006.06.006.

Wang, B.Z., 2011, The study and investigation on the assembly and coupling Petrotectonic assemblage during Paleozoic-Mesozoic period at Qimantage geological corridor domain [Ph.D. thesis] [in Chinese with English abstract]: Beijing, China, China University of Geosciences, 237 p.

Wang, C.Y., Yu, S., Sun, D., Lv, P., Feng, Z., Wang, G., and Gou, J., 2021, Mesoproterozoic tectonic-thermal events in the Oulongbuluke Block, NW China: Constraints on the transition from supercontinent Columbia to Rodinia: Precambrian Research, v. 352, no. 106010, https://doi.org/10.1016/j.precamres.2020.106010.

Wang, G., Sun, F.Y., Li, B.L., Li, S.J., Zhao, J.W., Yang, Q.A., and Ao, C., 2013a, Zircon U-Pb geochronology and geochemistry of the Early Devonian syenogranite in the Xiarihamu Ore District from East Kunlun, with implications for the geodynamic setting [in Chinese with English abstract]: Geotectonica et Metallogenia, v. 37, no. 4, p. 685–697.

Wang, G., Sun, F.Y., Li, B.L., Ao, Z., Li, S.J., Zhao, J.W., and Yang, Q.A., 2016, Geochronology [in Chinese with English abstract]: Geochemistry and tectonic implication of early Neoproterozoic monzogranite in Xiarihamu Ore District from East Kunlun: Geotectonica et Metallogenia, v. 40, no. 6, p. 1247–1260.

Wang, G.C., Chen, N.S., Zhu, Y.H., and Zhang, K.X., 2003, Late Caledonian ductile thrusting deformation in the central East Kunlun Belt, Qinghai, China and its significance: Evidence from geochronology: Acta Geologica Sinica, v. 77, no. 3, p. 311–319, https://doi.org/10.1111/j.1755-6724.2003.tb00747.x.

Wang, G.L., Chen, F.B., Li, W.F., Cao, J.S., Han, H.C., Liu, R., and Bao, G.P., 2018a, Discussion on the relationship between the Longwangshan granite mass and the Huashixia W-Mo deposit in the transitional belt of northern-central Qilian [in Chinese with English abstract]: Northwest Geology, v. 51, no. 4, p. 227–243.

Wang, G.L., Ren, E.F., Bao, G.P., Li, J.F., and Chang, Y.Y., 2013b, U-Pb age of zircons of Qimantage late-Devonian intrusive rocks, geochemical characteristics and its geological significance, Qinghai [in Chinese with English abstract]: Mineral Exploration, v. 4, no. 4, p. 421–434.

Wang, J., Xie, G., Shi, G.H., and Wang, Y., 2018b, Geochronology of the Chuancigou A-type granite in the North Qilian belt and its significances [in Chinese with English abstract]: Yanshi Xuebao, v. 34, no. 6, p. 1657–1668.

Wang, L.Q., Pan, G.T., Ding, J., and Yao, D.S., 2013c, Geological Map of the Tibetan Plateau at a Scale of 1:1.5 M with Explanations: Beijing, China, Geological Publishing House, 288 p.

Wang, N., Wu, C.L., Lei, M., Chen, H.J., Li, M.Z., and Zheng, W.H., 2017a, Geochronology and petrogenesis of granite in Shibaocheng area from the North Qilian orogenic belt [in Chinese with English abstract]: Yanshi Xuebao, v. 33, no. 12, p. 3909–3924.

Wang, Q., Chen, N., Li, X., Hao, S., and Chen, H., 2008, LA-ICPMS zircon U-Pb geochronological constraints on the tectonothermal evolution of the early Paleoproterozoic Dakendaban Group in the Quanji Block, NW China: Chinese Science Bulletin, v. 53, p. 2849–2858.

Wang, Q., Yang, D., and Xu, W., 2012, Neoproterozoic basic magmatism in the southeast margin of North China Craton: Evidence from whole-rock geochemistry, U-Pb and Hf isotopic study of zircons from diabase swarms in the Xuzhou-Huaibei area of China: Science China. Earth Sciences, v. 55, p. 1461–1479, https://doi.org/10.1007/s11430-011-4237-7.

Wang, Q.H., Luo, Y.H., and Li, Z.P., 2017b, Geochemistry characteristics and tectonic setting analysis of Zhahuaqiangzi granite in western Qilian, Gansu [in Chinese]: Gansu Science and Technology, v. 33, no. 11, p. 21–25.

Wang, Z.Z., Han, B.F., Feng, C.Y., and Li, G.C., 2014, Geochronology, geochemistry and tectonic significance of granites in Baiganhu area, Xinjiang [in Chinese with English abstract]: Acta Petrologica et Mineralogica, v. 33, no. 4, p. 597–616.

Webb, L.E., and Johnson, C.L., 2006, Tertiary strike-slip faulting in southeastern Mongolia and implications for Asian tectonics: Earth and Planetary Science Letters, v. 241, no. 1–2, p. 323–335, https://doi.org/10.1016/j.epsl.2005.10.033.

Wei, X.L., Zhang, D.X., Gan, C.P., and Chen, L.B., 2016, Discovery and geological significance of Neoproterozoic intrusive body in the Kaerqueka area of the East Kunlun mountain [in Chinese with English abstract]: Contributions to Geology and Mineral Resources Research, v. 31, no. 2, p. 236–244.

Weislogel, A.L., 2008, Tectonostratigraphic and geochronologic constraints on evolution of the northeast Paleotethys from the Songpan-Ganzi complex, central China: Tectonophysics, v. 451, p. 331–345, https://doi.org/10.1016/j.tecto.2007.11.053.

Wen, B., Evans, D.A., and Li, Y.X., 2017, Neoproterozoic paleogeography of the Tarim Block: An extended or alternative "missing-link" model for Rodinia?: Earth and Planetary Science Letters, v. 458, p. 92–106, https://doi.org/10.1016/j.epsl.2016.10.030.

Wen, B., Evans, D.A., Wang, C., Li, Y.X., and Jing, X., 2018, A positive test for the Greater Tarim Block at the heart of Rodinia: Mega-dextral suturing of supercontinent assembly: Geology, v. 46, no. 8, p. 687–690, https://doi.org/10.1130/G40254.1.

Windley, B.F., Alexeiev, D., Xiao, W., Kröner, A., and Badarch, G., 2007, Tectonic models for accretion of the Central Asian Orogenic Belt: Journal of the Geological Society, v. 164, no. 1, p. 31–47, https://doi.org/10.1144/0016-76492006-022.

Wu, C.C., Yang, J.S., Wooden, J.L., Shi, R.D., Chen, S.Y., Meibom, A., and Mattinson, C., 2004a, Zircon U-Pb SHRIMP dating of the Yematan batholith in Dulan, North Qaidam, NW China: Chinese Science Bulletin, v. 49, no. 16, p. 1736–1740, https://doi.org/10.1007/BF03184308.

Wu, C., Yin, A., Zuza, A.V., Zhang, J., Liu, W., and Ding, L., 2016a, Pre-Cenozoic geologic history of the central and northern Tibetan Plateau and the role of Wilson cycles in constructing the Tethyan orogenic system: Lithosphere, v. 8, no. 3, p. 254–292, https://doi.org/10.1130/L494.1.

Wu, C., Liu, C., Zhu, Y., Zhou, Z., Jiang, T., Liu, W., and Ye, B., 2016b, Early Paleozoic magmatic history of central Inner Mongolia, China: implications for the tectonic evolution of the Southeast Central Asian Orogenic Belt: International Journal of Earth Sciences, v. 105, no. 5, p. 1307–1327, https://doi.org/10.1007/s00531-015-1250-7.

Wu, C., Zhou, Z., Zuza, A.V., Wang, G., Liu, C., and Jiang, T., 2018, A 1.9-Ga Mélange Along the Northern Margin of the North China Craton: Implications for the Assembly of Columbia Supercontinent: Tectonics, v. 37, no. 10, p. 3610–3646, https://doi.org/10.1029/2018TC005103.

Wu, C., Zuza, A.V., Yin, A., Liu, C.F., Reith, R.C., Zhang, J.Y., Liu, W.C., and Zhou, Z.G., 2017, Geochronology and geochemistry of Neoproterozoic granitoids in the central Qilian Shan of northern Tibet: Reconstructing the amalgamation processes and tectonic history of Asia: Lithosphere, v. 9, no. 4, p. 609–636, https://doi.org/10.1130/L640.1.

Wu, C., Zuza, A.V., Chen, X., Ding, L., Levy, D.A., Liu, C., Liu, W., Jiang, T., and Stockli, D.F., 2019a, Tectonics of the Eastern Kunlun Range: Cenozoic Reactivation of a Paleozoic-Early Mesozoic Orogen: Tectonics, v. 38, no. 5, p. 1609–1650, https://doi.org/10.1029/2018TC005370.

Wu, C., Zuza, A.V., Zhou, Z.G., Yin, A., McRivette, M.W., Chen, X.H., Ding, L., and Geng, J.Z., 2019b, Mesozoic-Cenozoic evolution of the Eastern Kunlun Range, central Tibet, and implications for basin evolution within the Indo-Asian collision: Lithosphere, v. 11, no. 4, p. 524–550, https://doi.org/10.1130/L1065.1.

Wu, C., Liu, C.F., Fan, S., Zuza, A.V., Ding, L., Liu, W.C., Ye, B., Yang, S., and Zhou, Z., 2020, Structural analysis and tectonic evolution of the western domain of the Eastern Kunlun Range, northwest Tibet: Geological Society of America Bulletin, v. 132, no. 5–6, p. 1291–1315, https://doi.org/10.1130/B35388.1.

Wu, C., Zuza, A. V., Yin, A., Chen, X. H., Haproff, P. J., Li, J., Li, B., and Ding, L., 2021, Punctuated orogeny during the assembly of Asia: Tectonostratigraphic evolution of the North China Craton and the Qilian Shan from the Paleoproterozoic to early Paleozoic: Tectonics, v. 40, no. 4, https://doi.org/10.1029/2020TC006503.

Wu, C.L., Yang, J.S., Yang, H.Y., Wooden, J.L., Shi, R.D., Chen, S.Y., and Zheng, Q.G., 2004b, Dating of two types of granite from north Qilian, China [in Chinese with English abstract]: Yanshi Xuebao, v. 20, no. 3, p. 425–432.

Wu, C.L., Gao, Y.H., Wu, S.P., Chen, Q.L., Wooden, J.L., Mazadab, F.K., and Mattinson, C., 2007, Zircon SHRIMP U-Pb dating of granites from the Da Qaidam area in the north margin of Qaidam basin, NW China [in Chinese with English abstract]: Yanshi Xuebao, v. 23, no. 8, p. 1861–1875.

Wu, C.L., Wooden, J.L., Robinson, P.T., Gao, Y., Wu, S., Chen, Q., Mazdab, F.K., and Mattinson, C., 2009a, Geochemistry and zircon SHRIMP U-Pb dating of granitoids from the west segment of the North Qaidam: Science in China. Series D, Earth Sciences, v. 52, no. 11, p. 1771–1790, https://doi.org/10.1007/s11430-009-0147-3.

Wu, C.L., Yang, J., Robinson, P.T., Wooden, J.L., Mazdab, F.K., Gao, Y., and Chen, Q., 2009b, Geochemistry, age and tectonic significance of granitic rocks in north Altun, northwest China: Lithos, v. 113, no. 3–4, p. 423–436, https://doi.org/10.1016/j.lithos.2009.05.009.

Wu, C.L., Xu, X.Y., Gao, Q.M., Li, X.M., Lei, M., Gao, Y.H., Frost, R.B., and Wooden, J.L., 2010, Early Paleozoic granitoid magmatism and tectonic evolution in North Qilian, NW China [in Chinese with English abstract]: Yanshi Xuebao, v. 26, no. 4, p. 1027–1044.

Wu, C.L., Gao, Y., Frost, B.R., Robinson, P.T., Wooden, J.L., Wu, S.P., Chen, Q.L., and Lei, M., 2011a, An early Palaeozoic double-subduction model for the North Qilian oceanic plate: Evidence from zircon SHRIMP dating of granites: International Geology Review, v. 53, no. 2, p. 157–181, https://doi.org/10.1080/00206810902965346.

Wu, L., Liu, C.F., Liu, W.C., and Zhang, H.Y., 2021, The detrital-zircon U-Pb dating and provenance analysis for the Triassic sandstone in Qilianshan Orogen, NE Margin of Tibetan Plateau (in Chinese with English abstract): Geoscience, v. 35, no. 5, p. 1–16, https://doi.org/10.19657/j.geoscience.1000-8527.2020.096.

Wu, W.Z., Ma, R.Y., Zhang, X.D., Ma, F.H., Pan, J.L., and Wang, Z.J., 2019c, Geochemical characteristics, zircon U-Pb ages of the gabbro in Xiji region in the Eastern segment Northern Qilian Mountains and their significance [in Chinese with English abstract]: Dizhi Lunping, v. 65, no. 1, p. 211–220.

Wu, X.K., Meng, F.C., Xu, H., and Cui, M.H., 2011b, Zircon U-Pb dating, geochemistry and Nd-Hf isotopic compositions of the Maxingdaban Late Triassic granitic pluton from Qimantag in the eastern Kunlun [in Chinese with English abstract]: Yanshi Xuebao, v. 27, no. 11, p. 3380–3394.

Xi, R.G., Xiao, P.X., Wu, Y.Z., Dong, Z.C., Guo, L., and Gao, X.F., 2010, The geological significances, composition and age of the monzonitic granite in Kendekeke Iron Mine [in Chinese with English abstract]: Northwest Geology, v. 43, no. 4, p. 195–202.

Xia, L.Q., Xia, Z.C., and Xu, X.Y., 2003, Magmagenesis in the Ordovician in back basins of the northern Qilian Mountains, China: Geological Society of America Bulletin, v. 115, p. 1510–1522, https://doi.org/10.1130/B25269.1.

Xia, L.Q., Li, X.M., Yu, J.Y., and Wang, G.Q., 2016, Mid-late Neoproterozoic to early Paleozoic volcanism and tectonic evolution of the Qilianshan, NW China: GeoResJ, v. 9, p. 1–41, https://doi.org/10.1016/j.grj.2016.06.001.

Xiao, W.J., Windley, B.F., Yong, Y., Yan, Z., Yuan, C., Liu, C.Z., and Li, J.L., 2009, Early Paleozoic to Devonian multiple-accretionary model for the Qilian Shan, NW China: Journal of Asian Earth Sciences, v. 35, p. 323–333, https://doi.org/10.1016/j.jseaes.2008.10.001.

Xiao, Y., Feng, C.Y., Liu, J.N., Yu, M., Zhou, J.H., Li, D.X., and Zhao, Y.M., 2013, LA-MC-ICP-MS zircon U-Pb dating and sulfur isotope characteristics of Kendekeke Fe-polymetallic deposit [in Chinese with English abstract]: Qinghai Province: Mineral Deposits, v. 32, no. 1, p. 177–186.

Xie, Q.F., Zhou, L.F., and Liu, Y., 2014, LA-ICP-MS zircon U-Pb ages of Gangchadasi granite in Qinghai Province and their geological significance [in Chinese with English abstract]: Geological Bulletin of China, v. 33, no. 9, p. 1379–1390.

Xiong, Z.L., Zhang, H.F., and Zhang, J., 2012, Petrogenesis and tectonic implications of the Maozangshi and Huangyanghe granitic intrusions in Lenglongling area, the eastern part of North Qilian Mountains, NW China [in Chinese with English abstract]: Earth Science Frontiers, v. 19, no. 3, p. 214–227.

Xu, W.C., Zhang, H.F., and Liu, X.M., 2007, U-Pb zircon dating constraints on formation time of Qilian highgrade metamorphic rock and its tectonic implications: Chinese Science Bulletin, v. 52, no. 4, p. 531–538, https://doi.org/10.1007/s11434-007-0082-7.

Xu, X., Song, S., Su, L., Li, Z., Niu, Y., & Allen, M. B., 2015, The 600–580 Ma continental rift basalts in north Qilian Shan, northwest China: Links between the Qilian-Qaidam block and SE Australia, and the reconstruction of east Gondwana: Precambrian Research, v. 257, no. 47–64, https://doi.org/10.1016/j.precamres.2014.11.017.

Xu, Y.J., Du, Y.S., Cawood, P.A., Guo, H., Huang, H., and An, Z.H., 2010, Detrital zircon record of continental collision: assembly of the Qilian Orogen, China: Sedimentary Geology, v. 230, no. 1–2, p. 35–45, https://doi.org/10.1016/j.sedgeo.2010.06.020.

Xu, Y.L., Ba, J., Wang, Q.Y., Zhang, L., Wang, X.Y., and Chen, N.S., 2011, LA-ICP-MS zircon U-Pb age of the Halihadeshan granite-gneiss in northeastern Dulan, Qinghai, and its tectonic implications [in Chinese with English abstract]: Geological Bulletin of China, v. 30, no. 7, p. 1037–1042.

Xue, N., Wang, J., Tan, S.X., Lin, H., Li, W.F., Ren, J.Q., and Liu, S.J., 2009, Geological significance of granite of Jinningian age in Yeniugou-Tuole region on the northern margin of central Qilian Block [Nature Science]: Journal of Qinghai University, v. 27, no. 4, p. 23–28.

Yan, Z., Xiao, W., Wang, Z., and Li, J., 2007, Integrated analyses constraining the provenance of sandstones, mudstones, and conglomerates, a case study: The Laojunshan conglomerate, Qilian orogen, northwest China: Canadian Journal of Earth Sciences, v. 44, no. 7, p. 961–986, https://doi.org /10.1139/e07-010.

Yan, Z., Xiao, W.J., Windley, B.F., Wang, Z.Q., and Li, J.L., 2010, Silurian clastic sediments in the North Qilian Shan, NW China: Chemical and isotopic constraints on their forearc provenance with implications for the Paleozoic evolution of the Tibetan Plateau: Sedimentary Geology, v. 231, no. 3–4, p. 98–114, https://doi.org/10.1016/j.sedgeo.2010.09.001.

Yan, Z., Aitchison, J., Fu, C., Guo, X., Niu, M., Xia, W., and Li, J., 2015, Hualong Complex, South Qilian terrane: U-Pb and Lu-Hf constraints on Neoproterozoic micro-continental fragments accreted to the northern Proto-Tethyan margin: Precambrian Research, v. 266, p. 65–85, https://doi.org/10.1016/j.precamres.2015.05.001.

Yan, Z., Fu, C., Aitchison, J.C., Buckman, S., Niu, M., and Cao, B., 2019, Retro-foreland basin in the NE Tibet Plateau: Tectonics, v. 38, p. 4229–4248, https://doi.org/10.1029/2019TC005560.

Yang, H., 2016, Early Paleozoic intrusive magmatism and geodynamic processes in the eastern segment of the Central Qilian [Ph.D. thesis] [in Chinese with English abstract]: Wuhan, China, China University of Geosciences, 154 p.

Yang, H., Wu, G., Kusky, T.M., Chen, Y., and Xiao, Y., 2018, Paleoproterozoic assembly of the North and South Tarim terranes: New insights from deep seismic profiles and Precambrian granite cores: Precambrian Research, v. 305, p. 151–165, https://doi.org/10.1016/j.precamres.2017.11.015.

Yang, H., Zhang, H., Xiao, W., Luo, B., Gao, Z., Tao, L., Zhang, L., and Guo, L., 2020, Petrogenesis of Early Paleozoic high Sr/Y intrusive rocks from the North Qilian orogen: Implication for diachronous continental collision: Lithosphere, v. 12, no. 1, p. 53–73, https://doi.org/10.1130/L1129.1.

Yang, J.H., Du, Y.S., Cawood, P.A., and Xu, Y.J., 2009, Silurian collisional suturing onto the southern margin of the North Craton: Detrital zircon geochronology constraints from the Qilian orogen: Sedimentary Geology, v. 220, p. 95–104, https://doi.org/10.1016/j.sedgeo.2009.07.001.

Yang, J.S., Robinson, P.T., Jiang, C.F., and Xu, Z.Q., 1996, Ophiolites of the Kunlun Mountains, China, and their tectonic implications: Tectonophysics, v. 258, p. 215–231, https://doi.org/10.1016/0040-1951(95)00199-9.

Yang, S., Pei, X.Z., Li, R.B., Liu, C.J., Chen, Y.X., Li, Z.C., Wang, X.B., Sang, J.Z., Chen, G., and Deng, W.B., 2016, Provenance analysis and structural implications of Gequ Formation at the Buqingshan area in the eastern segment of the East Kunlun region [in Chinese with English abstract]: Geological Bulletin of China, v. 35, no. 5, p. 674–686.

Yao, L., Lv, Z.C., Zhao, C.S., Pang, Z.S., Yu, X.F., Zhu, X.Y., Li, Y.S., Liu, P., Li, S.T., and Zhang, M.C., 2016, Geochronological study of granitoids from the Niukutou and B section of the Kaerqueka deposits, Qimantag area, Qinghai Province: Implications for Devonian magmatism and mineralization [in Chinese with English abstract]: Geological Bulletin of China, v. 35, no. 7, p. 1158–1169.

Yin, A., and Harrison, T.M., 2000, Geologic evolution of the Himalayan-Tibetan orogen: Annual Review of Earth and Planetary Sciences, v. 28, p. 211–280, https://doi.org/10.1146/annurev.earth.28.1.211.

Yin, A., and Nie, S., 1996, A Phanerozoic palinspastic reconstruction of China and its neighboring regions, *in* Yin, A., and Harrison, T.M., The Tectonic Evolution of Asia: New York, USA, Cambridge University Press, p. 442–485.

Yin, A., Manning, C.E., Lovera, O., Menold, C.A., Chen, X., and Gehrels, G.E., 2007, Early Paleozoic tectonic and thermomechanical evolution of ultrahigh-pressure (UHP) metamorphic rocks in the northern Tibetan Plateau, northwest China: International Geology Review, v. 49, no. 8, p. 681–716, https://doi.org/10.2747/0020-6814.49.8.681.

Yin, A., Dang, Y.-Q., Wang, L.-C., Jiang, W.-M., Zhou, S.-P., Chen, X.-H., Gehrels, G.E., and McRivette, M.W., 2008a, Cenozoic tectonic evolution of Qaidam basin and its surrounding regions (Part 1): The southern Qilian Shan-Nan Shan thrust belt and northern Qaidam basin: Geological Society of America Bulletin, v. 120, no. 7–8, p. 813–846, https://doi.org/10.1130/B26180.1.

Yin, A., Dang, Y.Q., Zhang, M., Chen, X.H., and McRivette, M.W., 2008b, Cenozoic tectonic evolution of the Qaidam basin and its surrounding regions (Part 3): Structural geology, sedimentation, and regional tectonic reconstruction: Geological Society of America Bulletin, v. 120, no. 7–8, p. 847–876, https://doi.org/10.1130/B26232.1.

Yong, Y., Xiao, W.J., Yuan, C., Li, J.L., Yan, Z., and Mao, Q.G., 2008, LA-ICP-MS Zircon U-Pb ages of granitic plutons from the eastern sector of the central Qilian and their geologic implication [in Chinese with English abstract]: Xinjiang Geology, v. 26, no. 1, p. 62–70.

Yu, J.Y., Li, X.M., Ma, Z.P., Tang, Z., Wang, G.Q., Sun, J.M., and Wu, P., 2012, The LA-ICP-MS U-Pb age and geological significance of Hualong rock group in South Qilian Mountains [in Chinese with English Abstract]: Northwest Geology, v. 45, no. 1, p. 79–85.

Yu, M., Feng, C.Y., Santosh, M., Mao, J.W., Zhu, Y.F., Zhao, Y.M., and Li, B., 2017a, The Qiman Tagh orogen as a window to the crustal evolution in northern Qinghai-Tibet Plateau: Earth-Science Reviews, v. 167, p. 103–123, https://doi.org/10.1016/j.earscirev.2017.02.008.

Yu, S., Peng, Y., Zhang, J., Li, S., Santosh, M., Li, Y., Liu, Y., Gao, X., Ji, W., Lv, P., Li, C., Jiang, X., Qi, L., Xie, W., and Xu, L., 2021, Tectono-thermal evolution of the Qilian orogenic system: Tracing the subduction, accretion and closure of the Proto-Tethys Ocean: Earth-Science Reviews, v. 215, no. 103547, https://doi.org/10.1016/j.earscirev.2021.103547.

Yu, S.Y., Zhang, J., del Real, P.G., Zhao, X., Hou, K., Gong, J., and Li, Y., 2013a, The Grenvillian orogeny in the Altun-Qilian-North Qaidam mountain belts of northern Tibet Plateau: Constraints from geochemical and zircon U-Pb age and Hf isotopic study of magmatic rocks: Journal of Asian Earth Sciences, v. 73, p. 372–395, https://doi.org/10.1016/j.jseaes.2013.04.042.

Yu, S.Y., Zhang, J., Li, H., Hou, K., Mattinson, C.G., and Gong, J., 2013b, Geochemistry, zircon U-Pb geochronology and Lu-Hf isotopic composition of eclogites and their host gneisses in the Dulan area, North Qaidam UHP terrane: New evidence for deep continental subduction: Gondwana Research, v. 23, no. 3, p. 901–919, https://doi.org/10.1016/j.gr.2012.07.018.

Yu, S.Y., Zhang, J.X., Qin, H.P., Sun, D.Y., Zhao, X.L., Cong, F., and Li, Y.S., 2015, Petrogenesis of the early Paleozoic low-Mg and high-Mg adakitic rocks in the North Qilian orogenic belt, NW China: Implications for transition from crustal thickening to extension thinning: Journal of Asian Earth Sciences, v. 107, p. 122–139, https://doi.org/10.1016/j.jseaes.2015.04.018.

Yu, X., Fu, S., Wang, Z., Li, Q., and Guo, Z., 2017b, The discovery of early Paleoproterozoic high-Na trondhjemite in the northeastern Qaidam basin: Evidence from the drilling core samples: Precambrian Research, v. 298, p. 615–628, https://doi.org/10.1016/j.precamres.2017.04.002.

Yu, X.L., Cai, C.L., Wei, X.L., Liu, X.X., and Yue, X., 2018a, Zircon U-Pb geochronology, geochemical characteristics and geological significance of middle Ordovician intrusive rocks in Shulenanshan area of South Qilian [in Chinese with English abstract]: Mineral Exploration, v. 9, no. 11, p. 2049–2058.

Yu, X.L., Cai, C.L., Zhang, S.L., Wei, X.L., and Liu, X.X., 2018b, Petrogenesis of early Silurian intrusive rocks in Yeniujishan area of South Qilian: Constraints from geochemistry and LA-ICP-MS zircon U-Pb geochronology [in Chinese with English abstract]: Northwest Geology, v. 51, no. 4, p. 133–146.

Yu, X., Guo, Z., Guan, S., Du, W., Wang, Z., Bian, Q., and Li, L., 2019, Landscape and tectonic evolution of Bayin River watershed, northeastern Qaidam basin, northern Tibetan Plateau: Implications for the role of river morphology in source analysis and low-temperature thermochronology: Journal of Geophysical Research. Earth Surface, v. 124, p. 1701–1719, https://doi.org/10.1029/2018JF004989.

Zhang, G., Song, S., Zhang, L., and Niu, Y., 2008a, The subducted oceanic crust within continental-type UHP metamorphic belt in the North Qaidam, NW China:

Evidence from petrology, geochemistry and geochronology: Lithos, v. 104, no. 1–4, p. 99–118, https://doi.org/10.1016/j.lithos.2007.12.001.

Zhang, G.D., Xu, Z.Q., Gong, J., Feng, J., Han, Y.B., Zhang, J.W., Zhou, Y., Huang, Z.S., Zeng, X.F., Zhang, K.J., Wang, J.K., and Cheng, J., 2016a, Geochronology and significance of intermediate-acid intrusive rocks in Quanji Area, Gangcha, Qinghai [in Chinese with English abstract]: Gaoxiao Dizhi Xuebao, v. 22, no. 1, p. 113–126.

Zhang, H.R., Zhao, J.L., and Yu, H.Y., 2019, Petrogenesis and tectonic implications of the Laohushan quartz diorite from the eastern part of North Qilian Orogen, NW China [in Chinese with English abstract]: Gaoxiao Dizhi Xuebao, v. 25, no. 5, p. 641–653.

Zhang, L.L., 2014, The geochemistry and its tectonic significance of granitic rocks in Danghenanshan region, South Qilian Mt. [M.A. thesis] [in Chinese with English abstract]: Lanzhou, China, Lanzhou University, 93 p.

Zhang, L.T., Yu, J.P., Zhao, J.C., Fan, X.X., and Chen, S.X., 2018a, LA-ICP-MS zircon U-Pb age, geochemistry of Chaidano Mountain granite mass in the western part of north Qilian [in Chinese with English abstract]: Gansu Geology, v. 37, no. 3–4, p. 8–16.

Zhang, J., Mattinson, C.G., Meng, F., Wan, Y., and Tung, K., 2008b, Polyphase tectonothermal history recorded in granulitized gneisses from the north Qaidam HP/UHP metamorphic terrane, western China: Evidence from zircon U-Pb geochronology: Geological Society of America Bulletin, v. 120, no. 5–6, p. 732–749, https://doi.org/10.1130/B26093.1.

Zhang, J.M., Chen, G.T., Cai, H.J., and Fu, Y.W., 2018b, Zircon U-Pb age dating of the diorite in the Suli area of central Qilian Mountains: Its geological significance [in Chinese with English abstract]: Journal of Mineral Petrology, v. 38, no. 1, p. 20–26.

Zhang, J.X., Meng, F.C., and Wan, Y.S., 2007, A cold early Palaeozoic subduction zone in the North Qilian Mountains, NW China: Petrological and U-Pb geochronological constraints: Journal of Metamorphic Geology, v. 25, p. 285–304, https://doi.org/10.1111/j.1525-1314.2006.00689.x.

Zhang, J.X., Yu, S., and Mattinson, C.G., 2017a, Early Paleozoic polyphase metamorphism in northern Tibet, China: Gondwana Research, v. 41, p. 267–289, https://doi.org/10.1016/j.gr.2015.11.009.

Zhang, J.Y., Ma, C.Q., Xiong, F.H., and Liu, B., 2012a, Petrogenesis and tectonic significance of the Late Permian-Middle Triassic calc-alkaline granites in the Balong region, eastern Kunlun Orogen, China: Geological Magazine, v. 149, no. 5, p. 892–908, https://doi.org/10.1017/S0016756811001142.

Zhang, J.Y., Ma, C.Q., Xiong, F.H., Liu, B., Li, J.W., and Pan, Y.M., 2014a, Early Paleozoic high-Mg diorite-granodiorite in the eastern Kunlun Orogen, western China: Response to continental collision and slab break-off: Lithos, v. 210–211, p. 129–146, https://doi.org/10.1016/j.lithos.2014.10.003.

Zhang, L.Q., Zhang, H., Zhang, S., Xiong, Z., Luo, B., Yang, H., Pan, F.B., Zhou, X.C., Xu, W.C., and Guo, L., 2017b, Lithospheric delamination in post-collisional setting: Evidence from intrusive magmatism from the North Qilian orogen to southern margin of the Alxa block, NW China: Lithos, v. 288–289, p. 20–34, https://doi.org/10.1016/j.lithos.2017.07.009.

Zhang, L.Y., Ding, L., Pullen, A., Xu, Q., Liu, D.L., Cai, F.L., Yue, Y.H., Lai, Q.Z., Shi, R.D., Ducea, M.N., Kapp, P., and Chapman, A., 2014b, Age and geochemistry of western Hoh-Xil-Songpan-Ganzi granitoids, northern Tibet: Implications for the Mesozoic closure of the Paleo-Tethys ocean: Lithos, v. 190–191, p. 328–348, https://doi.org/10.1016/j.lithos.2013.12.019.

Zhang, Q., Ding, Q.F., Song, K., and Chen, L., 2018c, Detrital zircon U-Pb geochronology and Hf isotope of phyllite of Langyashan Formation in Hongshuihe Iron Ore District of Eastern Kunlun and their geological significance [Earth Science Edition]: Journal of Jilin University, v. 48, no. 4, p. 1085–1104.

Zhang, X., Zhang, L. L., Wang, L. B., Liu, B., Dai, S., Jin, Z. P., Meng, Z., & Yang, H. Y., 2015a, Zircon U-Pb geochronology and geochemical characteristics of neutral-acidic intrusions of Wuligou in South Qilian Mountains: Their implications on forming gold deposit [in Chinese with English abstract]: Journal of Chengdu University of Technology (Science & Technology Edition), v. 42, no. 5, p. 596–607.

Zhang, X.Y., Wang, C.T., Ouyang, G.W., and Li, R.B., 2018d, Zircon U-Pb ages and their geological significance of Aoguotunwulan pluton in South Qilian, China [in Chinese with English abstract]: Diqiu Kexue Yu Huanjing Xuebao, v. 40, no. 5, p. 546–562.

Zhang, Y., Zhao, Y.L., Li, H.H., Zhang, S., Zhou, Q.L., and Xiong, Y.L., 2016b, Zircon U-Pb dating and geological significance of monzonitic granite of Kayakedeng zinc polymetallic deposit in Qinghai [in Chinese with English abstract]: Contributions to Geology and Mineral Resources Research, v. 31, no. 1, p. 47–54.

Zhang, Y.P., Zhang, J., Chen, X.H., Wang, Y.N., Zhao, H., Nie, F.J., and Zhang, B.H., 2017c, Late Palaeozoic tectonic setting of the southern Alxa Block, NW China: Constrained by age and composition of diabase: International Geology Review, v. 59, no. 8, p. 1028–1046, https://doi.org/10.1080/00206814.2016.1253036.

Zhang, Z.W., Li, W.Y., Gao, Y.B., Zhang, J.W., Guo, Z.P., and Li, K., 2012b, ID-TIMS zircon U-Pb age of Yulonggou intrusive rocks in southern Qilian Mountain and its geological significance [in Chinese with English abstract]: Geological Bulletin of China, v. 31, no. 2–3, p. 455–462.

Zhang, Z.W., Li, W.Y., Gao, Y.B., Li, C.S., Ripley, E.M., and Kamo, S., 2014c, Sulfide mineralization associated with arc magmatism in the Qilian Block, western China: Zircon U-Pb age and Sr-Nd-Os-S isotope constraints from the Yulonggou and Yaqu gabbroic intrusions: Mineralium Deposita, v. 49, p. 279–292, https://doi.org/10.1007/s00126-013-0488-x.

Zhang, Z.W., Li, W.Y., Wang, Y.L., and Gao, Y.B., 2015b, The genesis study on Xiashentang basic-ultrabasic intrusion associated with Ni-Cu mineralization in Hualong, southern Qilian Mountains: Zircon geochronology, geochemistry and Sr-Nd isotopic constraints [in Chinese with English abstract]: Yanshi Xuebao, v. 31, no. 9, p. 2539–2548.

Zhao, G.B., Yang, H.Q., Ren, H.N., Jia, J., Wang, Y.H., Li, J.C., and Zhou, H., 2013, LA-ICP-MS zircon U-Pb ages of Heishishan granite bodies in north Qilian and their geological significance [in Chinese with English abstract]: Geological Bulletin of China, v. 32, no. 10, p. 1575–1583.

Zhao, P., He, J., Deng, C., Chen, Y., and Mitchell, R.N., 2021, Early Neoproterozoic (870–820 Ma) amalgamation of the Tarim craton (northwestern China) and the final assembly of Rodinia: Geology, https://doi.org/10.1130/G48837.1.

Zhao, X.M., Guo, Z.P., Wang, Y.X., Gao, Y.W., Zhang, L., Bai, Y., and Yang, S.F., 2018, Zircon U-Pb age, geochemical characteristics and geological significance of granitoids in the Maozangsi deposit, Northern Qilian Mountain [in Chinese with English abstract]: Geological Bulletin of China, v. 37, no. 4, p. 669–681.

Zhao, X.M., Zhang, Z.H., Liu, M., Li, Y.S., and Guo, S.F., 2014, Zircon U-Pb geochronology, geochemistry and petrogenesis of the granites from the Xiaoliugou deposit in the western of the North Qilian [in Chinese with English abstract]: Yanshi Xuebao, v. 30, no. 1, p. 16–34.

Zhao, Z.M., Ma, H.D., Wang, B.Z., Bai, Y.S., Li, R.S., and Ji, W.H., 2008, The evidence of intrusive rocks about collision-orogeny during Early Devonian in Eastern Kunlun Area [in Chinese with English abstract]: Dizhi Lunping, v. 54, no. 1, p. 47–56.

Zheng, Y., Chen, G.T., Zhang, X.Y., Song, T.Z., and Liang, K.X., 2017, Geochemical characteristics and chronology significance of Ordovician quartz diorite from Suli area in Middle Qilian Mountains [in Chinese with English abstract]: Northwest Geology, v. 50, no. 4, p. 9–17.

Zhou, B., Zheng, Y.Y., Tong, H.K., Xu, R.K., Nie, X.L., Ma, C., and Liu, Q., 2014, Zircon dating of early adakitic granite on the northern margin of Qaidam Basin and its geological significance [in Chinese with English abstract]: Geoscience, v. 28, no. 5, p. 875–883.

Zhou, C.A., Song, S., Allen, M.B., Wang, C., Su, L., and Wang, M., 2021, Post-collisional mafic magmatism: Insights into orogenic collapse and mantle modification from North Qaidam collisional belt, NW China: Lithos, v. 398–399, no. 106311, https://doi.org/10.1016/j.lithos.2021.106311.

Zhou, J.H., Feng, C.Y., Shen, D.L., Li, D.X., Wang, H., Zhang, M.Y., and Ma, S.C., 2015, Geochronology, geochemistry and tectonic implications of granodiorite in the northwest of Weibao Deposit, Xinjiang Qimantage [in Chinese with English abstract]: Acta Geologica Sinica, v. 89, no. 3, p. 473–486.

Zhou, J.H., Feng, C.Y., Li, D.X., and Li, G.C., 2016, Geological, geochemical, and geochronological characteristics of Caledonian W-Sn mineralization in the Baiganhu orefield, southeastern Xinjiang, China: Ore Geology Reviews, v. 75, p. 125–149, https://doi.org/10.1016/j.oregeorev.2015.12.009.

Zhu, X.H., Chen, D.L., Liu, L., Wang, C., Yang, W.Q., Cao, Y.T., and Kang, L., 2013, Geochemistry, geochronology, and Hf isotopic compositions of the Tuanyushan pluton from the western segment of the Northern Qaidam [in Chinese with English abstract]: Gaoxiao Dizhi Xuebao, v. 19, no. 2, p. 233–244.

Zhu, X.H., Wang, H.L., and Yang, M., 2016, Zircon U-Pb age of the monzogranite from the middle segment of the Qaidam Mountain composite granite on the south margin of the Qilian Mountain [in Chinese with English abstract]: Geology in China, v. 43, no. 3, p. 751–767.

Zhu, X.L., Ren, E.F., Kang, W.H., Guan, S., Yang, Q.P., and Du, M., 2019, Zircon U-Pb age and geological significance of the granodiorite from the Bahan rock in the eastern part of South Qilian [in Chinese with English abstract]: Journal of Qinghai University, v. 37, no. 3, p. 94–98.

Zuza, A.V., and Yin, A., 2017, Balkatach hypothesis: A new model for the evolution of the Pacific, Tethyan, and Paleo-Asian oceanic domains: Geosphere, v. 13, no. 5, p. 1664–1712, https://doi.org/10.1130/GES01463.1.

Zuza, A.V., and Yin, A., 2013, Testing the TWINS hypothesis: Were Greater North China and Laurentia linked in the Archean and Proterozoic?: Geological Society of America Abstracts with Programs, v. 45, no. 7, p. 463.

Zuza, A.V., Cheng, X., and Yin, A., 2016, Testing models of Tibetan Plateau formation with Cenozoic shortening estimates across the Qilian Shan-Nan Shan thrust belt: Geosphere, v. 12, no. 2, p. 501–532, https://doi.org/10.1130/GES01254.1.

Zuza, A.V., Wu, C., Reith, R.C., Yin, A., Li, J.H., Zhang, J.Y., Zhang, Y.X., Wu, L., and Liu, W.C., 2018, Tectonic evolution of the Qilian Shan: An early Paleozoic orogen reactivated in the Cenozoic: Geological Society of America Bulletin, v. 130, no. 5–6, p. 881–925, https://doi.org/10.1130/B31721.1.

Zuza, A.V., Wu, C., Wang, Z., Levy, D.A., Li, B., Xiong, X., and Chen, X., 2019, Underthrusting and duplexing beneath the northern Tibetan Plateau and the evolution of the Himalayan-Tibetan orogen: Lithosphere, v. 11, no. 2, p. 209–231, https://doi.org/10.1130/L1042.1.

Zuza, A.V., Gavillot, Y., Haproff, P.J., and Wu, C., 2020, Kinematic evolution of a continental collision: Constraining the Himalayan-Tibetan orogen via bulk strain rates: Tectonophysics, v. 797, no. 228642, https://doi.org/10.1016/j.tecto.2020.228642.

Science Editor: Brad S. Singer
Associate Editor: Timothy Kusky

Manuscript Received 24 August 2021
Revised Manuscript Received 23 September 2021
Manuscript Accepted 28 October 2021

Printed in the USA